Development and Evaluation of a Classification-Based Binary-QSAR Model for Identifying Key Molecular Fingerprints in Histone Deacetylase 11 (HDAC11) Inhibition

Submitted by

Rinki Prasad Bhagat

EXAM ROLL NO.: M4PHP24012
CLASS ROLL NO.: 002211402050
REG. NO.: 163690
Department of Pharmaceutical Technology
Jadavpur University
Session- 2022-2024

Under The Guidance Of

Dr. Shovanlal Gayen
Assistant Professor
Laboratory of Drug Design and Discovery
Department of Pharmaceutical Technology
Jadavpur University, Kolkata-700032

Thesis submitted in partial fulfilment of the requirements for the Degree of Master of Pharmacy
Department of Pharmaceutical Technology
Faculty of Engineering and Technology
Jadavpur University, Kolkata

2024

Jadavpur University

Jadavpur, Kolkata-700032

CERTIFICATE OF APPROVAL

This is to certify that ***Rinki Prasad Bhagat*** (Exam Roll No. ***M4PHP24012***, Reg. No. ***163690*** of 2022-2024) has sincerely carried out the research work on the subject entitled ***"Development and Evaluation of a Classification-Based Binary-QSAR Model for Identifying Key Molecular Fingerprints in Histone Deacetylase 11 (HDAC11) Inhibition"*** under the supervision of **Dr. Shovanlal Gayen**, Laboratory of Drug Design and Discovery, Department of Pharmaceutical Technology of Jadavpur University. She has incorporated her findings in this thesis submitted by her in partial fulfillment of the requirements for the degree of **Masters of Pharmacy** (Pharmaceutical Technology) of Jadavpur University. She has carried out the research work independently and sincerely with proper care and attention to our entire satisfaction.

29/8/24

Head of the Department

Department of Pharmaceutical Technology

Jadavpur University

Kolkata-700032

Head
Dept. of Pharmaceutical Technology
Jadavpur University
Kolkata - 700 032, W.B. India

Shovanlal Gayen 29.8.24

Dr. Shovanlal Gayen

Laboratory of Drug Design and Discovery

Jadavpur University

Kolkata-700032

Department of Pharmaceutical Technology

DR. SHOVANLAL GAYEN
Assistant Professor
Dept. of Pharmaceutical Technology
Jadavpur University
Kolkata - 700 032, INDIA

Dipak Laha 29.8.24

Dean

Faculty of Engineering and Technology

Jadavpur University

Kolkata-700032

DEAN
Faculty of Engineering & Technology
JADAVPUR UNIVERSITY
KOLKATA-700 032

Acknowledgment

The outcome of this thesis required a lot of guidance and assistance from many people. I am extremely fortunate to have had these all along the completion of my work. Whatever I have done is only due to such guidance and assistance and I would not forget to thank them.

I am highly obliged and like to express my deep gratitude and profoundness to my reverend mentor **Dr. Shovanlal Gayen** of the Department of Pharmaceutical Technology, Jadavpur University, Kolkata for his excellent and constant guidance and help, endless encouragement, thoughtful and freedom and stupendous cooperation throughout the term paper till its successful completion. I am greatly indebted to his motivation, fruitful suggestions, and inspiration.

I owe my deep respect to **Prof. Amalesh Samanta**, Head of the Department, Department of Pharmaceutical Technology, Jadavpur University, Kolkata for all the necessary help and encouragement. I would like to convey my sincere gratitude to AICTE and Jadavpur University for their financial and equipment support for my M. Pharm course.

I would like to thank **Prof. Tarun Jha**, Natural Science Laboratory, Jadavpur University, Kolkata for the continuous encouragement, necessary help, and support to perform my work. I express my sincere thanks to **Prof. Tapan Kumar Maity**, **Prof. Kunal Roy**, **Dr. Probir Kumar Ojha**, **Dr. Emdad Hossain**, and **Dr. Nilanjan Adhikari** sir for their cooperation, help, and support.

I am extremely grateful to my seniors **Ms. Samima Khatun**, **Arijit Bhattacharya,** and **Sourav Sardar** for their guidance and support which assisted me in gathering knowledge about the different aspects of this work. I would express my sincere thanks to my laboratory colleague **Mr. Totan Das** and my juniors **Indrasis Das Gupta** and **Biplab Das** from the Laboratory of Drug Design and Discovery, Department of Pharmaceutical Technology, Jadavpur University, Kolkata-700032.

Finally, I would like to express my deep respect to my father **Mr. Ranjit Prasad Bhagat**, mother **Mrs. Ratna Prasad Bhagat**, my younger brother **Mr. Ritesh Prasad Bhagat** and my friends **Mr. Biswajit Pradhan**, **Mr. Sai Satyaprakash Mishra**, **Mr. Abhisek Shamal** for their continuous help, love, encouragement, and moral support throughout the period of my work.

Finally, I would like to thank one and all who were directly or indirectly there to help me with the successful completion of my dissertation work.

Rinki Prasad Bhagat

[Rinki Prasad Bhagat]

Date: 29.08.2024

Place: Department of Pharmaceutical Technology, Jadavpur University

Kolkata, India.

Declaration of Originality and Compliance

Of Academic Ethics

I hereby declare that this thesis contains a literature survey and original research work performed by me (**Rinki Prasad Bhagat**) as a part of my Masters of Pharmacy studies. All the information in this document has been obtained and presented in accordance with academic rules and ethical conduct.

I also declare that, as required by these rules and conduct, I have cited and referenced the materials and results that are not original to this work.

Name: ***Rinki Prasad Bhagat***

Exam Roll Number: ***M4PHP24012***

Class Roll Number: ***002211402050***

Registration Number: ***163690***

Thesis Title: ***"Development and Evaluation of a Classification-Based Binary-QSAR Model for Identifying Key Molecular Fingerprints in Histone Deacetylase 11 (HDAC11) Inhibition".***

Signature with Date

Rinki Prasad Bhagat
29.08.2024
(Rinki Prasad Bhagat)

Dedicated to

My Parents, Teachers, Seniors

and

Friends

Contents

Preface

This thesis, titled "Development and Evaluation of a Classification-Based Binary-QSAR Model for Identifying Key Molecular Fingerprints in Histone Deacetylase 11 (HDAC11) Inhibition," represents the culmination of my research and studies towards the Master of Pharmacy degree. The field of drug discovery and development is continuously evolving, driven by the need to understand complex biological targets and develop effective therapeutic agents. HDAC11 has emerged as a significant target due to its role in the regulation of gene expression, cell cycle progression, and oncogenesis. Inhibition of HDAC11 holds promise for therapeutic applications in cancer and other diseases.

Quantitative Structure-Activity Relationship (QSAR) modeling is a pivotal tool in computational chemistry, allowing researchers to predict the biological activity of chemical compounds based on their molecular structures. The binary-QSAR model, a subset of QSAR, focuses on classifying compounds as active or inactive, thus aiding in the identification of potential drug candidates.

The objective of this research is to develop and evaluate a classification-based binary-QSAR model to explore and identify the essential molecular fingerprints responsible for HDAC11 inhibition. This work involves the integration of molecular modeling, and statistical analysis to derive a robust predictive model. By identifying key molecular features, this study aims to contribute valuable insights into the design of potent HDAC11 inhibitors.

The journey of this research has been both challenging and rewarding. It has deepened my understanding of computational drug discovery and provided me with the skills to handle complex data and derive meaningful conclusions. I am grateful for the guidance and support of my supervisors and seniors, the collaboration with my peers, and the encouragement from my family and friends. This thesis is a testament to the collective effort and dedication towards advancing the field of pharmaceutical sciences.

I hope this work will serve as a foundation for future research and inspire continued exploration in the quest for innovative therapeutic solutions.

Rinki Prasad Bhagat

(Rinki Prasad Bhagat)

LIST OF FIGURES

Figure 14: Top 20 favorable fingerprints identified from the Bayesian classification model.

Figure 15: Molecular structures of some *active* HDAC11 inhibitors with favourable Bayesian fingerprint.

Figure 16: Top 20 unfavourable fingerprints identified from the Bayesian classification study.

Figure 17: Structure of some *inactive* HDAC11 inhibitors with bad Bayesian fingerprints.

Figure 18: Classification of HDAC11 inhibitors through the decision tree into *active* and *inactive* classes by using the RP model.

Figure 19: *FCFP_6* fingerprints obtained from the RP Study.

Figure 20: Compounds containing different fingerprints through Bayesian study, RP study, SARpy, and machine-learning-based QSAR techniques.

Figure 21: Analysis of zinc-binding interactions in the compounds **A004**, **A007**, **A013**, and **A053** using molecular docking studies. All the compounds are coordinated with zinc metal via the carboxamide group (CONHOH). The dotted lines indicate different interactions: black lines (metal coordination with zinc metal), green lines (H-bonding), white lines (π-alkyl), blue lines (π-σ), orange lines (π-cation), and purple lines (halogen interaction).

LIST OF TABLES

Chapter 1: Introduction

Chapter 1: Introduction

A class of enzymes known as histone deacetylases (HDACs) regulates the acetylation status of both histones and non-histone proteins, which is important in regulating gene expression. Acetylation and deacetylation of histones are pivotal processes in chromatin remodeling, impacting the accessibility of transcriptional machinery to DNA and thereby influencing gene transcription (Kouzarides *et al*., 2007). HDACs catalyze the removal of acetyl groups from lysine residues on histone tails, leading to a more condensed chromatin structure and transcriptional repression. Conversely, histone acetyltransferases (HATs) add acetyl groups, resulting in an open chromatin conformation and active transcription (Shogren-Knaak *et al.,* 2006; Shanmugam *et al.,* 2022).

The HDAC family is divided into four classes based on sequence homology and domain organization: Class I, Class II (subdivided into IIa and IIb), Class III (sirtuins), and Class IV. Class I HDACs (HDAC1, 2, 3, and 8) are primarily located in the nucleus and are involved in regulating cell cycle progression and differentiation. Class II HDACs (HDAC4, 5, 6, 7, 9, and 10) can shuttle between the nucleus and cytoplasm, and they play roles in tissue-specific functions and developmental processes. Class III HDACs (SIRT1-7), or sirtuins, are NAD+-dependent deacetylases involved in metabolic regulation, aging, and stress responses. Class IV is represented by a single member, HDAC11, which exhibits properties of both Class I and II enzymes and is the least characterized among the HDACs (Ruijter *et al.,* 2003; Witt *et al.,* 2009).

HDACs are implicated in a wide array of physiological processes, including cell proliferation, differentiation, apoptosis, and DNA repair (Hauer *et al.,* 2017). Dysregulation of HDAC activity is associated with various diseases, most notably cancer, where aberrant deacetylation can lead to the silencing of tumor suppressor genes and the activation of oncogenes. This has made HDACs attractive targets for therapeutic intervention (Pan *et al.,* 2012; Glozak *et al.,* 2009). Several HDAC inhibitors (HDACi), such as vorinostat, romidepsin, and panobinostat, have been developed and approved for the treatment of certain cancers, underscoring the therapeutic potential of targeting HDACs (West *et al.,* 2014; Moinul *et al.,* 2023).

Recent research has extended beyond cancer, exploring the role of HDACs in neurodegenerative diseases, cardiovascular disorders, and inflammatory conditions. For instance, HDAC inhibitors have shown promise in the treatment of Huntington's disease and

amyotrophic lateral sclerosis by promoting neuronal survival and reducing neuroinflammation. In cardiovascular diseases, HDAC inhibition can modulate cardiac hypertrophy and fibrosis, offering potential therapeutic benefits (Amin *et al.,* 2023; Yoon *et al.,* 2016; Sardar *et al.,* 2024; Bhattacharya *et al.,* 2023; Khatun *et al.,* 2024).

Despite the progress in understanding and targeting HDACs, challenges remain, particularly in achieving isoform selectivity to minimize side effects and enhance therapeutic efficacy. The development of isoform-selective HDAC inhibitors is a burgeoning area of research, focusing on elucidating the distinct biological functions and regulatory mechanisms of individual HDAC isoforms (Sardar *et al.,* 2024; Bhattacharya *et al.,* 2023; Khatun *et al.,* 2024; Khatun *et al.,*2023; Balasubramanian *et al.,* 2009).

In this study, we have focused on HDAC11 which is the smallest and latest discovered only known HDAC enzyme that belongs to class IV (Gao *et al.,* 2002). Its encoding gene, which is an open reading frame with a 347-residue protein, is found on the human chromosome 3q25.1 (Cao *et al.,* 2019). It plays a crucial role in regulating gene expression through chromatin remodeling. It has been also demonstrated that HDAC11 is the first isozyme in the HDAC family to favour physiologically relevant acyl groups over acetyl groups. It effectively degrades long-chain acyl modifications on side chains of lysine. Strong lysine de-fatty acylase HDAC11 is found to function more than 10,000 times better than its deacetylase counterpart. HDAC11 is the most efficient fatty-acid deacetylase, with catalytic efficiencies towards dodecanoylated and myristoylated peptides of 77,700 and 149,000 M− 1s− 1, respectively (Kutil *et al.,* 2018; Sahakian *et al.,* 2017; Villagra *et al.,* 2009). HDAC11 has garnered significant interest in recent years due to its potential as a therapeutic target in various diseases, including cancer, neurodegenerative disorders, immunological diseases, metabolic diseases, and so on. Inhibiting HDAC11 can modulate the acetylation status of histones and non-histone proteins, thereby influencing key cellular processes such as proliferation, differentiation, and apoptosis (Woods *et al.,* 2017; Yanginlar *et al.,* 2018).

The development of HDAC11 inhibitors has become a focal point in drug discovery. However, identifying potent and selective inhibitors remains challenging due to the conserved nature of the active sites across the HDAC family and the absence of experimental structure. Therefore, there is a compelling need to develop computational models that can accurately predict HDAC11 inhibition and guide the design of selective inhibitors (Khatun *et al.,* 2024).

Quantitative Structure-Activity Relationship (QSAR) models have been instrumental in the drug discovery process by establishing a relationship between the chemical structure of

compounds and their biological activity (Tropsha *et al.,* 2010). Among the various types of QSAR models, classification-based binary-QSAR models are particularly useful when the primary interest is in distinguishing between *active* and *inactive* compounds (Ahamed *et al.,* 2018). These models employ Bayesian classification, Recursive partitioning, SARpy analysis, and different machine learning (ML) algorithms to identify molecular fingerprints, and specific structural features that are crucial for biological activity.

We aim to develop and evaluate a classification-based binary-QSAR model to identify key molecular fingerprints associated with HDAC11 inhibition. This study will leverage a comprehensive dataset of known/unknown HDAC11 inhibitors and non-inhibitors, applying advanced feature selection techniques to extract relevant molecular fragments, decision trees, and descriptors. By employing classification-based QSAR methods, we will construct a robust predictive model that can accurately classify compounds based on their potential to inhibit HDAC11 (Amin *et al.,* 2022).

The primary objectives of this research are to compile a dataset of HDAC11 inhibitors and non-inhibitors from databases and literature sources, ensuring data quality and relevance; removing duplicates from the dataset; and balancing the dataset in a justified manner. Subsequently, in the case of Bayesian classification and Recursive partitioning, constructing a predictive model and evaluating the performance of the developed models using metrics such as accuracy, precision, recall, and receiver operating characteristic curve (*ROC*); will generate relevant good/bad molecular fragments, and decision trees which will be crucial for identifying inhibitors from non-inhibitors (Sardar *et al.,* 2024; Bhattacharya *et al.,* 2023).

Moreover in the case of ML algorithms, utilizing genetic algorithms and other feature selection methods to identify the most relevant molecular descriptors that contribute to HDAC11 inhibition; to implement various classification algorithms, including Random Forest Classifier (*RFC*), Support Vector Classifier (*SVC*), Logistic Regression (*LR*) and Linear Discriminant Analysis (*LDA*), to build predictive models; to assess the performance of the developed models using metrics such as accuracy, precision, recall, and area under the receiver operating characteristic curve (*AUC-ROC*); and to analyze the models to extract and interpret the key molecular fingerprints that are critical for HDAC11 inhibition (Banerjee *et al.,* 2023).

The successful development of a reliable binary-QSAR model will provide valuable insights into the structural requirements for HDAC11 inhibition, facilitating the design of novel inhibitors with improved potency and selectivity. This approach not only enhances our understanding of HDAC11 biology but also accelerates the drug discovery process for therapeutic interventions targeting HDAC11.

1.1 Mechanism of action of HDAC11

The mode of action of HDAC11 is similar to that of other HDAC isoforms. Interestingly, research on chromatin remodeling by histone deacetylation has gained traction during the past few decades. Histone acetyltransferases (HAT) and histone deacetylases (HDAC) are two enzymes that balance the acetylation (relaxed chromatin) and deacetylation (condensed chromatin) of histones (**Figure 1**). HDACs remove the acetyl group from the ε-NH2 group of lysine residues in proteins, while HATs primarily catalyze the transfer of an acetyl group from acetyl-CoA to the lysine residue's ε-NH2 group (Liu *et al.,* 2009). One important epigenetic alteration that alters the chromatin architecture and controls gene expression by opening or shutting the chromatin structure is histone acetylation. The nucleosomes found in chromatin are made up of an octamer with four histone cores (H2A, H2B, H3, and H4) encircled by 146 base pairs of DNA. The ε amino groups present in the N-terminal of lysine residues are the site of acetylation, which aids in transcription factor binding. It weakens the bond that holds DNA and core nucleosome proteins together. Consequently, this increases accessibility to the transcription factor binding sites (Ruijter *et al.*, 2003). But according to Jenke *et al.*, these HDACs also deacetylate several non-histone proteins such p53, c-Myc, NF-κB, and E2F (Jenke *et al*., 2021).

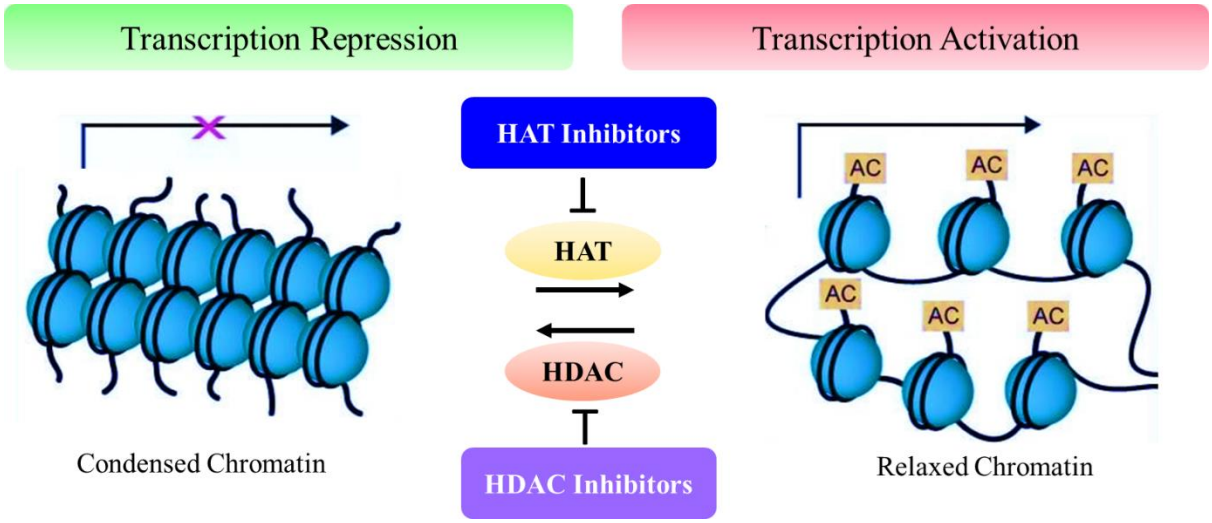

Figure 1: Mode of action of HAT and HDAC protein

1.2 Location of HDAC11

HDAC11 is localized in both the cytoplasm and the nucleus. Unlike some other HDACs, it does not exhibit a preference for either site, and it dynamically shuttles between these

compartments, similar to other class II HDACs (Tiwari *et al*., 2014; Schlüter *et al*., 2019). In freshly isolated, unstimulated T regulatory cells, HDAC11 is present in both the nucleus and cytoplasm. However, upon activation of these cells, HDAC11 predominantly localizes in the nucleus (Cheng *et al*., 2014). In retinal ganglion cells (RGC), HDAC11 also shows both nuclear and cytoplasmic distribution, but it is expelled from the nucleus in response to excitotoxicity induced by N-Methyl-D-aspartate (NMDA) receptors (Joshi *et al*., 2013). In adult neurons, RGCs, macrophages, and human T regulatory cells, HDAC11 is evenly distributed across the cytoplasm and nucleus (Tiwari *et al*., 2014; Schlüter *et al*., 2019; Cheng *et al*., 2014; Joshi *et al*., 2013; Takase *et al.*, 2013).

Additionally, the interactions of HDAC11 provide substantial evidence that it may play a role in regulating the cohesin complex and other cell cycle-related processes. Interestingly, HDAC11 is found in the perinuclear region of T regulatory cells, which aligns with its interaction with the survival of motor neuron (SMN) complexes, responsible for the assembly of the spliceosome. This positioning suggests a potential role in coordinating activities crucial for cell function and survival (Joshi *et al*., 2013). HDAC11 has been identified in specific subcellular locations in various studies. These locations include the cytoplasm of quiescent CD4+ cells, maturing oligodendrocytes, retinal pigmented cells, and neurons in the anterior cingulate cortex (Gao *et al*., 2002; Host *et al*., 2011; Hurtado *et al*., 2021; Keedy *et al*., 2009; Liu *et al*., 2008). Additionally, HDAC11 is notably abundant in brain synapses and mitochondria-rich skeletal muscle cells. The localization of HDAC11 varies across different systems. For example, HDAC11 is mostly located in the cytoplasm of mature cells and the progenitors of embryonic astrocytes, but it is also equally present in the cytoplasm and nucleus of immature oligodendrocytes (Tiwari *et al*., 2014).

1.3 Structural insights and the Catalytic domain of HDAC11

The HDAC11 protein consists of conserved residues within the catalytic key regions used by mammalian class I and II HDACs (Gao *et al*., 2002). While the deacetylase function and structure of HDAC11 for each domain remain to be determined, they have been accurately modeled with the help of the resolved structure of HDAC8 (Gao *et al*., 2002). The key characteristics of HDAC11's catalytic site are a conserved funnel-like channel outline that can accommodate a reformed lysine residue; a uniform catalytic residue at the base of the funnel; and four loops at the opening of the funnel, varying in length and shape, that interact with protein regions and may be involved in substrate identification (Hurtado *et al*., 2021; Bryant *et al*., 2017). Histidine residues 142 and 143 are crucial for the enzymatic activity of HDAC11,

specifically in catalyzing the hydrolysis of acyl groups within the catalytic region (**Figure 2**). These residues are among the invariant amino acids essential for this function. Research indicates that HDAC11 is more similar to class I HDACs than to class II, suggesting that HDAC11 may possess the full deacetylase activity characteristic of class I HDACs (Thangapandian *et al.*, 2012; Woods *et al.*, 2017).

Homology models of HDAC11, developed by Thangapandian *et al*. were aligned with the structure of HDAC8 to compare the dimensions of their catalytic tunnels. The analysis revealed that both HDAC8 and HDAC11 feature tunnels that are generally deep and narrow

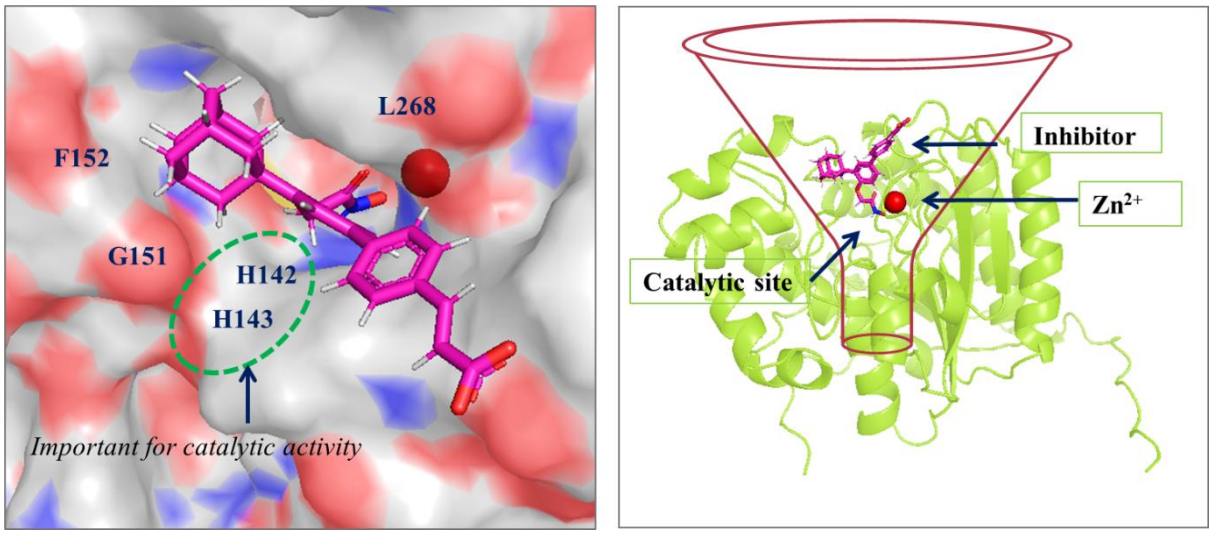

Figure 2: The alpha model of HDAC11 provides structural insights into the catalytic region of the enzyme.

from the top to the bottom, containing a charge relay system and divalent Zn2+ ions necessary for catalytic activity (Thangapandian *et al*., 2012). Kutil *et al.* noted that a narrow channel, extending from the surface of the protein to the zinc-dependent catalytic site, accommodates the lysine side chain of the substrate. This narrow channel branches into lateral and vertical internal tunnels. These tunnels are capable of accommodating substrates with long aliphatic fatty acid chains. The lateral tunnel, also known as the "foot pocket" in HDAC8, is thought to act as an escape pathway for unbound acetate and can be occupied by acyl groups from the substrates. Therefore, HDAC11, similar to HDAC8 and class I HDACs, has a deep lateral pocket, indicating a catalytic mechanism akin to that of HDAC8 (Kutil *et al.*, 2018).

1.4 Understanding the Functionality and Growing Importance of HDAC11

HDAC11 stands out among other HDACs due to its unique enzymatic activity, specifically targeting lysine residues' fatty acid modifications. This specialization differentiates HDAC11 from other HDACs that are involved in the deacetylation of histone and non-histone proteins, establishing it as a distinct entity in the realm of epigenetic regulation, expanding the substrate scope of HDACs beyond traditional acetyl lysine hydrolysis (Núñez-Álvarez *et al.*, 2022).

HDAC11 plays distinct roles in the myeloid compartment, particularly within neutrophils. In antigen-presenting myeloid cells, HDAC11 negatively regulates the production of interleukin-10 (IL-10) by promoting histone deacetylation and binding to the IL-10 promoter, thereby influencing immune system activation (Li *et al.*, 2016). In neutrophils, HDAC11 is upregulated during differentiation and maturation but inversely correlates with functional activity (Sahakian *et al.*, 2016). It also influences cytokine and chemokine biology in neutrophils, making HDAC11 a potential target for diseases involving these cells. Furthermore, HDAC11 regulates RNA splicing and immune cell functions, including those of neutrophils, T cells, regulatory T cells, and antigen-presenting cells (Sahakian *et al.*, 2017; Villagra *et al.*, 2009; Woods *et al.*, 2017).

HDAC11 is highly expressed in the rat brain, suggesting its significance in neurological functions (Broide *et al.*, 2007). Research indicates that inhibiting HDAC11 may be beneficial for treating conditions such as multiple sclerosis, obesity, and cancer (Ho *et al.*, 2023). In breast cancer cells, HDAC11 affects gene expression and interacts with the promoter of the adrenodoxin reductase tumor suppressor gene ARH1 (Feng *et al.*, 2007; Tao *et al.*, 2007). Additionally, HDAC11 inhibits hepatitis B virus (HBV) replication by reducing H3 acetylation on covalently closed circular DNA (cDNA) minichromosomes (Yuan *et al.*, 2019).

In oligodendrocytes, HDAC11 regulates maturation by modulating H3K9 and H3K14 acetylation on the proteolipid protein (Plp) and myelin basic protein (Mbp) genes (Liu *et al.*, 2009). In vitamin D-deficient intestinal epithelial cells, HDAC11 binds to promoters of tight junction proteins, reducing H3/H4 acetylation ratios and inhibiting gene transcription. HDAC11 is also associated with transcription factors such as TBX2, TBET, and EOMES in non-activated T cells, suppressing T-cell effector functions (Woods *et al.*, 2017). HDAC11's role extends to cell-specific transcription factors like KLF4, PU.1, GLI1, and MYOD, and it interacts with bromodomain-containing protein BRD2 (**Figure 3**). These interactions highlight

the potential therapeutic applications of HDAC11 inhibition for various conditions, including metabolic disorders, cancers, and inflammatory diseases (Bagchi *et al.*, 2018; Todd *et al.*, 2010; Chen *et al.*, 2022; Chen *et al.*, 2020). Although no specific HDAC11 inhibitors are currently approved, several naturally derived and synthetic inhibitors have shown promising preclinical therapeutic effects (Dallavalle *et al.*, 2022; Son *et al.*, 2020). Ongoing research continues to focus on developing specific HDAC11 inhibitors for disease treatment.

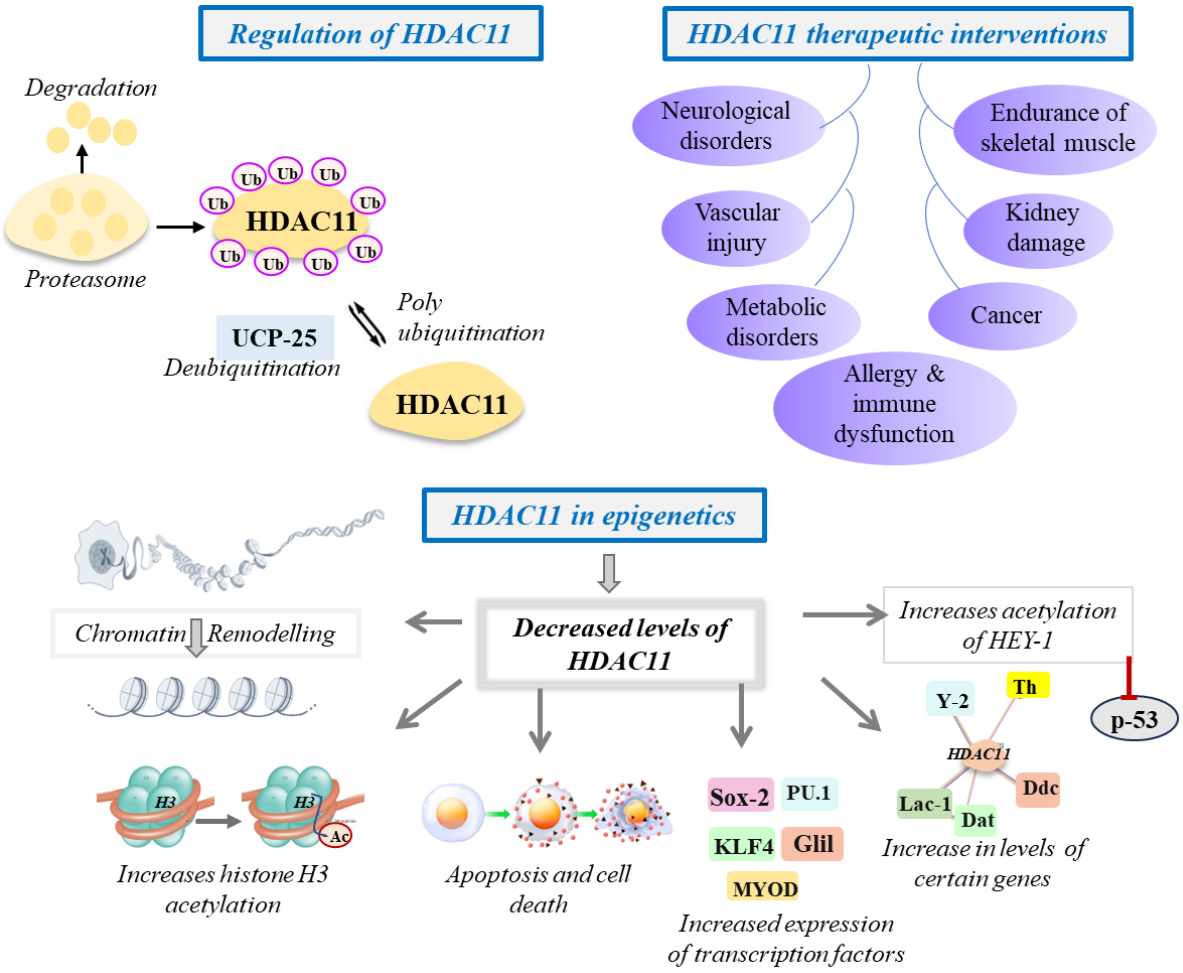

Figure 3: HDAC11 regulation and its involvement in epigenetics, as well as therapeutic treatments that target HDAC11. SOX-2 (SRY-box transcription factor 2), PU.1 (Polyomavirus enhancer-binding protein 2 alpha 1), GLI1 (glioma-associated oncogene family zinc finger-1), KLF4 (Krüppel-like factor 4), MYOD (myoblast determination protein 1), UCP-25 (uncoupling protein-25), HEY-1 (Hes Related Family BHLH transcription factor with YRPW motif 1), and DNA (deoxyribonucleic acid).

1.5 The Role of HDAC11 in Epigenetic Regulation

HDAC11 is expressed in particular tissues, including the brain, heart, testis, kidney, skeletal muscle, and gallbladder (Gao *et al.*, 2002; Núñez-Álvarez *et al.*, 2021; Boltz *et al.*, 2019). It

plays a vital role in epigenetic regulation by deacetylating both histone and non-histone proteins, thereby influencing the acetylation status of various proteins involved in transcriptional regulation and cell cycle control. In breast cancer cells, HDAC11 deacetylates transcription factors such as E2F1 and E2F4, affecting their function and expression levels, and thereby contributing to cancer progression. HDAC11 also deacetylates CDT1, promoting its proteasomal degradation and removing acetylation protection against ubiquitination (Feng *et al.,* 2007; Tao *et al.,* 2007). Additionally, HDAC11 decreases the acetylation of BubR1 without altering its protein levels, and this interaction occurs at the centrosome alongside HDAC6. In vitro experiments have shown that HDAC11-mediated deacetylation can inactivate BubR1 and enhance dendritic growth (Lozada *et al.,* 2016; Watanabe *et al.,* 2014).

HDAC11 is crucial for various biological traits such as migration, apoptosis, stemness, immune evasion, and cell invasion, all contributing to tumor growth and metastasis. Its overexpression in cancer is linked to the regulation of cell proliferation, differentiation, immune evasion, and treatment resistance (Liu *et al.,* 2023). HDAC11 depletion can double the acetylation levels of histone H3 at lysine residues 9 and 14 (H3K9/K14ac) in cells like oligodendrocytes compared to non-depleted cells (Liu *et al.,* 2009). Conversely, HDAC11 overexpression reduces acetylation on histone H3 at lysine residue 27 (H3K27ac) and decreases chromatin accessibility in retinal-pigmented cells (Wang *et al.,* 2018). The extent of histone acetylation is modulated by either the downregulation or overexpression of HDAC11. Interleukin-10 (IL-10) is the first known epigenetic target of HDAC11, which acts as a transcriptional repressor of IL-10 production by influencing H3/H4 acetylation levels at the IL-10 promoter and regulating immune system activation in antigen-presenting cells (APCs) (Villagra *et al.,* 2009).

1.6 Different Physiological Roles of HDAC11

HDAC11 plays a vital biological role in almost all systems in the human body and is recognized as a crucial regulator of cellular functions. It is notably expressed in the brain, kidneys, heart, and testis. HDAC11 is implicated in the development of numerous metabolic diseases, such as diabetes and obesity, and in the regulation of several immune cells, including T-cells and neutrophils. Additionally, it is associated with cardiovascular disease, chronic kidney disease, CNS-related disorders, and cancer. HDAC11 is among the top 1–4% of overexpressed genes in cancers like breast cancer and hepatocellular carcinoma. This section provides an overview of the latest research on the role and mechanisms of HDAC11 in the regulation of these various diseases.

1.6.1 Renal and Metabolic disorders

In today's world, metabolic illnesses such as obesity, hypertension, type II diabetes, cardiovascular diseases, and polycystic ovarian syndrome pose significant health risks (https://www.nhlbi.nih.gov/health/metabolic-syndrome/causes). The primary contributors to metabolic syndrome include overweight and obesity, which elevate blood pressure, low-density lipoprotein (LDL), triglycerides, and high-density lipoprotein (HDL) levels (Yang *et al.*, 2021). Additionally, obesity is linked to chronic metabolic inflammation and abnormal adipocyte growth and function. HDAC11 plays a crucial role in combating obesity by modulating the immune response; normal or high levels of HDAC11 activity can stimulate this response, while inhibition of HDAC11 increases IL-10 expression and affects metabolic inflammation. HDAC11 is also vital for regulating cell division, proliferation, migration, glucose homeostasis, and insulin sensitivity (**Figure 4**) (Villagra *et al.*, 2009).

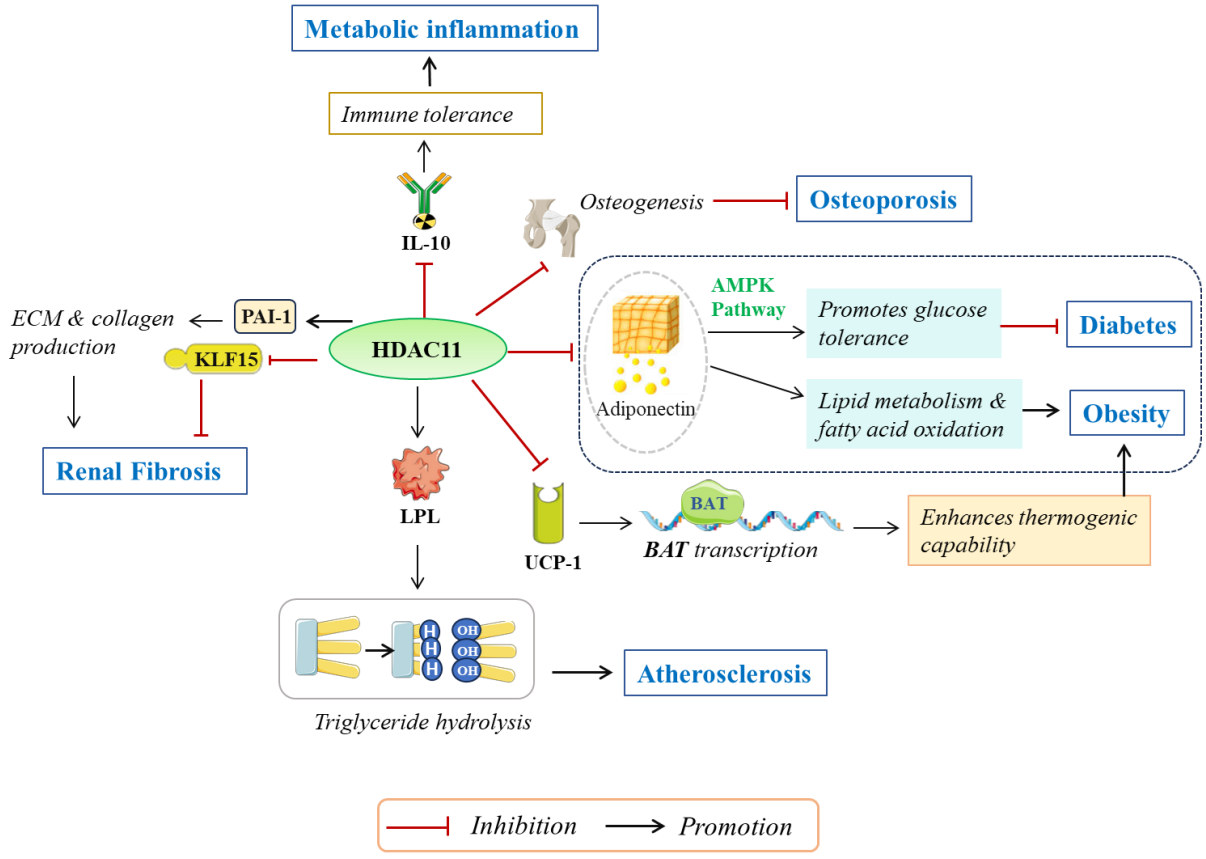

Figure 4: HDAC11's function in metabolic diseases. Histone deacetylase 11, PAI-1 (plasminogen agonist inhibitor type 1), KLF15 (Krugppel-like factor 15), IL-10 (interleukin-10), BAT (brown adipose tissue), LPL (lipoprotein lipase), UCP1 (uncoupling protein 1), and AMPK (AMP-activated protein kinase) are some of the proteins involved in this pathway.

However, some research suggests that depleting HDAC11 can significantly reduce liver fat and damage, while improving insulin sensitivity, lowering cholesterol levels, and enhancing glucose tolerance (Sun *et al.*, 2018). Significantly, lacking HDAC11 leads to a marked increase in metabolic rate and oxygen consumption, which boosts energy expenditure and fat oxidation (Bagchi *et al.*, 2018). Sun *et al.* found that the increase in uncoupling protein 1 (UCP1) expression and activity in brown adipose tissue due to HDAC11 deficiency enhances energy expenditure through improved thermogenesis. Moreover, HDAC11 deletion activates the adiponectin-AdipoR-activated protein kinase (AMPK) pathway in the liver, potentially reversing hepatosteatosis. Consequently, HDAC11 is recognized as a novel regulator of obesity with promising therapeutic implications for obesity-related diseases (Sun *et al.*, 2018).

Fan *et al.* highlighted the role of HDAC11 in maintaining healthy body weight and preventing lipid accumulation in diabetic hearts and adipose tissues. In a diabetic heart failure mouse model, reduced levels of HDAC11 led to oxidative stress, inflammation, decreased apoptosis, and dyslipidemia. This suggests that inhibiting HDAC11 expression might prevent or mitigate diabetes-associated cardiomyopathy. Furthermore, renal fibrosis, characterized by increased myofibroblast proliferation, inflammatory infiltrates, migration, and extracellular matrix proteins, is a poor prognostic indicator in chronic kidney disease. Among the HDACs, only HDAC11 has been shown to suppress PAI-1 (plasminogen activator inhibitor type 1) expression in kidneys subjected to ischemia-reperfusion (I/R) injury, particularly in gender-specific kidney models, and in monocytes and macrophages stimulated with lipopolysaccharide (LPS). Orchiectomy prevented the release of HDAC11 induced by ischemia-reperfusion (I/R) injury, while dihydrotestosterone therapy restored its levels. This suggests that reductions in HDAC11 binding and expression due to I/R injury are influenced by male gender and hormones, leading to increased PAI-1 expression (Fan *et al.*, 2018; Kim *et al.*, 2013; Mrug Kim *et al.*, 2013).

Mao *et al.* explored various models of renal fibrosis, finding that HDAC11 expression was elevated in the kidneys. In cultured renal tubular epithelial cells (RTECs), treatment with angiotensin II (Ang II) also increased HDAC11 levels. Additionally, inhibiting HDAC11 with quisinostat or siRNA reduced the Ang II-induced fibrogenic response in these cells. The interaction between HDAC11 and activator protein 2 alpha (AP-2α) was found to suppress the transcription of Kruppel-like factor 15 (KLF15). Consequently, Ang II promoted fibrogenesis in RTECs by counteracting the effects of HDAC11 inhibition or depletion through KLF15

knockdown. This led to the identification of a critical AP-2α-HDAC11-KLF15 pathway involved in renal fibrosis (Mao *et al.,* 2020).

1.6.2 Neurological diseases

Epigenetic alterations, such as histone acetylation, are essential for normal brain function. HDAC11 is predominantly expressed in the brain and some other tissues in the human body. At the cellular level, the HDAC11 protein is primarily located in the cell nuclei of mature oligodendrocytes, with a lesser presence in astrocytes (Liu *et al*., 2008). The acetylation of histone core proteins decreases as neural cells in the CNS grow. Consequently, using RNA interference to inhibit HDAC11 expression enhances histone H3 acetylation in an oligodendroglial cell line (Liu *et al*., 2008). Additionally, HDAC11 is considered a potential therapeutic target for mental conditions, including depression, Parkinson's disease, and schizophrenia, due to its role in neuronal differentiation. It is also relevant in the treatment of malignant hematopoiesis and myeloproliferative neoplasms (Baek *et al*., 2023; Kumar *et al*., 2022; Sun *et al*., 2018). Some studies suggest that the removal of HDAC11 leads to a significant decrease in chemokine C–C motif ligand 2 (CCL2) levels. This reduction is associated with a lower number of monocytes and dendritic cells infiltrating the spinal cords of animals with experimental autoimmune encephalomyelitis (EAE), aiding in the treatment of CNS demyelinating diseases (**Figure 5**) (Baek *et al*., 2023; Kumar *et al*., 2022; Sun *et al*., 2018).

Baek *et al.* achieved a revolutionary discovery by pharmacologically controlling HDAC11, which induces autophagy and balances reactive nitrogen species in microglia. This discovery suggests a new therapeutic approach for depressive conditions and an anti-inflammatory strategy for brain disorders involving microglia (Baek *et al.*, 2023). Jagielska *et al.* found that during the development of oligodendrocytes, HDAC11 decreases histone 3 acetylation and promotes the transcription of the Mbp and Plp genes (Jagielska *et al.*,2017). He *et al.* demonstrated that HDAC11 affects the expression of the human microRNA hsa-miR-4639-5p, which could potentially serve as both a diagnostic tool and a treatment option for Parkinson's disease (He *et al.,* 2017). Additionally, Bryant *et al.* observed decreased expression of the schizophrenia-associated gene FEZ1 in differentiating brain cells. Since FEZ1 interacts with DISC1, it is associated with the risk of schizophrenia and the dendritic development of neurons (Bryant *et al.*, 2017).

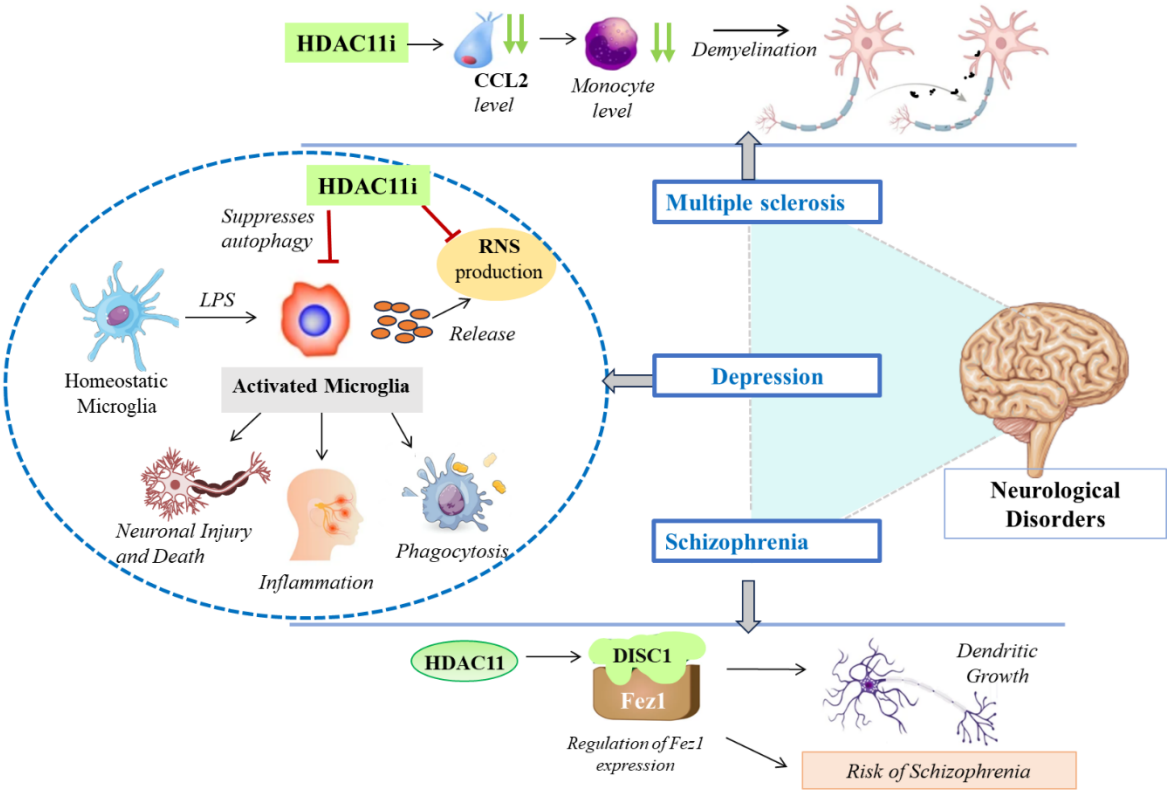

Figure 5: HDAC11's function in neurological conditions. FEZ1, fasciculation and elongation protein zeta 1; DISC1, disturbed in schizophrenia 1; LPS, lipopolysaccharides; RNS, reactive nitrogen species; CCL2, chemokine (C-C motif) ligand 2.

1.6.3 Functions of Immune system

HDAC11 acts as a negative regulator of IL-10 gene expression. IL-10 is an anti-inflammatory cytokine that modulates macrophages and dendritic cells, while also controlling the production of pro-inflammatory cytokines (Sahakian *et al.*, 2015). It prevents the differentiation of dendritic cells from monocyte precursors and limits macrophages' ability to combat intracellular infections by inhibiting TNF (tumor necrosis factor) production (Bryant *et al.*, 2017; Sahakian *et al.*, 2015; Kumar *et al.*, 2022). Recent studies have shown that HDAC11 negatively affects the phenotype and function of T-cells and neutrophils. HDAC11-deficient myeloid-derived suppressor cells displayed increased inhibitory activity against CD8+ T-cells (Chen *et al.*, 2021). Additionally, lactate from *Staphylococcus aureus* biofilms inhibits HDAC11, enhancing IL-10 transcription through unchecked HDAC6 activity, which promotes the anti-inflammatory properties of macrophages and myeloid-derived suppressor cells (Heim *et al.*, 2020).

Emerging evidence suggests that HDAC11 could be an inflammatory biomarker in Huntington's disease (Kumar *et al.*, 2022), as it directly suppresses IL-10 production, leading

to inflammation and disease progression (Shao *et al.*, 2018). In Parkinson's disease, hyperimmune activation, characterized by elevated IL-10 gene expression, promotes neuronal loss through the activation and release of CD4+ and T-cells (Kumar *et al.*, 2022). Overexpression of HDAC11 lowers IL-10 production, which boosts the functioning of inflammatory antigen-presenting cells, potentially activating naïve T cells and increasing the responsiveness of tolerant CD4+ T cells (Kumar *et al.*, 2022; Villagra *et al.*, 2009).

HDAC11 plays a dual role in neutrophil biology: it increases as neutrophils mature, and a decrease in HDAC11 correlates with neutrophil functional activity (Sahakian *et al.*, 2017). TNF upregulates HDAC11 expression in B cells, inhibiting IL-10 synthesis and contributing to allergic rhinitis (Shao *et al.*, 2018). Nasal polyp development is mediated by IL-4, which also suppresses IL-10 production in dendritic cells by modulating HDAC11 (Luo *et al.*, 2017). In Hodgkin's lymphoma (HL) cell lines, HDAC inhibitors increased OX40 ligand (OX40L) surface expression in a dose-dependent manner. Suppressing HDAC11 transcripts elevated TNF- and IL-17 production in HL cell supernatants. Furthermore, OX40L produced by HDAC11 suppressed Type-1 T-regulatory (Treg) cells that generate IL-10 (Buglio *et al.*, 2011). OX40 activation reduces the suppressive effect of IL-10-producing Type 1 Treg cells and CD4+ CD25+ Foxp3+ Treg cells, as well as the transformation of antigen-specific CD4+ naive T cells to CD4+ CD25+ Foxp3+ Treg cells (Ito *et al.*, 2006).

Finally, individuals with food allergies show elevated expression of IL-13 and HDAC11 in their blood and local tissues. Mechanistically, IL-13 binds to HDAC11 in the IL-10 promoter area, which prevents B-cells from producing IL-10 and hence contributes to food allergies (Liu *et al.*, 2020).

1.6.4 Vascular Injury

Vascular injury refers to damage to a blood vessel, such as an artery that supplies blood to an organ or limb, or a vein that returns blood to the heart (https://vascular.org/patients-and-referring-physicians/conditions/vasculartrauma). This injury triggers inflammation within blood vessels, leading to a transformation of vascular smooth muscle cells from a contractile state to a synthetic state, which plays a crucial role in the development of cardiovascular diseases (Núñez-Álvarez *et al.*, 2016). Vascular smooth muscle cells have become a significant focus of research as a model for flexible gene expression (Miano *et al.*, 2010). Studies suggest that Kruppel-like factor 4 (KLF4) recruits HDAC11 to silence histone acetylation, which deactivates the chromatin around the angiogenic factor with G-Patch and FHA domain 1

(Aggf1) promoter, thereby repressing Aggf1 transcription. Consequently, the modulation of the vascular smooth muscle cell phenotype was halted, and Aggf1 expression was restored when either HDAC11 or KLF4 was depleted. Administering an HDAC11 inhibitor to mice ultimately reduced vascular injury (Zhou *et al.*, 2017). Zhou *et al.* experimented on rats, where intraperitoneal treatment with quisinostat reduced vascular injury in rats with carotid artery ligation-induced vascular injury by restoring Aggf1 levels and contractile gene expression (Zhou *et al.*, 2017).

1.6.5 HDAC11 in Skeletal muscle

Skeletal muscle, comprising over 40% of total body mass in mammals, plays a crucial role in determining basal metabolic rate (BMR) and maintaining overall energy homeostasis (Hurtado *et al.*, 2021). Although HDAC11 is highly expressed in skeletal muscle, its specific biological functions and physiological roles remain largely unknown. Recent research suggests that HDAC11 deficiency enhances muscle strength and endurance, thereby improving muscular function (Zhang *et al.*, 2022). The loss of HDAC11 facilitates a shift from glycolytic to oxidative muscle fibers, increasing the number of oxidative myofibers without significantly affecting the overall structure of skeletal muscle (Núñez-Álvarez *et al.*, 2016). Additionally, HDAC11 depletion boosts mitochondrial fatty acid β-oxidation by lowering acylcarnitine levels in vivo and activating the AMP-activated protein kinase-acetyl-CoA carboxylase pathway, which helps maintain the balance between different muscle fiber types and mitochondrial lipid oxidation (Morales *et al.*, 2017).

Nunez-Alvarez *et al.* investigated the impact of HDAC11 genetic deficiency on skeletal muscle regeneration, a process primarily dependent on local stem cells along with stromal and immune cells. Their findings indicate that HDAC11 is not essential for adult muscle development or the formation of the stem cell population. However, HDAC11 deficiency accelerates muscle healing following injury. This acceleration is partly due to the inappropriate rise in IL-10 levels, creating a pro-regenerative and anti-inflammatory environment, which promotes more effective muscle regeneration in the absence of HDAC11 (Nunez-Alvarez *et al.*, 2021).

1.6.6 HDAC11 in Cancer

HDAC11 is upregulated in various cancers and plays a significant role in tumor development, influencing cell proliferation, differentiation, apoptosis, migration, stemness, immune evasion, and therapeutic tolerance (Liu *et al.*, 2023). These processes are mediated through signaling

pathways such as AMPK and JAK/STAT. The involvement of HDAC11 in cancer is multifaceted and varies across different cancer types. For instance, HDAC11 enhances cell invasion and migration in esophageal squamous cell carcinoma (Yang *et al.*, 2022), while in colorectal cancer (Mármol *et al.*, 2017) and non-small-cell lung cancer (Gridelli *et al.*, 2015), it inhibits these processes. Additionally, HDAC11 has dual roles in hepatocellular carcinoma (HCC) (Wang *et al.*, 2020) and breast cancer (Leslie *et al.*, 2019), affecting cell invasion and migration differently (**Figure 6**).

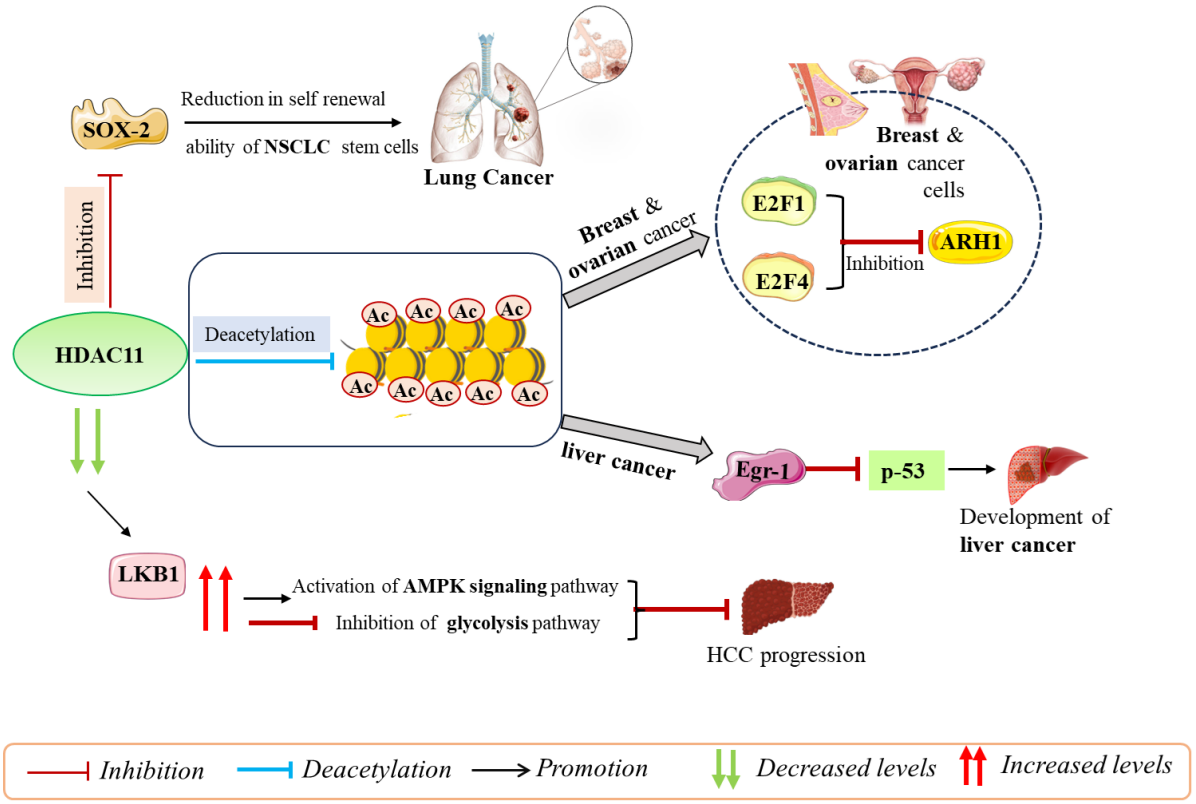

Figure 6: HDAC11's involvement in many cancer types. LKB1, liver kinase B1; AMPK, AMP-activated protein kinase; NSCLC, non-small cell lung cancer; ARH1, ADP-ribosylhydrolase 1; EGR1, Early Growth Response Protein 1.

In the context of tumor immunity, HDAC11 acts as a "gatekeeper" of immune cell demise and regulates various immune cells, including neutrophils, CD8+ T cells, macrophages, natural killer cells, T-helper 1 (Th1) cells, and bone marrow-derived suppressor cells (Kirchner *et al.*, 2021). Deficiency in HDAC11 leads to cell death and suppresses metabolic processes in ovarian (SK-OV-3), colon (HCT-116), prostate (PC-3), and breast (MCF-7) cancer cell lines (Deubzer *et al.*, 2013). Aiming HDAC11 might be beneficial for treating HCC and overcoming resistance to kinase inhibitors, as HDAC11 decreases Liver Kinase B1 (LKB1) expression in HCC, promoting progression and cancer stemness (Bi *et al.*, 2021). Recent studies (Yang *et*

al., 2024) indicate that inhibiting or depleting HDAC11 significantly reduces the self-renewal capacity of cancer stem cells in non-small-cell lung cancer and diminishes the expression of SOX-2, essential for cancer stem cell maintenance. HDAC11 has been observed to inhibit SOX2 production through GLI1, a transcription factor in the Hedgehog pathway (Bora-Singhal *et al.,* 2020).

Silencing HDAC11 decreases protein deacetylation, enhances the apoptotic response to mitogen-activated protein kinase inhibitors (MEKi), and inhibits proliferation in various uveal melanoma cell lines during long-term colonization experiments (Sriramareddy *et al.,* 2022). HDAC11 is also thought to negatively affect liver cancer cell death by suppressing the p53 gene (Gong *et al.,* 2019). Higher HDAC11 expression is associated with improved overall survival in breast cancer patients, making HDAC11 a potential prognostic marker due to its partial inhibition of breast cancer cell invasion and proliferation (Zhao *et al.,* 2023).

Li *et al.* discovered that HDAC11 is abnormally expressed in 25 different cancer types, with its expression either positively or negatively correlated with prognosis. HDAC11 may have a suppressive role in cancers such as kidney renal papillary cell carcinoma, brain lower-grade glioma, rectum adenocarcinoma, kidney renal clear cell carcinoma, pheochromocytoma and paraganglioma, and uveal melanoma, challenging the notion that HDAC11 functions universally as an oncogene (Li *et al.,* 2022). Currently, few highly selective inhibitors target HDAC11 with precision, and the low selectivity of existing HDAC inhibitors often results in dose-dependent toxicities. Cancer remains a critical target for HDAC11 research, with significant potential for future investigations.

1.7 Inhibitors of HDAC11

The development of selective HDAC11 inhibitors is still in its nascent stages compared to inhibitors for other HDAC family members. However, some promising compounds have been identified:

1.7.1 Hydroxamic Acids

These compounds are common in many HDAC inhibitors and have shown potential in inhibiting HDAC11. Hydroxamic acids can chelate the zinc ion in the active site of HDAC11, leading to effective inhibition.

- **SAHA:** Suberoylanilide Hydroxamic Acid (SAHA), also known as Vorinostat, is a well-known HDAC inhibitor approved for treating cutaneous T-cell lymphoma. SAHA is a pan-HDAC inhibitor that can inhibit multiple HDAC enzymes, including Class I and II HDACs.

While SAHA is primarily known for its broad-spectrum inhibition of HDACs, its role in inhibiting HDAC11 is of particular interest due to the unique biological functions and therapeutic potential associated with HDAC11 inhibition (Auzzas *et al.*, 2010).

- **FT895:** FT895 is an emerging HDAC inhibitor under investigation for its potential therapeutic applications, particularly in cancer treatment. These inhibitors work by blocking the activity of HDAC enzymes, leading to increased acetylation of histones, which can result in altered gene expression, cell cycle arrest, apoptosis, and enhanced immune responses. This novel compound has demonstrated promising selectivity and efficacy in preclinical studies, representing a significant step forward in HDAC11 inhibitor development (Martin *et al.*, 2018).
- **Elevenostat:** Elevenostat represents a promising advancement in the field of selective HDAC11 inhibition, with potential therapeutic applications in cancer, immune regulation, and neurological disorders. While still in the early stages of development, ongoing research and development efforts are expected to further elucidate the therapeutic potential of Elevenostat, paving the way for new treatment strategies targeting HDAC11 (Kutil *et al.*, 2019).
- **MIR002:** MIR002 is a small molecule inhibitor specifically designed to target HDAC11. As a novel HDAC11 inhibitor, MIR002 represents a significant advancement in the development of selective inhibitors aimed at regulating the activity of this particular enzyme (Chen *et al.*, 2020).
- **Trichostatin A:** Trichostatin A is a valuable HDAC inhibitor with significant effects on HDAC11, among other HDACs. Understanding TSA's impact on HDAC11 is crucial for advancing our knowledge of HDAC biology and developing targeted therapies for diseases involving HDAC11 dysregulation (Auzzas *et al.*, 2010).
- **Quisinostat:** Quisinostat (JNJ-26481585) is a second-generation hydroxamic acid-based HDAC inhibitor. It is known for its potent and broad-spectrum activity against multiple HDACs, with a particular emphasis on its efficacy in cancer therapy due to its ability to induce cell cycle arrest, differentiation, and apoptosis in cancer cells. Further research is needed to fully understand Quisinostat's specific effects on HDAC11 and optimize its therapeutic applications (Arts *et al.*, 2009).
- **Belinostat (PXD101):** Belinostat (PXD101) is a pan-HDAC inhibitor belonging to the hydroxamic acid class. It is approved for treating peripheral T-cell lymphoma (PTCL) and

is being investigated for other types of cancers due to its ability to induce apoptosis, cell cycle arrest, and differentiation in malignant cells.

Its inhibition of HDAC11 contributes to its therapeutic effects in cancer treatment, particularly in inducing apoptosis and modulating immune responses. Further studies on Belinostat's specific interaction with HDAC11 will enhance our understanding of its mechanisms and therapeutic potential (Rana *et al.,* 2020; Li *et al.,* 2016).

- **Aes-135:** Aes-135 is a novel HDAC inhibitor that has shown potential in targeting HDAC11. HDAC inhibitors work by blocking the activity of HDAC enzymes, leading to increased acetylation of histone proteins, which can alter gene expression, inhibit cell proliferation, and induce apoptosis. Aes-135 is a promising selective HDAC inhibitor targeting HDAC11. Its ability to inhibit HDAC11 specifically positions it as a potential candidate for targeted cancer therapy and other diseases where HDAC11 plays a crucial role. Further research on Aes-135 will enhance our understanding of HDAC11 and optimize its therapeutic applications (Shouksmith *et al.,* 2019).
- **Fimepinostat:** Fimepinostat is a potent dual inhibitor of HDACs, including HDAC11, and PI3Ks. Its inhibition of HDAC11 contributes to its anti-cancer effects, promoting apoptosis and disrupting cancer cell proliferation. Fimepinostat’s dual action enhances its therapeutic potential, making it a promising candidate for targeted cancer therapies and further research into the specific roles of HDAC11 in disease (Cheshmazar *et al.,* 2022; Kutil *et al.,* 2019).
- **Dacinostat:** Dacinostat is a powerful HDAC inhibitor with broad-spectrum activity, including inhibition of HDAC11. Its ability to target HDAC11 contributes to its therapeutic effects in cancer treatment, particularly by inducing apoptosis and modulating immune responses (Auzzas *et al.,* 2010).
- **Pracinostat:** Pracinostat is an influential HDAC inhibitor with broad-spectrum activity, including targeting HDAC11. Its inhibition of HDAC11 enhances its therapeutic effects in cancer treatment by promoting apoptosis, regulating immune responses, and influencing metabolic pathways. Continued research into Pracinostat's specific interactions with HDAC11 will improve our understanding of its mechanisms and refine its therapeutic use (Kutil *et al.,* 2019; Rana *et al.,* 2020).
- **Panobinostat:** Panobinostat, also known as LBH589, is a potent pan-HDAC inhibitor that includes HDAC11 in its spectrum of targets. It is primarily used in the treatment of multiple myeloma, particularly in patients who have not responded to other treatments. By inhibiting

HDAC activity, Panobinostat alters gene expression, leading to anti-proliferative and pro-apoptotic effects in cancer cells (Li *et al.*, 2014).

1.7.2 Benzamides and Thiols

These chemical classes have also been explored for HDAC11 inhibition. They offer an alternative to hydroxamic acids, potentially providing different selectivity profiles and pharmacokinetic properties.

- **Mocetinosta:** Mocetinostat, also known as MGCD0103, is an orally bioavailable inhibitor of HDACs, with a preference for Class I and IV HDACs. It has shown promise in the treatment of various hematological malignancies and solid tumors. By inhibiting HDACs, Mocetinostat induces changes in gene expression that can lead to anti-tumor effects (Rana *et al.*, 2020; Zhou *et al.*, 2008).

1.7.3 Cyclic peptides

Cyclic peptides are a class of peptides characterized by a circular structure, which is formed through peptide bonds between the amino and carboxyl termini or through side-chain linkages. This cyclic structure imparts unique stability and binding properties, making cyclic peptides an attractive scaffold for drug development. Their enhanced stability, resistance to proteolytic degradation, and ability to bind to protein targets with high affinity have positioned them as potential therapeutics, including inhibitors of HDACs (Olsen *et al.*, 2009).

- **TD034:** TD034 is a small molecule inhibitor designed to target histone deacetylases (HDACs). While it is primarily recognized for its inhibitory action on HDAC11, it may also exhibit effects on other HDACs to a lesser extent. HDAC inhibitors, such as TD034, are of significant interest in the field of oncology and other therapeutic areas due to their ability to modulate gene expression and cellular functions (Ho *et al.*, 2023).
- **Romidepsin:** Romidepsin, also known as Istodax or FK228, is a potent HDAC inhibitor approved for the treatment of cutaneous T-cell lymphoma (CTCL) and peripheral T-cell lymphoma (PTCL). It is a cyclic peptide that selectively inhibits Class I HDACs, including HDAC1, HDAC2, HDAC3, and HDAC8, leading to the re-expression of silenced genes that regulate cell cycle arrest and apoptosis in cancer cells. Although Romidepsin primarily targets Class I HDACs, its inhibitory effects also extend to HDAC11. While challenges such as selectivity and resistance need to be addressed, the development of Romidepsin and similar inhibitors holds promise for advancing targeted therapies in oncology and beyond (Yao *et al.*, 2015).

- **Trapoxin A:** Trapoxin A is a naturally occurring cyclic tetrapeptide that functions as a potent HDAC inhibitor. It was originally isolated from the culture broth of the fungus *Helicoma ambiens*. Trapoxin A is well-known for its ability to inhibit HDACs irreversibly, leading to increased acetylation of histones and subsequent changes in gene expression. While Trapoxin A is a broad-spectrum HDAC inhibitor, its effects on HDAC11 have garnered significant interest. Trapoxin A inhibits HDAC activity by covalently binding to the enzyme's active site, leading to the accumulation of acetylated histones. This results in a more open chromatin structure, promoting the transcription of genes involved in cell cycle regulation, apoptosis, and differentiation. The irreversible nature of Trapoxin A's inhibition provides a prolonged effect on gene expression (Furumai *et al.*, 2001; Kutil *et al.*, 2019).

1.7.4 Hydrazides

Hydrazides are a class of organic compounds characterized by the presence of the functional group -CONHNH2. They are known for their diverse biological activities and have been explored extensively in medicinal chemistry for their potential as therapeutic agents. Hydrazides have shown promising results as HDAC inhibitors, including the inhibition of HDAC11 (Carreiras *et al.*, 2024).

- **SIS7:** SIS7 is an investigational compound designed to selectively inhibit HDAC11, a protein involved in regulating gene expression, immune responses, and cellular metabolism. By targeting HDAC11, SIS7 disrupts its deacetylase activity, leading to an accumulation of acetylated proteins that alter chromatin structure and gene expression. This inhibition holds potential therapeutic benefits across various diseases. In cancer treatment, SIS7 could reduce tumor growth and induce apoptosis in cancer cells with high HDAC11 expression. Inflammatory diseases may benefit from SIS7's ability to modulate immune responses and reduce inflammation. Additionally, by impacting neuronal function and neuroinflammation, SIS7 shows promise for neurodegenerative disorders like Alzheimer's and Parkinson's. Despite its potential, SIS7 faces challenges related to achieving high selectivity for HDAC11 over other HDACs and ensuring safety and efficacy through rigorous preclinical and clinical studies. Ongoing research is necessary to optimize SIS7 and validate its therapeutic benefits (Son *et al.*, 2019).
- **SIS17 -** SIS17 is a compound under investigation for its potential to inhibit HDAC11. HDAC11 is a key enzyme involved in regulating gene expression, cellular metabolism, and immune responses. Its inhibition by specific compounds like SIS17 is of significant interest

for therapeutic development, particularly in cancer, inflammatory diseases, and neurodegenerative disorders (Son *et al.*, 2019).

Table 1. Different HDAC11 inhibitors along with their chemical class, inhibitory activity in different HDAC isoforms and clinical status.

HDAC11*is*	**HDACs IC_{50} (nM)**											**Clinical Status**	**Ref**
	11	**1**	**2**	**3**	**4**	**5**	**6**	**7**	**8**	**9**	**10**		
CYCLIC PEPTIDES													
Trapoxin A 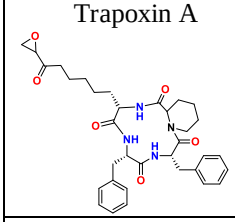	10	0.82					524					—	(Furumai et al., 2001; Kutil et al., 2019)
Romidepsin 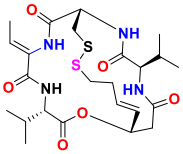	*a*	1050	6070	62	*a*	*a*	1220	*a*	*a*	*a*	11	Completed ClinicalTrials.gov ID – NCT02850016	(Yao et al., 2015)
TD034* 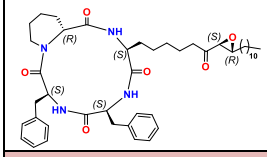	5.1	-	-	-	-	-	-	-	-	-	-	—	(Ho *et al.*, 2023)
BENZAMIDES													
Mocetinostat 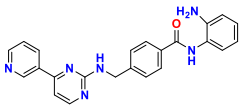	590	150	290	1660	*a*	*a*	-	*a*	*a*	-	-	Phase II ClinicalTrials.gov ID - NCT02236195	(Rana et al., 2020; Zhou et al., 2008)
HYDRAZIDES													
SIS7* 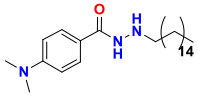	910,760	-	-	-	-	-	-	-	-	-	-	—	(Son et al., 2019)
SIS17* 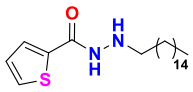	830, 270	-	-	-	-	-	-	-	-	-	-	—	(Son et al., 2019)
HYDROXAMIC ACIDS													
SAHA 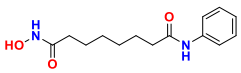	362	258	921	350	493	378	28.60	344	243	316	456	Completed ClinicalTrials.gov ID-NCT01319383	(Auzzas et al., 2010)
Trichostatin A	15.15	7.12	22.95	10.32	12.07	16.48	0.42	22.46	89.53	38.12	20.10	Phase I ClinicalTrials.gov ID-NCT03838926	(Furumai et al., 2001; Kutil et al.,

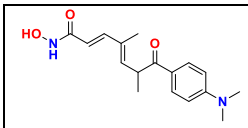													2019)
Quisinostat 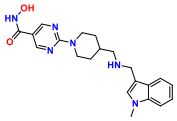	0.37	0.11	0.33	4.86	0.64	3.69	76.8	119	4.26	32.1	0.46	Phase II ClinicalTrials.gov ID-NCT01486277	(Arts et al., 2009)
Belinostat (PXD101) 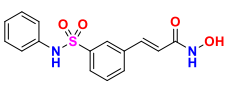	25,000	41	125	30	115	-	82	67	216	128	-	Completed ClinicalTrials.gov ID-NCT01583777	(Rana et al., 2020; Li et al., 2016)
Aes-135 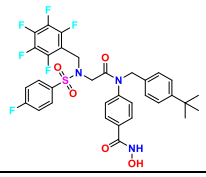	636	-	-	654	-	-	190		*b*	-	-	—	(Shouksmith et al., 2019)
Fimepinostat 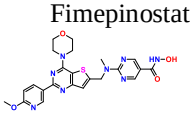	23	1.7	5	1.8	-	-	-	-	-	-	2.8	Phase II ClinicalTrials.gov ID-NCT05971758	(Cheshmazar et al., 2022; Kutil et al., 2019)
Dacinostat 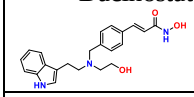	5.58	3.23	15.70	10.50	5.82	5.58	5.93	6.11	3.84	8.24	8.41	—	(Auzzas et al., 2010)
Pracinostat 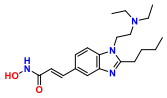	93	49	96	43	56	47	1008	137	140	70	40	Phase II ClinicalTrials.gov ID-NCT03151304	(Kutil et al., 2019; Rana et al., 2020)
Panobinostat 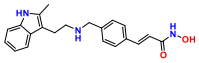	2.7	2.5	13.3	2.1	203	7.8	10.5	531	277	5.7	2.3	Completed ClinicalTrials.gov ID-NCT01680094	(Li et al., 2014)
MIR002* 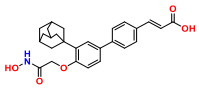	6090	-	-	-	-	-	-	-	-	-	-	—	(Chen et al., 2020)
FT895* 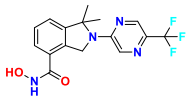	3	*a*	*a*	*a*	*a*	*a*	*a*	*a*	5600	*a*	*a*	—	(Martin et al., 2018)
Elevenostat* 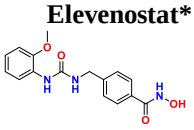	235	-	-	-	-	-	-	-	-	-	-	—	(Kutil et al., 2019)

* Indicates selective HDAC11 inhibitors as reported by Ho *et al.*, 2023, Chen *et al.*, 2020, Dallavalle *et al.*, 2022, Martin *et al.*, 2018, and Son *et al.*, 2019. (*a* indicates IC50 > 10,000 nM, and *b* indicates IC50 > 1000 nM).

Chapter 2: Literature Review

Chapter 2: Literature Review

There is no molecular modeling analysis on HDAC11, so we are reporting some review articles and research articles based on synthesis. In this scenario, we want to give more emphasis on drug discovery and biological investigations.

2.1 Son *et al.* (**2020**) represented a significant breakthrough in understanding the mechanism of action of Garcinol. It provides a natural product-derived lead that could be further optimized to enhance its potency and specificity. The observed similarities between the phenotypes of Garcinol treatment and HDAC11 knockout in mouse models further support this hypothesis. The authors discovered that Garcinol is a potent and selective inhibitor of HDAC11, with an IC_{50} of approximately 5 μM in vitro and 10 μM in cellular assays. The discovery of Garcinol as a potent and selective HDAC11 inhibitor opens new avenues for developing natural product-derived therapeutic agents for various diseases, including obesity, diabetes, and multiple sclerosis. It underscores the importance of continued research into the molecular mechanisms of natural products and their potential therapeutic applications. This discovery not only provides a new lead for the development of HDAC11 inhibitors but also offers a deeper understanding of the biological activities of Garcinol (Son *et al.,* 2020).

2.2 Baek *et al*. (**2023**) introduced a novel HDAC inhibitor, compound 5, which selectively targets HDAC11. HDACs are enzymes that regulate gene expression and cellular processes, with HDAC11 being highly expressed in the brain and immune cells. The study demonstrates that compound 5 can significantly alleviate depression-like behaviors in mice by inhibiting microglial activation and inducing autophagy. Microglia are immune cells in the central nervous system that play a crucial role in neuroinflammation, which is implicated in depressive disorders. By targeting HDAC11, inhibitor 5 effectively suppresses the production of nitric oxide, a key mediator of neuroinflammation, and induces autophagy in microglial cells. This dual action of inhibiting microglial activation and enhancing autophagy makes HDAC11 a promising therapeutic target for treating depressive disorders. The research provides new insights into the molecular mechanisms underlying depression and opens new avenues for the development of targeted therapies for various neuropsychiatric diseases (Baek *et al.,* 2023).

2.3 Huang *et al*. (**2017)** investigated the role of HDAC11 in enhancing the function of Foxp3+ T-regulatory (Treg) cells, particularly in the context of transplantation and autoimmune diseases. By using mice with constitutive or conditional deletion of HDAC11 within Foxp3+

Treg cells and employing small molecule HDAC11 inhibitors in allograft models, the researchers demonstrate that targeting HDAC11 can significantly boost Treg function and suppress allograft rejection. The findings suggest that HDAC11-selective inhibitors may offer new therapeutic options for managing transplantation and autoimmune diseases, by enhancing the suppressive activity of Tregs and promoting long-term allograft survival (Huang *et al.* (2017).

Tian *et al.* (**2017**) presented a novel method for assaying slow-binding inhibitors against the unstable protein HDAC11, a poorly studied member of the human HDAC family. By employing the fast-binding inhibitor SAHA as a chaperone molecule, the researchers stabilized HDAC11, significantly reducing the protein's activity loss from 40% to less than 10% over a 3-hour period. This stabilization allowed for a more accurate determination of the inhibitory capacity of the benzamide HDAC inhibitor MS275, with the true IC_{50} being established at 0.65 μM. The optimized assay conditions were then applied to a one-dose screening assay, revealing that several benzamide derivatives showed moderate inhibition strength against HDAC11, which would have been missed using traditional methods. This approach not only enhances the accuracy of HDAC11 inhibitor assays but also improves the discovery of potential inhibitors, particularly in the hit-discovery stage (Tian *et al.,* 2017).

Sui *et al.* (**2020**) investigated the role of HDAC11 in mouse oocyte maturation, revealing that HDAC11 inhibition disrupts meiosis progression, spindle organization, chromosome alignment, kinetochore-microtubule attachment, and spindle assembly checkpoint (SAC) function. The inhibition also increases the acetylation levels of H4K16 and α-tubulin, suggesting that HDAC11 promotes meiotic apparatus assembly by modulating these acetylation statuses. The findings underscore the importance of HDAC11 in ensuring accurate chromosome segregation during oocyte meiosis, providing insights into the regulatory mechanisms of meiosis and potential pathways for modulating meiotic apparatus assembly (Sui *et al.,* 2020).

Villagra *et al.* (**2009**) examined the function of HDAC11 in the regulation of interleukin 10 (IL-10) expression within antigen-presenting cells (APCs) and its effect on the immune system's decision between activation and tolerance. The authors demonstrate that HDAC11 negatively regulates IL-10 expression, with overexpression leading to decreased IL-10 and increased inflammatory responses, capable of priming naive T cells and reversing tolerance in

CD4+ T cells. Conversely, disrupting HDAC11 results in higher IL-10 expression and reduced antigen-specific T-cell responses. The study also shows that HDAC11 interacts with the distal segment of the IL-10 promoter, influencing its transcriptional activity through changes in histone acetylation and transcription factor binding. These findings identify HDAC11 as a key molecule in the balance between immune tolerance and activation, with potential implications for treating autoimmune diseases, managing transplant rejection, and enhancing cancer immunotherapy (Villagra *et al.,* 2009).

Baselious *et al.* (**2023**) explored the application of AlphaFold models in drug discovery, focusing on HDAC11, an enzyme with potential therapeutic implications for cancer and other diseases. Despite the lack of a crystal structure for HDAC11, the authors successfully optimized an AlphaFold model by incorporating a catalytic zinc ion and assessed its reliability through docking simulations with known inhibitors. Molecular dynamics simulations confirmed the stability of the optimized model and its complexes with various inhibitors. The study demonstrates that the optimized HDAC11 model can be utilized for structure-based drug design, emphasizing the potential of AlphaFold in aiding drug discovery efforts, even for proteins with limited structural data (Baselious *et al.*, 2023).

Baselious *et al.* (**2024**) demonstrate the successful application of an optimized AlphaFold protein model for the design of a novel and selective inhibitor targeting HDAC11, which has potential implications for treating neuroblastoma. The authors address the challenge of using AlphaFold models in drug discovery, particularly in the absence of ligands and cofactors, by refining the HDAC11 model and employing it to predict the binding mode of a known inhibitor, FT895. Based on this prediction, they design and synthesize a series of compounds, with one compound, 5a, showing the most promise, having an IC_{50} of 365 nM for HDAC11 and displaying selective inhibition. Molecular docking and dynamics simulations validate the predicted binding mode of compound 5a, which also exhibits anti-neuroblastoma activity with an EC_{50} of 3.6 µM. The research signifies the potential of optimized AlphaFold models in guiding the development of novel therapeutic agents, particularly for cancer targets like HDAC11 (Baselious *et al.*, 2024).

Chapter 3: Rationale Behind the Study

Chapter 3: Rationale Behind the Study

HDAC11 plays a crucial role in various diseases, including cancer, neurodegenerative disorders, and inflammatory conditions (Amin *et al.,* 2023; Yoon *et al.,* 2016; Sardar *et al.,* 2024; Bhattacharya *et al.,* 2023; Khatun *et al.,* 2024). However, creating selective inhibitors for HDAC11 is challenging due to the necessity to distinguish its activity from other HDAC family members.

The significance of HDAC11 inhibition is underscored by its involvement in modulating gene expression, immune responses, and key cellular processes such as apoptosis and differentiation. Overexpression of HDAC11 is linked to several pathological conditions, including tumor progression and inflammation (Bagchi *et al.,* 2018; Chen *et al.,* 2022; Chen *et al.,* 2020; Liu *et al.,* 2009; Todd *et al.,* 2010). Developing specific HDAC11 inhibitors could offer new therapeutic options for these diseases. However, achieving selectivity is a major challenge, as many current HDAC inhibitors affect multiple HDAC isoforms, leading to potential off-target effects and toxicity. A classification-based binary-QSAR model is proposed to help identify and optimize inhibitors with high specificity for HDAC11, thereby minimizing unwanted side effects.

Binary-QSAR models are essential in drug discovery as they elucidate the relationship between molecular structure and biological activity. These models predict the inhibitory potential of new compounds based on their molecular fingerprints, facilitating the design of more effective and selective inhibitors. By employing a classification-based approach, researchers can gain insights into the structural features contributing to HDAC11 inhibition, leading to the identification of key molecular determinants.

The development of a classification-based binary-QSAR model for HDAC11 inhibition could significantly advance drug discovery efforts. It offers a systematic approach to screen and optimize potential inhibitors, improving the efficiency of the drug development process. This approach aligns with current trends in computational drug design and personalized medicine, where predictive models play a crucial role in identifying and developing new therapeutic agents. Some studies such as bayesian classification, recursive partitioning, SARpy analysis, and machine learning study have been conducted to find important fingerprints for potent HDAC11 inhibitory activity. This research is valuable for studying the molecular docking of selected compounds. It provides insights into the binding mechanisms between inhibitors and their targets, helping to optimize drug design and improve binding affinity.

Chapter 4: Materials and Methods

4. Materials and Methods

4.1 Collection and preparation of data set

In this work, a total of 1191 compounds having HDAC11 inhibitory activity (IC_{50}) in nanomolar (nM) concentration was compiled from Binding Data Base also known as Binding DB (https://www.bindingdb.org/rwd/bind/index.jsp). It provides three-dimensional structures of compounds in the .sdf format. For ease of work, the "*prepare ligands for QSAR*" protocol of Discovery Studio version 3.0 (*D.S. 3.0*) (Accelrys Inc., CA, USA, 2015) was applied, removing duplicate compounds from the dataset. As a result, 382 duplicate compounds were detected and permanently removed from the dataset. The duplicate-free dataset contains a total of 809 compounds. In the next step, the duplicate-free dataset was filtered with the "*Filter using Lipinski and Verber's rule*" protocol of *D.S. 3.0* (Accelrys Inc., CA, USA, 2015) to prepare a dataset of drug-like compounds only. The protocol produced a dataset containing 712 drug-like compounds which passed Lipinski and Verber's rule (Lipinski *et al.*, 2004). Then the inhibitor's HDAC11 inhibitory activities (IC_{50}) were converted to negative logarithm values (pIC_{50}). Therefore, the activity profile of the compounds in this dataset had been segregated into binary manner, having HDAC11 inhibitory activity equal to or more than the pIC_{50} value of 6.001 ($IC_{50} \leq 1000$ nM) were labeled as '1' (*active*) whereas compounds with indefinite HDAC11 inhibitory action and activity range less than the pIC_{50} value of 6.001 ($IC_{50} \geq 1000$ nM) was labeled as '0' (*inactive*). The binarized dataset shows the number of *actives* = 307 (training=237, test=70) and the number of *inactive* compounds = 405 (training=297, test=108).

4.2 Division of Dataset

The dataset division in a justified manner is the most necessary step for any QSAR model development process. In this study, the dataset contains a large number of structurally diverse compounds (N_{set} = 712, where the highest active compound with IC_{50} = 0.3 nM and least active compound with IC_{50} = 80,020 nM). The whole dataset was divided into two distinct sets i.e., the training set and test set through the "*Generate Training and Test Data*" module in *D.S. 3.0* (Accelrys Inc., CA, USA, 2015), which were used to build and evaluate the QSAR models respectively. The dataset was divided with the "random per cluster" method based on various parameters like cluster, distance to the closest, cluster centre, and cluster size, to create the training set (which contained almost 70% of the dataset compounds) and the test sets (which contained nearly 30% of the dataset compounds). All training sets (N_{Train} = 534, **Annexure-I**) were used to build the QSAR models, which were then verified using their equivalent test set

(N_{Test} = 178, **Annexure-I**). Several molecular descriptors of the selected compounds were evaluated such as the number of aromatic rings (*nAR*), rings (*nR*), and rotatable bonds (*nRB*); molecular weight (*MW*), octanol/water partitioning coefficient (*AlogP*) and molecular fractional polar surface area (*M_FPSA*); number of hydrogen bond (*nHBD*) donors and acceptors (*nHBA*) (Amin *et al.*, 2004) as well as topological fingerprint descriptors such as extended connectivity fingerprints of diameter 6 (*ECFP_6*) (Rogers *et al.*, 2010) and functional-class fingerprints of diameter 6 (*FCFP_6*) for the modeling study in *D.S. 3.0* (Accelrys Inc., CA, USA, 2015). Further with the help of this divided dataset classification-based Bayesian classification, Recursive partitioning, and SARpy analysis were conducted. Also, the workflow of the study is illustrated in **Figure 7**.

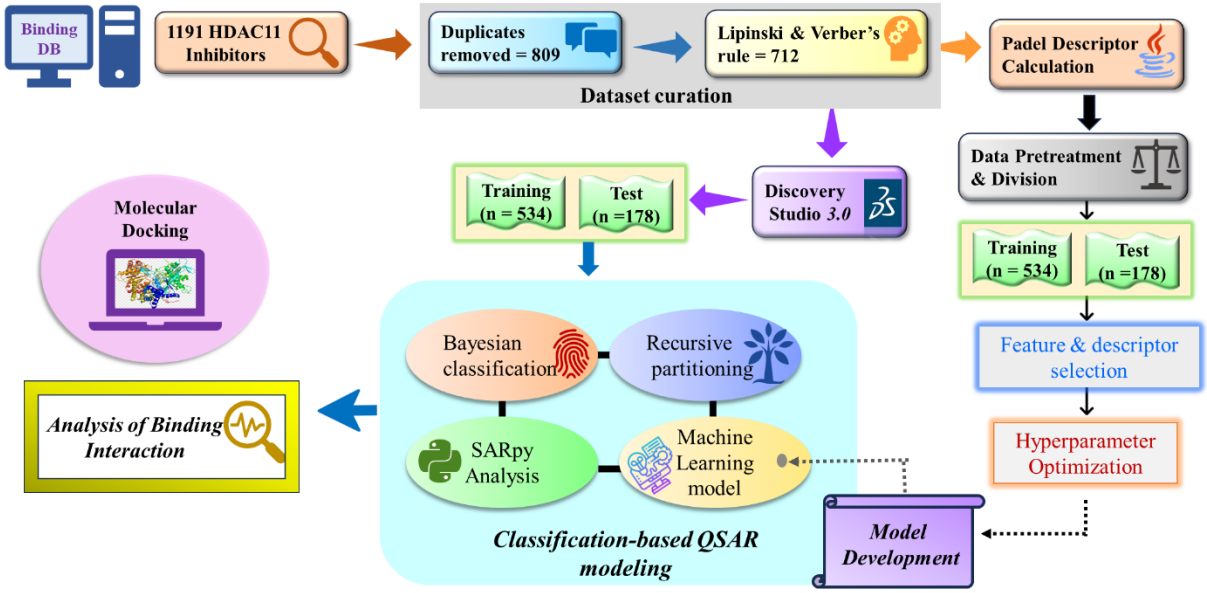

Figure 7: Overall workflow of the study

4.3 Machine learning (ML) models utilizing multiple 2D Descriptors

a. Molecular Descriptor Calculation

To perform ML modeling, the curated dataset containing 712 compounds (.sdf file format) was used for calculating *2D* descriptors through *PaDEL* software (Yap *et al.*, 2011). The *PaDEL*-Descriptor program was used to construct several classes of *2D*-descriptors, such as molecular features, electro-topochemical atom descriptors, detour matrix descriptor, auto-correlation descriptors, etc.

b. Data pre-treatment and dataset division

To ensure the accuracy of our modeling analysis, we performed data pre-treatment to remove undesired features such as missing values, constant values across all compounds, and highly inter-correlated features. We used the Java-based tool DataPreTreatmentGUI 1.2, available at http://teqip.jdvu.ac.in/QSAR_Tools/, for this purpose (Ambure *et al.,* 2015). This tool helped us eliminate descriptors with intercorrelation cut-off values above 0.85 and those with a variance cut-off below 0.0001. After pre-treating the data, we divided the dataset into a training set (N_{Train}= 534) and a test set (N_{Test}= 178) consistent with the sets used for Bayesian and Recursive models. The pre-treated training set was then used for feature selection.

c. Selection of features and model development

Before conducting classification-based modeling analysis, it is crucial to identify the essential features that accurately represent the response. Feature selection using appropriate algorithms is a significant challenge for modelers. So, we have utilized the Most Discriminating Features (*MDF*) selection tool (https://dtclab.webs.com/software-tools) to keep those features that appeared most often. Importantly, feature selection was performed exclusively on the training set, with no involvement of the test set compounds. The selected features were combined, and hyperparameter optimization was employed for building multiple classification-based ML models. These models were built using the ML classifier tool (https://sites.google.com/jadavpuruniversity.in/dtc-lab-software/home/machine-learning-model-development-guis).

d. Development of Classification-based ML models

ML entails programming computers to gather information from existing information to enhance their performance on subsequent duties, with usage in several fields like regulatory decision-making and predictive modeling (Chatterjee *et al.,* 2024; Jordan *et al.,* 2015). Subsequently, by utilizing the finalized list of selected features from the "*Feature selection*" step, various ML-based classification models were built including Random Forest Classifier (*RFC*) (Pal *et al.,* 2005), Support Vector Classifier (*SVC*) (Lau *et al.,* 2003), Logistic Regression (*LR*) (Kleinbaum *et al.,* 2002) and Linear Discriminant Analysis (*LDA*) (Xanthopoulos *et al.,* 2013). We developed ML-based models using Python-based scripts and executed them in Jupyter Notebook web tool (Kluyver *et al.,* 2016) with Anaconda Navigator version 2022.05 (https://www.anaconda.com/products/distribution) and Python version 3.10.4.

The best model for the prediction of test set compounds was selected after the related hyperparameters were optimized using the " CSL v 1.1 " tool (https://sites.google.com/jadavpuruniversity.in/dtc-lab-software/home/machine-learning-model-development-guis) by the Grid search technique utilizing 5-fold cross-validation mean squared error as the objective function in each of the ML approaches. Finally, the "*Machine Learning Classification v1.1"* tool was used to build the ML models.

e. SHAp analysis

SHapley Additive exPlanations (*SHAp*) analysis is a method used in ML to explain model predictions by assigning importance values to each feature based on their contribution to the prediction. Developed from cooperative game theory, SHAP values offer a unified approach to interpreting complex models by fairly distributing the prediction among the features. This analysis helps identify key features, understand their interactions, and enhance model transparency and trustworthiness (Mangalathu *et al.,* 2020).

This approach calculates Shapley values, which are the mean marginal contribution of every feature over all feasible combinations. The process begins by feeding the dataset into the model, and then *SHAp* gives a Shapley value to each feature, reflecting its involvement in the model's output (Štrumbelj *et al.*, 2011).

4.4 Bayesian classification study

The Bayesian classification is a statistical method that primarily utilizes probability principles (Box *et al.,* 2011) based on Bayes' theorem as indicated in *Eq. 1.*

$$P\,(h/d) = \frac{P(d/h)\,P(h)}{P(d)}; \qquad \begin{matrix} P(h/d) = Posterior\ probability \\ P(d/h) = Likelihood \\ P(h) = Prior\ belief \\ P(d) = Evidenced\ data \\ where\ h\ stands\ for\ hypothesis\ and\ d\ stands\ for\ observed\ data \end{matrix} \qquad (1)$$

The fundamental goal of Bayesian classification in our study is to identify important structural fingerprints using a probabilistic approach (Fang *et al.,* 2015). The "*Create Bayesian model*" protocol of *D.S. 3.0* (Accelrys Inc., CA, USA, 2015) involved building a Bayesian classification model on the training set molecules, comprising both calculated molecular descriptors and the extended connectivity fingerprint descriptors (Chen *et al.,* 2011). The models were then validated using the test set molecules.

4.5 Recursive partitioning (RP) study

RP is a classification-based QSAR approach that classifies dataset molecules based on their molecular features/descriptors into group/class-based groupings (Yadav *et al.,* 2022). RP generates multiple "*decision trees*" using key molecular features that separate the research samples into further smaller samples (nodes) based on whether a certain selected predictor is greater than or less than a given cut-off value (Amin *et al.,* 2022). Thus, the RP study was applied in our investigation to gather significant data and characterize HDAC11 inhibitors. RP models were built through the "*Create RP model*" module of the *D.S. 3.0* software (Accelrys Inc., CA, USA, 2015) utilizing the training set molecules (N_{Train}= 534) which were then validated using the test set compounds (N_{Test}= 178). These models depend on the combination of distinct molecular descriptors (as considered for Bayesian classification study) and *FPCP_6* (Chen *et al.,* 2011; Rogers *et al.,* 2010). Among the several models, the best RP model with the maximum discriminating capability was selected as the best RP tree model.

4.6 Statistical analysis and evaluation of QSAR-based models

To support the model's predictability and dependability, it is essential to evaluate various statistical parameters for fitness measurement and performance evaluation of the overall classification-based modeling study. In this work, to validate and justify the robustness of the QSAR models, a statistical evaluation based on the receiver operating characteristic (*ROC*)-based evaluation was exclusively examined (Fawcett *et al.,* 2005; Roy *et al.,* 2015). Both internal (ROC_{Train} and ROC_{CV}) and externally validated ROC (ROC_{Test}) scores have been examined using a test set for the developed classification-based models. The statistical models depend on some predicted values like true positive (*TP*), true negative (*TN*), false positive (*FP*), and false negative (*FN*). Similarly, the performance of the model was validated using statistical parameters including sensitivity (*Se*), specificity (*Sp*), accuracy (*Acc*), precision (*Pr*), and geometric mean (*G-means*) (Son *et al.,* 2020; Núñez-Álvarez *et al.,* 2021; Boltz *et al.,* 2019) using *Eqs 2-6*. Additionally, metrics including F1-measure (*F1*), area under the balanced accuracy ROC curve (AUC_b), Youden's index (γ), positive likelihood (ρ_+), negative likelihood (ρ_-), and Matthew's correlation coefficient *(MCC)* were calculated for both the training and test set compounds employing *Eqs 6 to 12* (Kar *et al.,* 2013; Das *et al.,* 2014; Toropova *et al.,* 2017; Toropova *et al.,* 2014).

$$Sensitivity\ (Se) = \frac{TP}{TP + FN};\ \begin{matrix} TP = Number\ of\ true\ positives \\ FN = Number\ of\ false\ negatives \end{matrix} \quad (2)$$

$$Specificity\ (Sp) = \frac{TN}{TN + FP} \tag{3}$$

$$Accuracy\ (Acc) = \frac{TP + TN}{TP + TN + FP + FN} \tag{4}$$

$$Precision\ (Pr) = \frac{TP}{TP + FP} \tag{5}$$

$$G - means = \sqrt{(Sensitivity * Specificity)} \tag{6}$$

$$F1 = \frac{2TP}{2TP + FP + FN} \tag{7}$$

$$AUC_b = \frac{Se + Sp}{2} \tag{8}$$

$$\gamma = Se - (1 - Sp); \quad \begin{array}{c} where, \quad \gamma = 0: Model\ has\ no\ discriminatory\ ability \\ (random\ classification) \\ \gamma = 1: Perfect\ discrimination\ (ideal\ classification) \end{array} \tag{9}$$

$$\rho_+ = \frac{Se}{(1 - Sp)}\ ; \quad \begin{array}{c} where,\ \rho_+ > 1: Model\ is\ more\ likely\ to\ correctly\ identify\ positive\ instances \\ \rho_+ = 1: Model\ has\ no\ discriminatory\ power \\ \rho_+ < 1: Model\ is\ less\ likely\ to\ correctly\ identify\ positive\ instances \end{array} \tag{10}$$

$$\rho_- = \frac{(1 - Se)}{Sp}\ ; \quad \begin{array}{c} where,\ \rho_- > 1: Model\ is\ more\ likely\ to\ correctly\ identify\ negativce\ instances \\ \rho_- = 1: Model\ has\ no\ discriminatory\ power \\ \rho_- < 1: Model\ is\ less\ likely\ to\ correctly\ identify\ negative\ instances \end{array} \tag{11}$$

$$MCC = \frac{(TP * TN) - (FP * FN)}{\sqrt{(TP + FP)(TP + FN)(TN + FP)(TN + FN)}}; \quad \begin{array}{c} where\ MCC\ ranges\ from - 1\ to + 1; \\ MCC = 1: Perfect\ prediction \\ MCC = 0: No\ better\ than\ random\ prediction \\ MCC = -1: Total\ disagreement\ between \\ prediction\ and\ observation \end{array} \tag{12}$$

4.7 SARpy Model

The SAR in Python (SARpy) program is a Python script based on the OpenBabel chemistry library (Banerjee *et al.*, 2022; Golbamaki *et al.*, 2016). SARpy is a QSAR technique designed to transparently discover significant molecular fragments utilizing categorized active and inactive compounds in a learning set and immediately extract a set of rules from data in a recursive manner, without the need for any previous knowledge (Ferrari *et al.*, 2013). The methodology builds molecular substructures of arbitrary complexity, and the fragments that are candidates for structural alerts are automatically chosen based on their performance in a learning set of predictions (Marzo *et al.*, 2016; Mombelli *et al.*, 2016).

The software generates substructures in a set using user-defined SMILES format depending on their likelihood ratio (LR) value and attempts to connect the specific molecular structures with their biological activity in three phases: fragmentation, evaluation, and extraction (Lombardo *et al.*, 2014).

$$\text{Likelihood ratio (LR)} = \frac{True\ positive}{False\ positive} \times \frac{negative}{positives} \quad (13)$$

LR value is a number between 1 and infinity. When the structural alert is only present in the positive observations then the LR can be regarded as infinite (inf) (Banerjee *et al.*, 2023).

In the fragmentation stage, a recursive simple fragmentation algorithm is employed to find chemical substructures in the training set molecules. It continues through each bond in the input structures, attempting to produce every possible pair of fragments (Yang *et al.*, 2017). After each substructure has been created, it is evaluated individually to look for any possible structural alerts (SA) in the evaluation step. Furthermore, to complete the process, only the reduced sets of estimated rules were applied from the collection of generated structural alerts (Baderna *et al.*, 2020). The rule sets in our present investigation were generated utilizing "OPTIMAL" single alert precision for fragments with atom numbers between 2 (minimum) and 26 (maximum) and a minimum number of 6 occurrences. Later, utilizing the SARpy software (https://www.vegahub.eu/portfolio-item/sarpy/) these generated structural alerts/active rulesets were further evaluated on the test set compounds.

4.8 Molecular Docking Analysis

Till now, the mammalian HDAC11 X-ray crystallographic structure has not been solved. So, the AlphaFold model of HDAC11 was downloaded from the AlphaFold database (https://alphafold.ebi.ac.uk/entry/B5MCU6). The zinc coordination motif of this protein was discovered by structural alignment analysis with the PDB ID: 1C3S (https://www.rcsb.org/structure/1C3S) as described in the previous research study by Baek *et al*., 2023. **Figure 8** shows that the binding motif of PDB ID: 1C3S and the Alphafold HDAC11 model is similar and can be considered an active site for molecular docking analysis with reference compound SAHA.

For molecular docking analysis, we used AutoDockZn, which is a freely available docking tool developed by Santos-Martins *et al.*, 2014 which uses a modified improved forcefield option for improvement in the performance of binding estimation and free energy calculation in case of molecular docking with zinc-specific metalloproteins. Some common initial steps of molecular processes, such as PDB to PDBQT conversion for protein and selected ligands, were done using the ADFR suite and mk-prepare.py python script of the MEEKO software package (https://pypi.org/project/meeko/). Then the tetrahedral zinc pseudo atom was added according to the protocol of the AutoDockZn. The grid box was generated (X, Y, Z dimensions of 60, spacing: 0.375 Å) by enclosing the prototype ligand SAHA and zinc ion (Grid centre: -7.605,

11.153, -9.269). Additionally, the AD4Zn.bat (specific parameter file for zinc) was added to the grid input file. Then, the grid generation (with AutoGrid4.2.7) and molecular docking (with AutoDock4) were done conventionally. Finally, the best docking pose for each compound (**A004**, **A007**, **A013**, **A053**) was selected by comparing the docked structure with the prototype compound. The 3D and 2D interactions of the compounds were analyzed with D.S. 3.0 (Accelrys Inc., CA, USA, 2015).

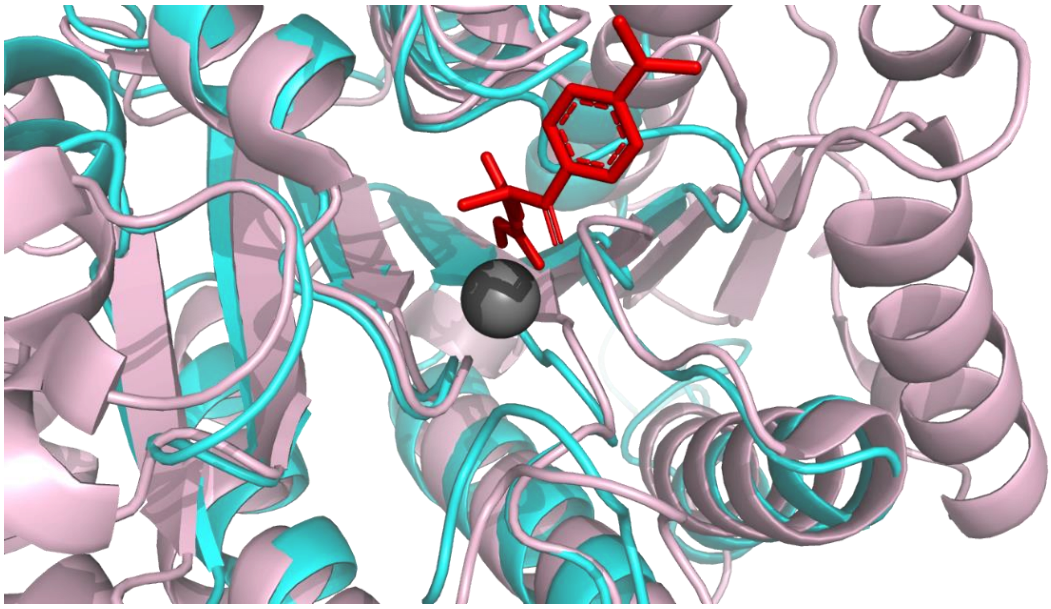

Figure 8: Structural alignment of alphafold HDAC11 model (Siam) with PDB ID:1c3s (Pink) bound with SAHA (Red). The structure showing same binding motif in both of their structure.

Chapter 5: Results and discussion

5. Results and discussion

5.1 Data Analysis

In this study, a dataset containing 712 compounds was used for the development of classification models. The dataset was split into training (N_{Train}=534) and test sets (N_{Test}=178) using the "*Random per Cluster*" method for the Bayesian and RP studies. The model was developed on the training set and validated on test set compounds. Before the model development, different molecular descriptors were calculated, including *nAR*, *nRB*, *nR*, *AlogP*, *MW*, *nHBD*, *nHBA*, *M_FPSA*, *ECFP_6*, and *FCFP_6*. In **Figure 9** multiple bin plots for physicochemical properties are illustrated, including *nAR*, *nRB*, *nR*, *AlogP*, *MW*, *nHBD*, *nHBA, and M_FPSA* for *active* and *inactive* compounds.

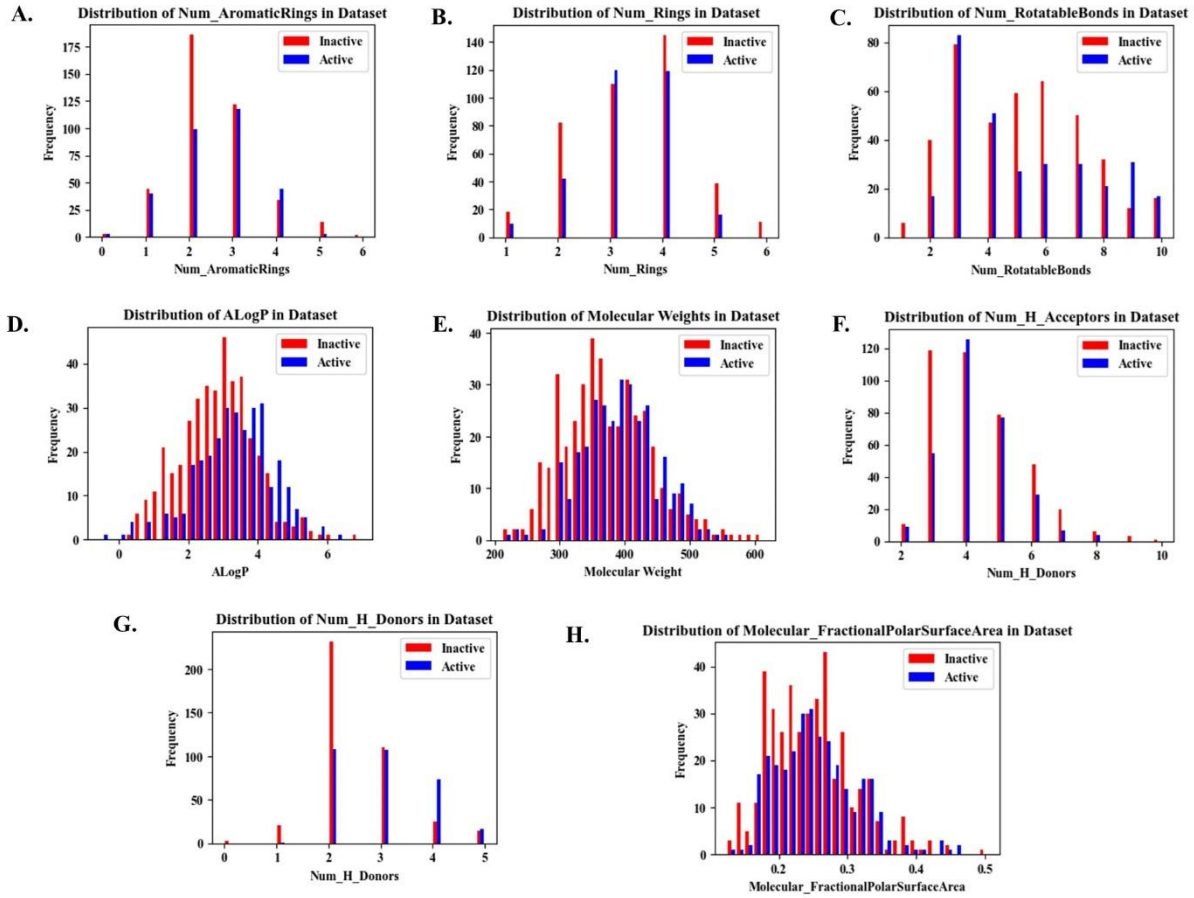

Figure 9: Distribution of HDAC11 inhibitory activity, **A.** *nAR*, **B.** *nRB*, **C.** *nR*, **D.** *AlogP*, **E.** *MW*, **F.** *nHBD*, **G.** *nHBA*, **H.** *M_FPSA*.

5.2 Machine Learning (ML)

A well-curated dataset of 712 HDAC11 inhibitors was used to build ML-based QSAR models, which included Random Forest Classifier (*RFC*), Support Vector Classifier (*SVC*), Logistic Regression (*LR*) and Linear Discriminant Analysis (*LDA*). At first, the *PaDEL*-Descriptor program was implemented to build a set of 1445 2D descriptors (Yap *et al.*, 2011). After that, the dataset was pre-treated, which yielded 496 2D descriptors, and then these descriptors were employed for model development and feature selection. Ultimately, 53 descriptors that the *MDF* tool determined to be the most discriminatory features were used to generate four classification-based ML models (*RFC*, *SVC*, *LDA*, and *LR*). The model was specified and configured through hyperparameter optimization [*RFC* (*'criterion'*: *'gini'*, *'max_depth'*: *None*, *min_samples_leaf'*: *4*, *'min_samples_split'*: *2*, *'n_estimators'*: *150*); *SVC* (*'C'*: *0.1*, *'gamma'*: *'scale'*, *'kernel'*: *'linear'*); *LR* (*'C'*: *0.1*, *'penalty'*: *None*, *'solver'*: *'lbfgs'*); *LDA* (*'solver'*: *'svd'*)] by utilizing Scikit-learn package in Python. These ML algorithms are easily available on the DTC Lab webpage (https://sites.google.com/jadavpuruniversity.in/dtc-lab-software/home/machine-learning-model-development-guis). A range of validation metrics based on classification was used to evaluate the ML models' performance. The *RFC* model with 53 descriptors turned out to be the best of them. **Table 2** presents a detailed analysis of validation outcomes using various approaches for each of the four models and **Figure 10** presents an illustration of the obtained *ROC* plots from the RFC models.

Several metrics were used to evaluate the model, including Cohen's kappa (*k*) coefficient, *F1* score, accuracy, precision, recall, and Matthews correlation coefficient (*MCC*). Specifically, the random forest (*RF*) model performed better, with an *AUC-ROC* of **0.985** for the training set and **0.831** for the test set, demonstrating adequate internal and external validation at 0.852 and 0.529, respectively. On the training set, the RF model yielded an accuracy of **0.927** and a precision of **0.934**; on the test set, it obtained an accuracy of **0.758** and a precision value of **0.651**. The training set demonstrated a specificity of **0.899** and a recall of **0.898**, while the test set showed a value of **0.828** for specificity and recall. Cohen's kappa coefficients for the training and test sets were 0.851 and 0.517, respectively. In addition, we used the RFC model to perform *SHAp* (SHapley Additive ExPlanations) analysis on the training dataset. This analysis aimed to assess each variable's (descriptor) local and global contributions to the predictions.

Table 2. Comparison of the performances of different ML models

Model Type	Set	*TP*	*FP*	*TN*	*FN*	*Acc*	*Pr*	*Sp*	*F1 score*	*Recall (Se)*	*Cohen's k*	*MCC*	*AUC-ROC*
RFC	Training	282	24	213	15	0.927	0.934	0.899	0.916	0.898	0.851	0.852	0.985
	Test	77	12	58	31	0.758	0.651	0.828	0.729	0.828	0.517	0.529	0.831
SVC	Training	242	59	178	55	0.786	0.763	0.751	0.757	0.751	0.567	0.567	0.822
	Test	77	15	55	31	0.741	0.639	0.785	0.705	0.785	0.479	0.488	0.820
LDA	Training	248	63	174	49	0.790	0.780	0.734	0.756	0.734	0.573	0.573	0.846
	Test	80	19	51	28	0.736	0.645	0.729	0.684	0.728	0.459	0.461	0.838
LR	Training	234	64	173	63	0.762	0.733	0.73	0.731	0.730	0.518	0.518	0.816
	Test	73	13	57	35	0.730	0.619	0.814	0.703	0.814	0.465	0.480	0.824

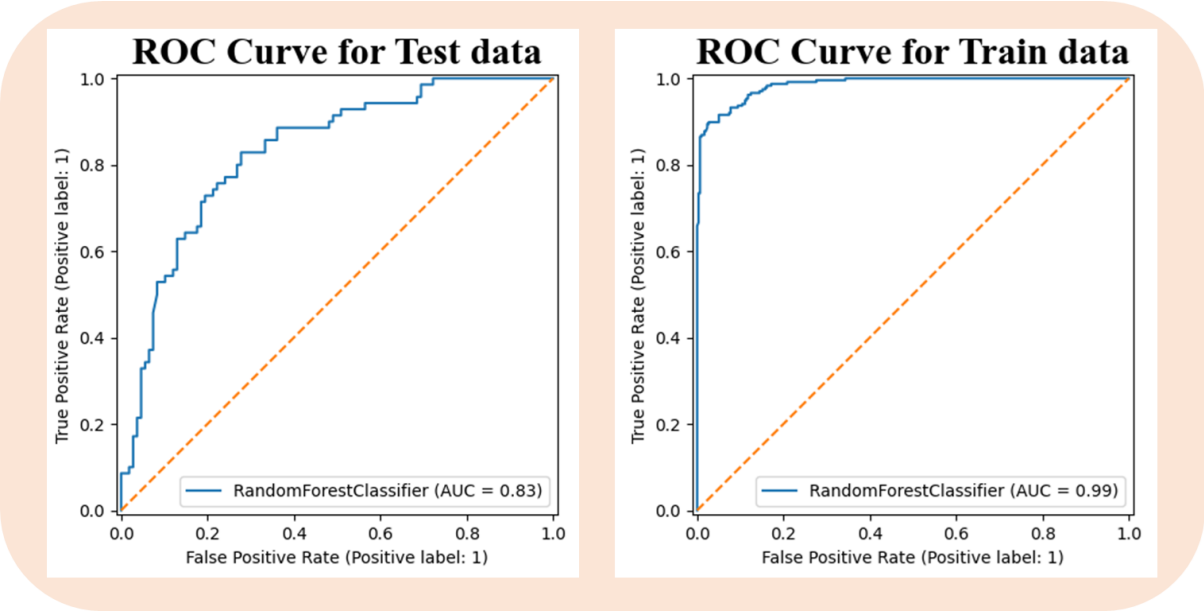

Figure 10: The *ROC* plots obtained in the RFC model

5.2.1 *Interpretation of the descriptors involved in Machine learning models*

Mechanistic interpretation is crucial for any QSAR model as per OECD Guidelines 5. The development of the final model utilizes some molecular descriptors *minHBint2, minHBint5, VE3_Dt, maxHdsCH, GATS1m, minHssNH, and minsssN* as illustrated in **Figure 11**. Understanding the contribution of these structural descriptors is essential for gaining insight into HDAC11 inhibition. Among these descriptors, *minHBint5* has the most significant impact

on HDAC11 inhibition (**Figure 12**). The *minHBint2* and *minHBint5* descriptors are 2D electro-topological state (E-state) descriptors, which represent the minimum E-State descriptors of strength for potential hydrogen bonds with path lengths of 2 (*minHBint2*) and 5 (*minHBint5*) respectively. These descriptors highlighted the relevance of hydrogen bonding with path lengths 2 and 5. Interestingly, compounds like **A043** (IC_{50} = 27 nM), **A073** (IC_{50} = 115 nM), **A117** (IC_{50} = 651 nM), and **A118** (IC_{50} = 659 nM) show both high *minHBint2* and *minHBint5* values and powerful HDAC11 inhibition, indicating that *minHBint2* and *minHBint5* positively contribute to HDAC11 inhibitory action. On the other hand, the descriptors *minHssNH* (**A117**, IC_{50} = 651 nM, **A130** = 750 nM), *maxHdsCH* (**A037** = 15 nM, **A084** = 180 nM, **A134** = 750 nM), and *minsssN* (**A046** = 31 nM, **A161** =776 nM) are also E-state fragments based on atoms that positively contribute to HDAC11 activity. These descriptors represent both the electronic and steric properties of atoms and molecules. *MinHssNH* denotes the bonding of amine groups while the feature *minsssN* refers to the >N- fragment's minimum nitrogen atom-type E-State. A high *minsssN* score indicates strong polarity and, thus, less toxicity since the presence of polar nitrogen atoms increases the hydrophilicity of molecules. In addition, *maxHdsCH* is one of the most essential descriptors for the model with only *PaDEL* descriptors. It represented the maximum atom-type H E-State: =CH-.

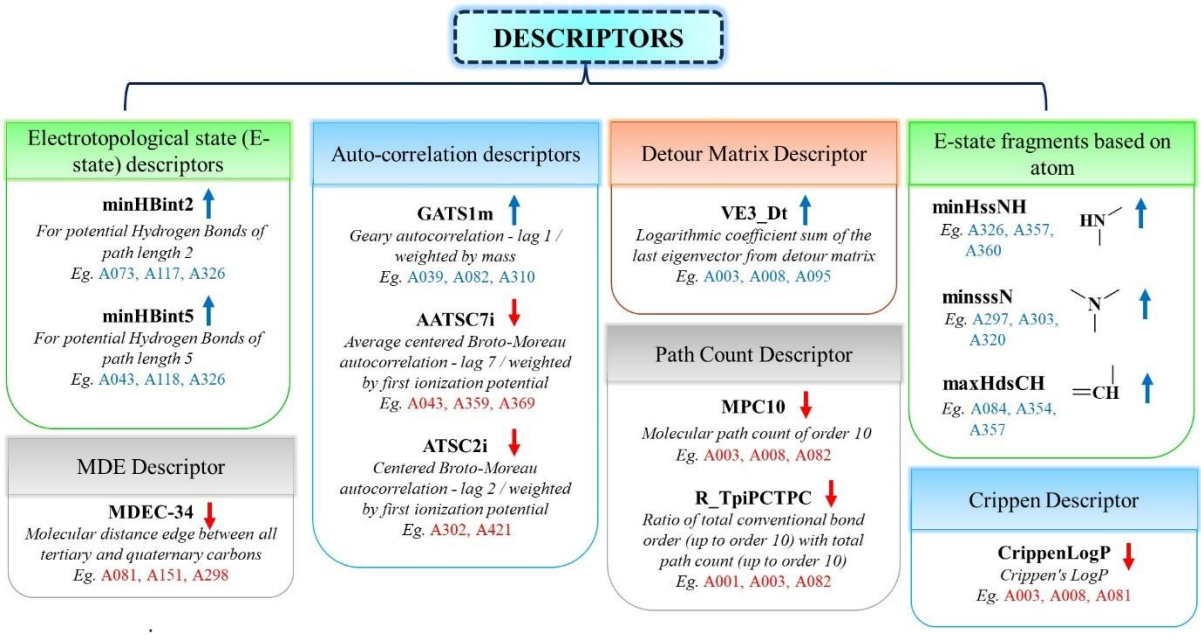

Figure 11: A summary of 13 significant descriptors used in ML models. Positive contributions are denoted by upward arrows in blue, while negative contributions are represented by downward arrows in red.

The *GATS1m* is a 2D autocorrelation descriptor that describes how a given attribute is distributed over a topological molecular structure. It defines mass distribution along a topological molecular structure. Higher values of *GATS1m* indicate increased HDAC11 activity, as observed in compounds like A**039** (IC_{50} = 21 nM), and **A082** (IC_{50} = 174 nM). Conversely, *ATSC2i* (**A630** and **A696**) and *AATSC7i* (**A691** and **A702**) contributed negatively to the HDAC11 activity. Moreover, the descriptor *VE3_Dt* denoted the logarithmic coefficient sum of the last eigenvector in the detour matrix. It has been found that *VE3_Dt* contributes positively to the HDAC11 activity, in compounds like **A003** (IC_{50} = 1 nM), and **A008** (IC_{50} = 2 nM). Furthermore, *CrippenLogP* a Crippen's LogP descriptor (**A528** and **A673**), *MDEC-34* MDE descriptor (**A586** and **A648**), *MPC10* (**A625** and **A699**) and *R_TpiPCTPC* (**A616** and **A625**) a path count descriptor each of them have a negative impact on HDAC11 activity.

5.2.2 SHAP Plots

SHapley Additive exPlanations (*SHAP*) illustrate the output of ML models. *SHAP* highlights each feature by itself and also, shows the importance of all the features together. *SHAP* is a model-nonspecific tool, organic to the application of any ML algorithm, and ensures that the sum of the *SHAP* values for each attribute is the difference between the prediction loss and the average prediction loss. To sum up, SHAP is a powerful method of increasing transparency and trust in ML models as it provides a comprehensive explanation of how each feature affects the predictions (Mangalathu *et al.*, 2020; Štrumbelj *et al.*, 2011).

These plots show the contribution of each descriptor to the prediction on the y-axis (SHAP values), with features plotted on the x-axis. Every point on the plot represents a data instance, and its colour indicates whether the feature value is high (usually blue) or low (usually red), depending on where the point falls on the x-axis. In complicated machine learning models like neural networks or tree-based models, SHAP plots help visualize the relative relevance of different features and how they contribute to individual predictions (Lundberg *et al.*, 2018). We trained the best machine learning model (*RFC*) from the dataset to investigate these visualizations.

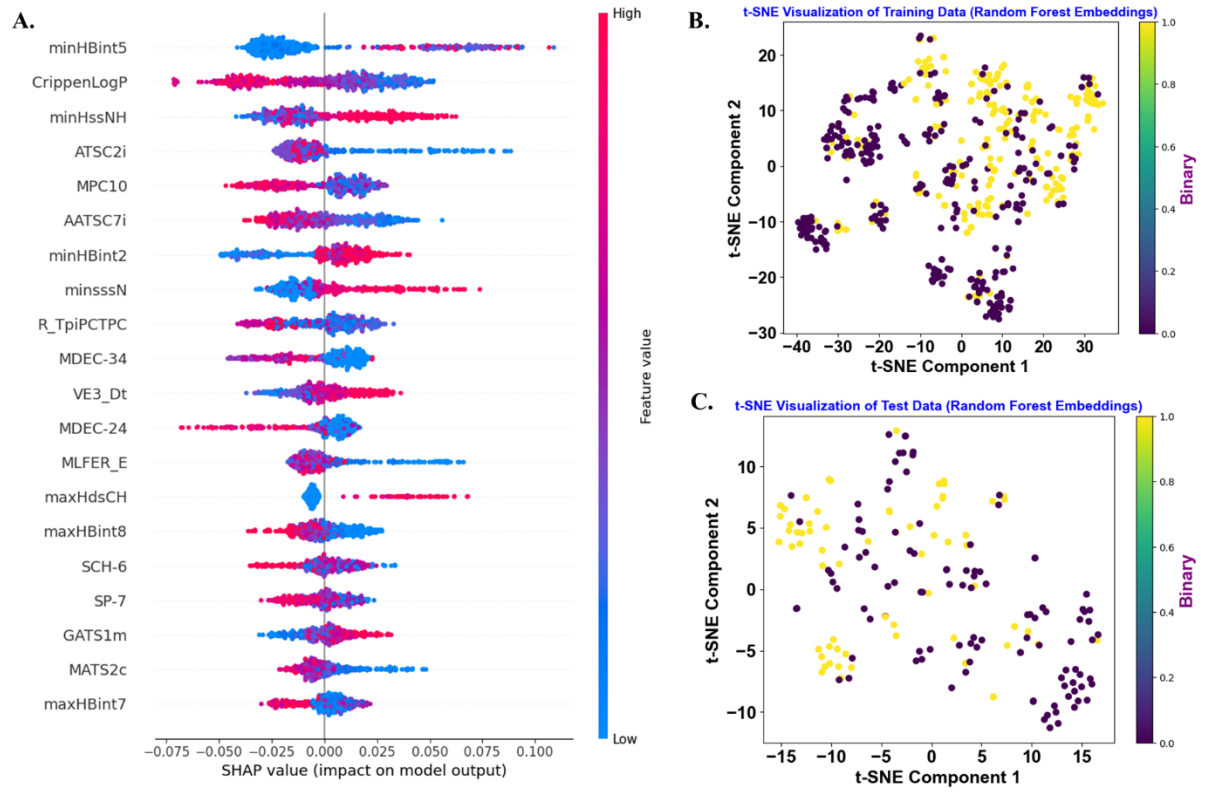

Figure 12: A. SHAP Summary plot providing a detailed overview of the directional effects of different features on the predictions for the Random Forest Classification (RFC) model. **B.** t-SNE Plot of SHAP embeddings for the training data set. **C.** t-SNE Plot of SHAP embeddings for the test data set.

5.2.3 SHAP Summary Plot

SHAP summary plots employ individual feature attributions to efficiently communicate multiple aspects of a feature's significance while maintaining the visualization simple and brief. These plots show dots representing SHAP values in a horizontal orientation, with characteristics arranged according to their total impact. The dots stack vertically in cases where there is insufficient room. The colour of each dot indicates the value of the feature, ranging from low (blue) to high (red). The colouring will exhibit a smooth transition if a feature's influence on the model varies gradually as its value changes.

The most significant element influencing the model's output at baseline is *minHBint5*, as seen in **Figure 12A**. The colouring of the *minHBint5* plot shows a smooth increase in the model's output (a log odds ratio) with higher *minHBint5* values, while the density of dots shows the frequency of different *minHBint5* values in the dataset. The pattern of dots that leans more to the right (as in the case of *maxHdsCH*) than to the left suggests that high values of these measures might considerably increase the influence on RFC. These depictions aid in

comprehending the behaviour of the model and highlighting significant characteristics that influence its evaluations. These descriptors strongly influence HDAC11 inhibitory activity.

5.2.4 t-SNE Plots

A technique for visualizing data that maps high-dimensional points to discrete locations in two or three dimensions is called t-distributed stochastic embedding, or *t-SNE*. This non-linear method of lowering complicated data dimensions is achieved by efficiently distilling the core of high-dimensional datasets and projecting them into lower-dimensional environments (Banerjee *et al.,* 2023). *t-SNE* plots showing various scenarios for the training and test set compounds are shown in **Figures 12B** and **12C**. In the first scenario (6B), *t-SNE* plots were generated for the training set of the best (RFC) model. In this instance, the data point clustering indicates total segregation. As we go to the next scenario (6C), t-SNE plots were generated for the test set of the best (RFC) model.

5.3 Bayesian Classification

The "*Create Bayesian Model*" module of *D.S. 3.0* (Accelrys Inc., CA, USA, 2015) generated the Bayesian classification model. However, the Bayesian model has been developed on a collection of 534 training set HDAC11 inhibitors and non-inhibitors using descriptors such as *nHBD, nHBA, ALogP, nRB, nR, nAR, MW,* and *M_FPSA* together with *ECFP_6* fingerprint. After analysis, it has been found that the proposed model accurately discriminated between favourable and unfavourable structural features which can be classified into distinct categories. Therefore, this approach is beneficial in identifying several essential molecular properties of diverse classes of HDAC11 inhibitors.

The results of the statistical analysis of the Bayesian classification model along with its parameter and predictive performance are discussed in **Table 3**. The developed model for both training (five-fold cross-validated, ROC_{5Cv}) and test sets demonstrated good *ROC* scores of 0.824 and 0.834 respectively, while the *ROC* plots are displayed in **Figure 13**. The training set (N_{Train}) model depicted a value of 77.2 % *Se*, 91.9 % *Sp*, 0.853 *Acc*, 0.884 *Pr*, and 0.842 *G-mean*. Similarly, in the case of external validation, the test set (N_{Test}) model also demonstrated satisfactory scores for the different statistical parameters (**Table 3**) such as 65.7 % *Se*, 79.3 % *Sp*, 0.741 *Acc*, 0.676 *Pr*, and 0.723 *G-mean*. The *G-mean* algorithm efforts to enhance the accuracy on each of the classes. Furthermore, to quantify the overall performance of the model, other measures such as the *F1*, AUC_b, *MCC*, γ, and likelihoods such as positive likelihood (ρ_+) and negative likelihood (ρ_-) were also determined. A good Youden's index (γ=0.691, N_{Train};

γ=0.453, N_{Test}) signifies a higher potential for discriminating the developed model. A higher positive likelihood score (ρ+=9.555, N_{Train}; ρ+=3.225, N_{Test}) indicates how well the model recognizes positive instances, while a lower negative likelihood value (ρ-=0.247, N_{Train}; ρ-=0.430, N_{Test}) indicates how well the model recognizes negative instances in comparison to the likelihood that it will incorrectly identify positive instances.

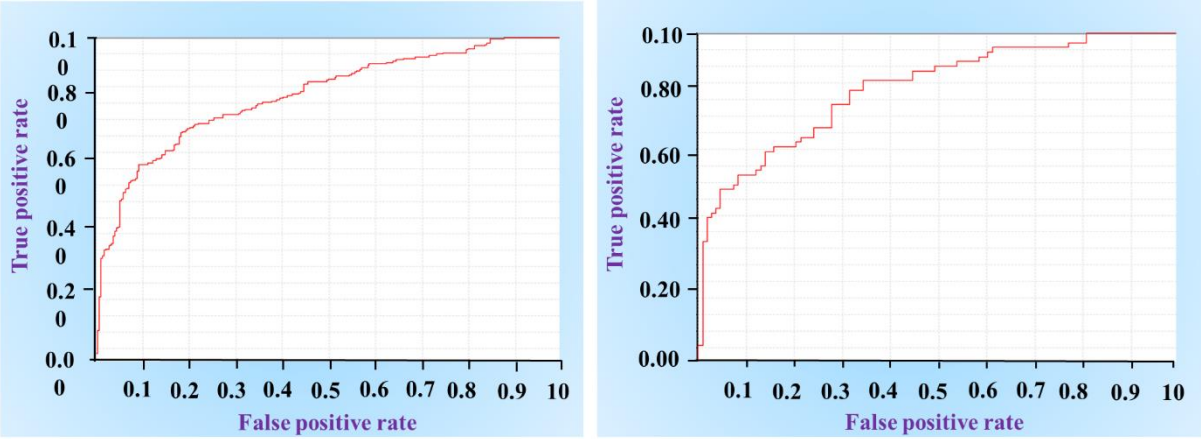

Figure 13: *ROC* plots obtained from the Bayesian model

Table 3. Validation metrics of the developed Bayesian model

Set	*ROC Score*	*ROC Rating*	*TP*	*FP*	*TN*	*FN*	*Se*	*Sp*	*Acc*	*Pr*	*G-mean*	*F1*	*AUC_b*	*MCC*	*γ*	*$ρ_+$*	*$ρ_-$*
Train#	0.824	Good	183	24	273	54	0.772	0.919	0.853	0.884	0.842	0.824	0.845	0.705	0.691	9.555	0.247
Test	0.834	Good	46	22	86	24	0.657	0.793	0.741	0.676	0.723	0.666	0.726	0.455	0.453	3.225	0.430

#5-fold cross-validation is used for the training set to evaluate the statistics, *ROC*= Receiver operating characteristics; *TP* = True positive; *FN* = False negative; *FP* =False positive; *TN* = True negative; *Se* =Sensitivity, *Sp* =Specificity, *Acc* =Accuracy, *Pr* = precision, *G-mean* = Geometric mean *F1* =F1 measure, AUC_b = area under the balanced accuracy *ROC* curve, *MCC* = Matthew's correlation co-efficient, γ = Youden's index, ρ_+ = positive likelihood, ρ- = negative likelihood.

5.3.1 Evaluation of structural fingerprints generated by a Bayesian classification model

The Bayesian classification model generated 20 favourable as well as unfavourable molecular fingerprints that may influence or hinder the HDAC11 inhibitory activities. Following the Bayesian score, the top 20 good (***G1-G20***) and bad (***B1-B20***) structural fingerprints (**Figures 14** and **16**) are taken for further identification and evaluation. The compounds having good fingerprints show significant behaviour for HDAC11 inhibitory activity.

Additionally, most of the good structural fingerprints are present in the developed compounds showing favourable activity and it has been illustrated in **Figure 15**. Similarly, the presence of fingerprint features ***G1***, ***G2***, ***G3***, ***G4***, ***G5***, ***G9***, ***G11***, ***G17***, ***G18***, ***G19***, *and* ***G20*** exhibit the favourable contribution of *benzimidazole* moiety in the biological activity of HDAC11 inhibitors for example, compound **A007** and **A008** (IC_{50} = 2 nM); **A013** (IC_{50} = 3 nM). The fragments ***G6***, ***G8***, and ***G10*** exhibit the significance of the *carboxamide* functional group present in the compound **A003** (IC_{50} = 1 nM); **A014** (IC_{50} = 3 nM); **A017** (IC_{50} =5 nM); **A053** (IC_{50} =47 nM).

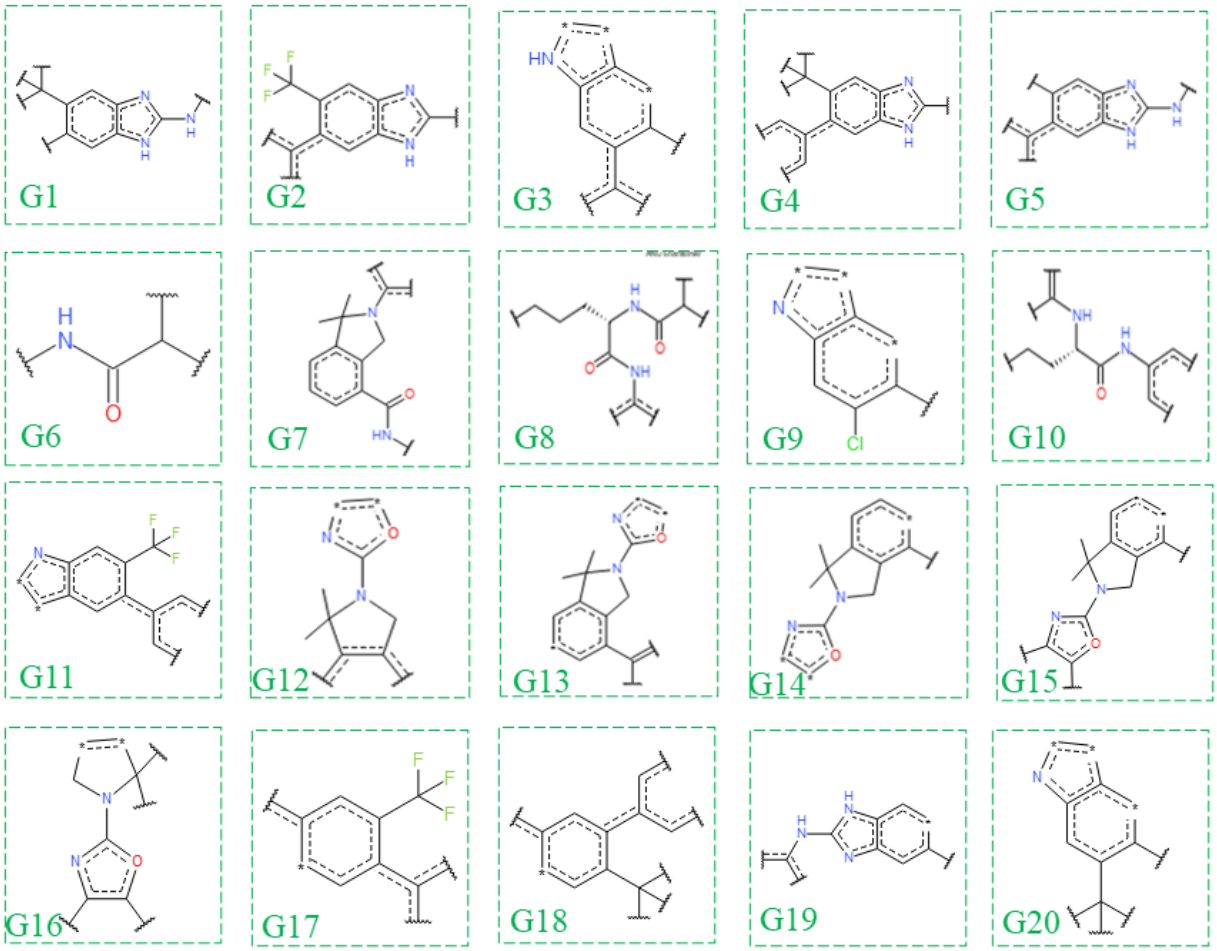

Figure 14: Top 20 favorable fingerprints identified from the Bayesian classification model

Furthermore, compounds **A004**, **A006**, **A007**, **A010**, **A012**, **A021** and **A022** with fingerprints like ***G7***, ***G12***, ***G13***, ***G14***, ***G15*** and ***G16*** exhibit a significant HDAC11 inhibitory action. Meanwhile, the mentioned fingerprints denote the existence of an *isoindoline* moiety attached to the substituted *oxazole* ring. Interestingly, some of the compounds have more than one good fingerprint such as **A004**, **A007**, **A008**, **A013**, and **A022** which revealed a clear picture, that they might be a potential candidate for HDAC11 inhibitory activity.

As a result, the Bayesian study revealed that the *benzimidazole* moiety, *carboxamide* group, and *isoindoline* moiety are essential for enhancing HDAC11 inhibitory action. Also, the study revealed certain bad fingerprints liable for HDAC11 inhibitory activity hindrances.

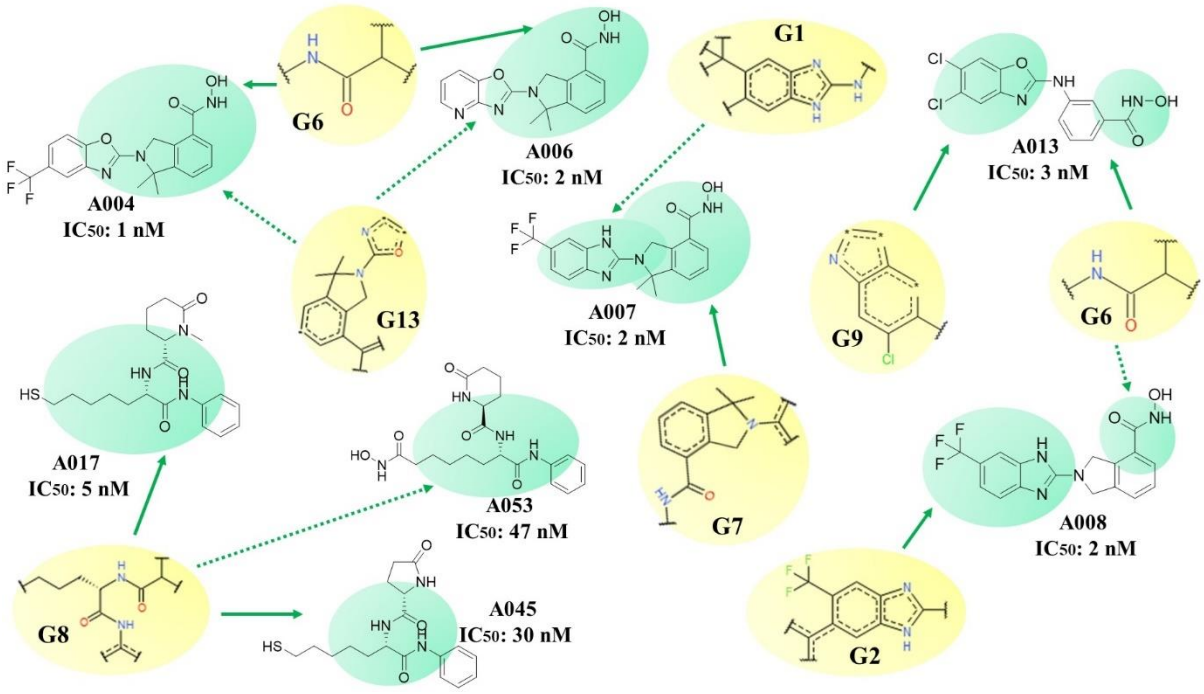

Figure 15: Molecular structures of some *active* HDAC11 inhibitors with favourable Bayesian fingerprint.

Considering the Bayesian classification of bad molecular fingerprints (***B1***-***B20***, **Figure 16**), the ***B1*** fragment makes it abundantly evident that the molecule containing the *1,3-dimethyl imidazolidine-2-one* scaffolds may not be able to boost the activity of any HDAC11 inhibitors, as it is observed in compounds **A501-A503** all exhibiting HDAC11 IC_{50} values exceeding 100,000 nM. Specifically, analogs containing *1,3-dimethyl-2,4-dimethylenehexahydropyrimidine* moiety (***B4***, ***B6***, ***B7***, ***B9***, ***B10***, ***B11***, ***B13***, ***B14*** and ***B15***) were responsible for detrimental characteristic of HDAC11 inhibition as illustrated in **Figure 17**, for example, compounds like **A237** (IC_{50} = 5686 nM); **A269** (IC_{50} = 15400 nM); **A284** (IC_{50} = 34370 nM); **A289** (IC_{50} = 52050). Additionally, ***B2*** and ***B16*** fingerprints possessing *propyl benzene* moiety, such as in compounds **A234** (IC_{50} = 5530 nM); and **A285** (IC_{50} = 37000 nM) are also responsible for poor activity. Similarly, scaffolds like *divinyl amine* having *1,3-methyl* or *ethyl* substitution in fingerprints ***B3***, ***B5***, ***B8***, and ***B12*** in compounds **A269** (IC_{50} = 15400 nM); **A289** (IC_{50} = 52050) is undesirable for HDAC11 inhibitory action. The negative fingerprint ***B17*** (**A697**, **A699**) suggests that the *1-ethyl-2,3-dimethyleneindoline* and *2-isopropyl oxazole* moiety (***B18***-***B20***) may also impede the HDAC11 inhibitory activities.

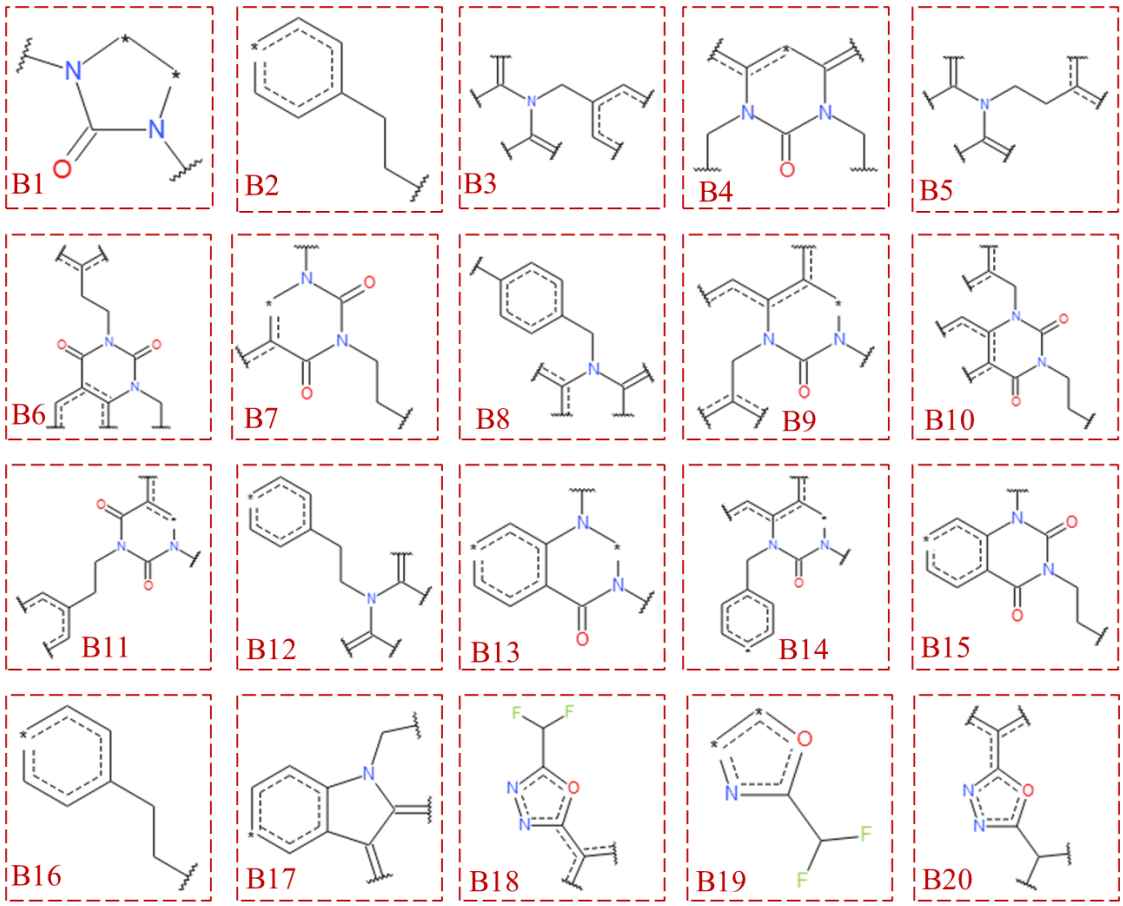

Figure 16: Top 20 unfavourable fingerprints identified from the Bayesian classification study

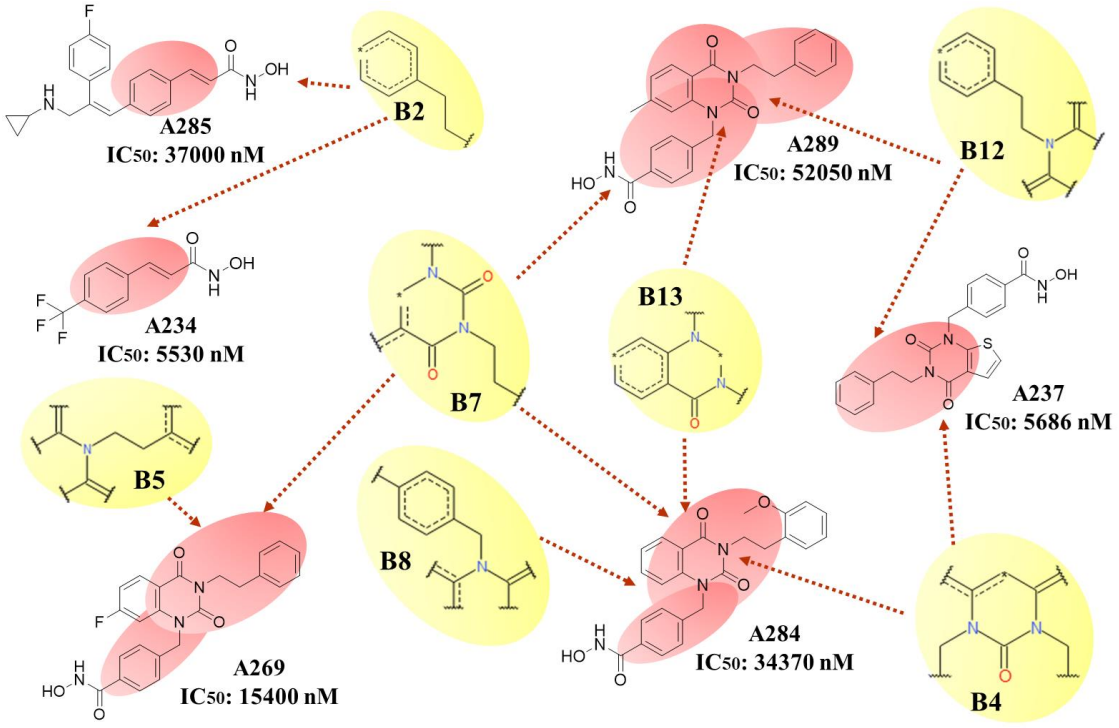

Figure 17: Structure of some *inactive* HDAC11 inhibitors with bad Bayesian fingerprints

In general, our Bayesian analysis shows that the majority of compounds with substituted *1,3-dimethyl-2,4-dimethylenehexahydropyrimidine*, *methyl substituted-divinyl amine*, and *2-propyloxazole* scaffolds have shown poor or less activity while compounds with *benzimidazole*, *isoindoline*, or *carboxamide* functional group have a significant outcome. Another intriguing finding is that compounds having both *benzimidazole* and *isoindoline* scaffolds have shown higher activity as compared to others.

5.4 Recursive partitioning (RP) study

The Recursive Partitioning (RP) analysis was carried out using a dataset encompassing 712 compounds as HDAC11 inhibitors with diverse hydroxamate and non-hydroxamate groups to develop clearer and more precise classification-based models by generating decision trees. RP modeling was done on the training (N_{Train} = 534) and test (N_{Test} = 178) sets developed by the "Random per cluster" method. Since the Bayesian classification models involving the training set performed better on the test set. Similar to the Bayesian classification research, this RP model was built in *D.S. 3.0* [125] with default settings utilizing a combination of fingerprint features (Feature-class fingerprint of diameter 6, *FPCP_6*) and different types of molecular descriptors like *AlogP, MW, nR, nAR, nRB, nHBD, nHBA, ECFP_6* and *MFPSA. 5-fold cross-validation* was utilized to assess the model's performance, which led to the generation of 9 tree(s) for differentiating the *active*s from *inactives*. Statistical analysis of the RP model's decision trees reveals that decision tree-1 outperformed the training and test sets in terms of *ROCCV*, *ROC* score, and other statistical metrics. **Table 4** shows the statistical performance of 9 decision trees built from the training set compounds, and **Table 5** has a full statistical description of the 9 decision trees for the test set.

Tree-1 has an ROC_{Train} score of 0.922 and is the least-trimmed tree. Consequently, it is a model with less error (Min alpha = 0) than the other eight trees. A thorough investigation revealed that Tree-1, with an ROC_{CV} score of 0.794, is the best model and the *ROC* score for the test set compounds was found to be 0.83. Based on the *FPCP_6* fingerprint, the decision tree with 26 leaves exported six molecular properties and twelve structural fingerprints (*FP-1* to *FP-12*), as shown in **Figure 18**. These twelve fingerprints (**Figure 19**) are essential in distinguishing between highly *active* and less active or *inactive* HDAC11 inhibitors. In addition, various statistical measures like sensitivity (*Se*), specificity (*Sp*), overall accuracy (*Acc*), precision (*Pr*), geometric-mean (*g-mean*), F1-measure (*F1*), and area under the balanced accuracy *ROC* curve (AUC_b), etc. were obtained for both the training and test set compounds. Moreover, both the

Table 4. Statistical results of the RP model for the training set

Tree No: *Depth:* *Leaves*	*ROC*	*ROC$_{CV}$*	*TP*	*FP*	*TN*	*FN*	*Se*	*Sp*	*Acc*	*Pr*	*G-mean*	*F1*	*AUC$_b$*	*MCC*	*γ*	*ρ+*	*ρ-*
1:26	**0.922**	**0.794**	**200**	**47**	**250**	**37**	**0.844**	**0.842**	**0.843**	**0.809**	**0.843**	**0.826**	**0.842**	**0.683**	**0.685**	**5.332**	**0.185**
2:20	0.941	0.796	200	47	250	37	0.844	0.842	0.843	0.809	0.843	0.826	0.842	0.683	0.685	5.332	0.185
3:18	0.931	0.792	200	49	248	37	0.844	0.835	0.839	0.803	0.839	0.823	0.844	0.676	0.679	5.115	0.186
4:15	0.921	199	199	55	242	38	0.840	0.815	0.826	0.783	0.827	0.810	0.827	0.652	0.654	4.534	0.196
5:12	0.896	0.788	183	43	254	54	0.772	0.855	0.818	0.810	0.813	0.790	0.813	0.630	0.627	5.333	0.266
6:11	0.887	0.785	190	57	240	47	0.802	0.808	0.805	0.77	0.805	0.785	0.805	0.607	0.609	4.177	0.245
7:5	0.879	0.764	134	29	268	103	0.565	0.902	0.753	0.822	0.714	0.67	0.734	0.504	0.467	5.790	0.481
8:4	0.861	0.764	111	21	276	126	0.468	0.929	0.725	0.840	0.660	0.601	0.698	0.457	0.398	6.623	0.572
9:2	0.794	0.733	69	14	283	168	0.291	0.953	0.659	0.831	0.527	0.431	0.622	0.334	0.244	6.176	0.744

The best RP model is shown in boldfaces

Table 5. Statistical results of the RP model for the test set

Tree No: *Depth:* *Leaves*	*ROC score*	*TP*	*FP*	*TN*	*FN*	*Se*	*Sp*	*Acc*	*Pr*	*G-mean*	*F1*	*AUC$_b$*	*MCC*	*γ*	*ρ+*	*ρ-*
1:26	**0.83**	**57**	**24**	**84**	**13**	**0.814**	**0.778**	**0.792**	**0.703**	**0.796**	**0.754**	**0.796**	**0.580**	**0.592**	**3.66**	**0.238**
2:20	0.827	57	24	84	13	0.814	0.778	0.792	0.703	0.796	0.754	0.796	0.580	0.592	3.66	0.238
3:18	0.802	55	33	75	15	0.786	0.694	0.730	0.625	0.739	0.696	0.740	0.47	0.480	2.57	0.308
4:15	0.731	51	39	69	19	0.729	0.639	0.674	0.566	0.682	0.637	0.683	0.36	0.367	2.01	0.424
5:12	0.724	49	32	76	21	0.700	0.704	0.702	0.605	0.702	0.650	0.701	0.40	0.403	2.36	0.426
6:11	0.725	54	34	74	16	0.771	0.685	0.719	0.613	0.727	0.683	0.728	0.446	0.456	2.45	0.333
7:5	0.711	42	21	87	28	0.600	0.806	0.725	0.666	0.695	0.631	0.702	0.414	0.405	3.08	0.496
8:4	0.678	33	11	97	37	0.471	0.898	0.730	0.75	0.651	0.578	0.684	0.418	0.37	4.63	0.588
9:2	0.57	15	8	100	55	0.214	0.926	0.646	0.652	0.445	0.322	0.570	0.204	0.140	2.9	0.848

The best RP model is shown in boldfaces

training and test set yielded *Se* at (0.844, 0.814); *Sp* (0.842, 0.778); *Acc* (0.843, 0.792); *Pr* (0.809, 0.703); *G-mean* (0.843, 0.796); *F1* (0.826, 0.754); *AUC$_b$* (0.842, 0.796); and so on (summarized in **Table 4** and 5). These obtained measures demonstrate Tree 1's supremacy as the best RP model over the other eight models and a graphical illustration with 12 fingerprints (FP-1 to FP-12) and 26 terminal leaves of Tree-1 is depicted in **Figure 18**.

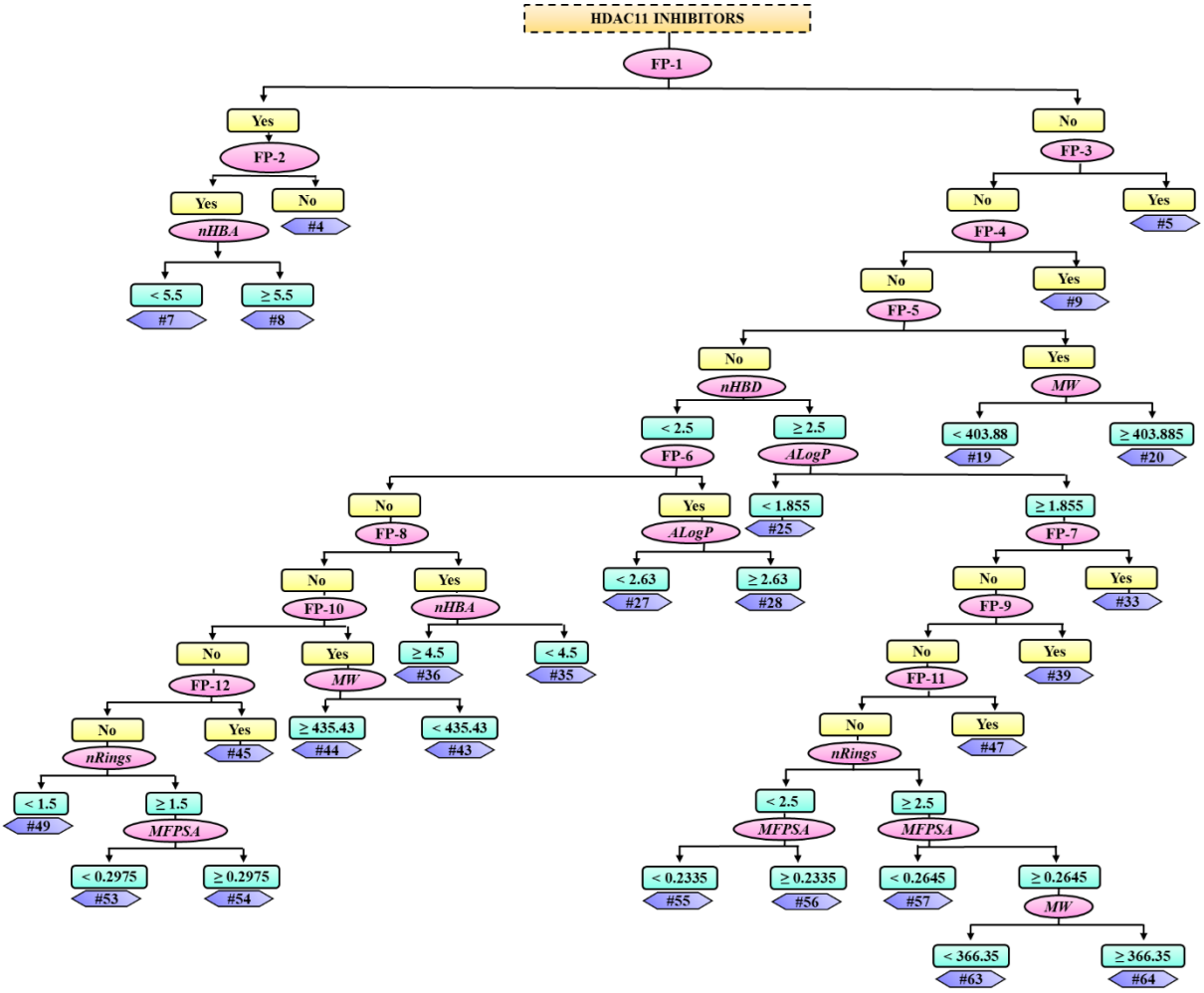

Figure 18: Classification of HDAC11 inhibitors through the decision tree into *active* and *inactive* classes by using the RP model.

5.4.1 Evaluation of the decision tree and structural fragments of the RP Model

The potential of Tree-1 in distinguishing between *active* and *inactive* HDAC11 inhibitors is strongly reliant on the twelve fragments (**Figure 19**) and these fragments plays an essential role in governing the activity of HDAC11 inhibitors.

Mechanistically, the number of hydrogen bond donors *(nHBD*), number of hydrogen bond acceptors *(nHBA*), number of rings (*nR*), octanol/water partitioning coefficient (*ALogP*), molecular fractional polar surface area (*MFPSA)*, and molecular weight (*MW*) are the prime molecular descriptors determined by the best decision tree (Tree-1) that has an impact on the activity of the compounds to be predicted as *active*/*inactive* classes of HDAC11 inhibitors. The RP model findings demonstrated the importance of different structural fragments in the formation of the decision tree. In particular, it is expected that the fragments FP-1 to FP-5, and FP-7 will improve HDAC11 inhibition.

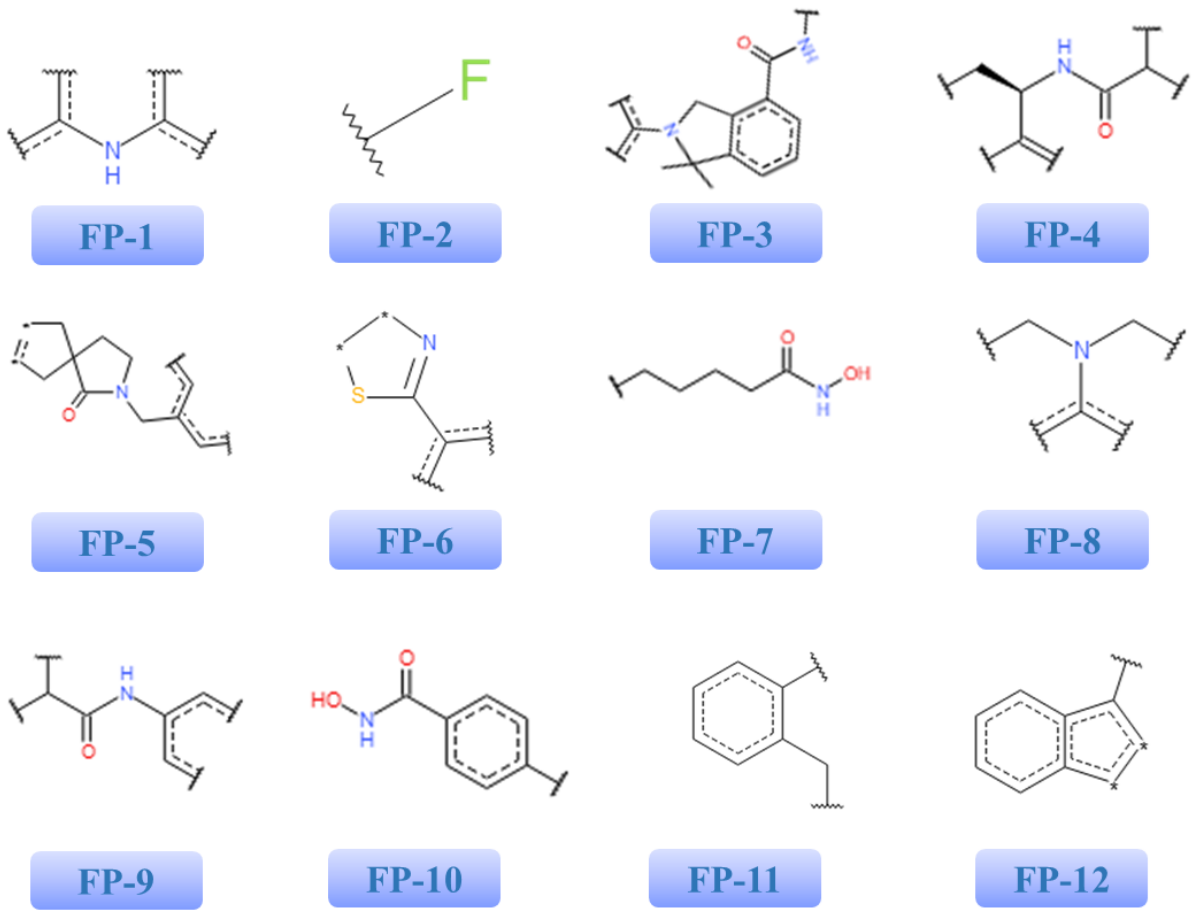

Figure 19: *FCFP_6* fingerprints obtained from the RP Study

On the other hand, probably, FP-6, FP-8, and FP-9 to FP-12 will negatively affect HDAC11 inhibition. In addition, each of the 26 terminal leaves of decision Tree-1 represents a cluster of *active* and *inactive* compounds. In this context, leaf #5, #7, #8, #9, #20, #33, #35, #44, #57 and #64 indicate clusters of *active* compounds, while leaf #4, #19, #25, #36, #49 and #53 represent clusters of *inactive* compounds.

In the decision tree (Tree-1), FP-1 (*diisopropyl amine* moiety) is split into compounds that contain *FP-2* (*fluromethane* scaffold) and that do not contain FP-3 (*isoindoline* moiety fused with *carboxamide*). Both *FP-1* and *FP-2* are believed to show good inhibitory activity. For instance, compound **A013** (IC_{50} = 3 nM), **A067** (IC_{50} = 190 nM) contains both FP-1 and FP-2. In addition, Leaf ID #7 and #8 are comprised of compounds with *nHBA* (<5.5 and ≥ 6.5). Mostly, compounds with *isoindoline* moiety with a *carboxamide* group belong to Leaf ID #5 that comprise FP-3 and seem to be excellent HDAC11 inhibitors for example compounds **A004** (IC_{50} = 1 nM), **A006** (IC_{50} = 2 nM), **A007** (IC_{50} = 2 nM), **A010** (IC_{50} = 3 nM), **A012** (IC_{50} = 3 nM)**, A013** (IC_{50} = 3 nM), **A030** (IC_{50} = 27 nM). Leaf ID #9 consists of compounds having FP-

4 (*carboxamide group*) and the rest do not contain FP-4. Interestingly, compounds with Leaf ID #9 possess a majority of *phenyl mercaptoheptanamide* and *6-oxopiperidine-2-carboxamide* kind of scaffolds which is responsible for good HDAC11 inhibitory activity such as in compounds **A001** (IC_{50} = 0.3 nM), **A003** (IC_{50} = 1 nM), **A011** (IC_{50} = 3 nM), **A025** (IC_{50} = 15 nM), **A036-A041**, etc. Further, analyzing compounds such as **A135-A139**, **A356-A370**, etc bearing FP-5 (*pyrrolidine* ring fused to *cyclic pentane*) have shown better activity. Next, Leaf ID #19 and #20 consist of compounds with *MW* <403.88 and ≥ 403.88 respectively (compounds **A133-A139, A354-A361**, **A365-A370**).

On the one hand, FP-5 does not contain compounds with *nHBD* <2.5 and ≥2.5 and is again split into other fingerprints such as FP-6 (*isopropyl thiazolidine* ring) from *nHBD* <2.5, which shows poor activity (**A703**, IC_{50} = >50000). Leaf ID #25 comprises compounds with *ALogP* <1.855. Then, Leaf ID #27 and #28 consist of compounds with *ALogP* < 2.63 and ≥ 2.63 independently. On the other hand, Leaf ID #35 and #36 consist of compounds with *nHBA* <4.5 and ≥ 4.5 which bear FP-8 (*diethyl propane amine*). Likewise, Leaf ID #33 comprises compounds having FP-7 (*N-hydroxy acetamide* attached to an *aliphatic chain*) that have shown good activity for example, compounds **A046** (IC_{50} = 38 nM), **A056** (IC_{50} = 51 nM), **A062** (IC_{50} = 75 nM), **A065** (IC_{50} = 79 nM), etc. In addition, Leaf ID #39 consist of compounds having FP-9 (compounds **A188**, **A199**, **A210**, **A214**, **A221**, **A222, A269, A284**). Here, FP-9 containing molecules belong to *isobutyramide* scaffolds indicating that this fingerprint has a negative influence on the inhibitory activities.

Further, Leaf ID #43 and #44 consist of compounds with *MW* <435.43 and ≥ 435.43 having FP-10 (*N-hydroxy-4-methylbenzamide*). Most of the compounds of Leaf ID #43 are inactive. Then Leaf ID #45 contains compounds with FP-12 (*methyl indene*) and the rest of the compounds do not contain FP-12. These fragments are responsible for the detrimental activity of the HDAC11 inhibitors. Again, Leaf ID #49 comprises compounds with *nRings* <1.5 whereas *nRings* ≥ 1.5 divides into *MFPSA* <0.2975 and ≥ 0.2975 having Leaf ID #53 and #54 respectively. Next, Leaf ID #47 consists of compounds with FP-11 (*m-substituted toluene*) and the remaining compounds do not contain FP-11 but are divided into *nRings* < 2.5 and ≥ 2.5, all these Leaf IDs contain *inactive* compounds. However, the decision tree is split into Leaf ID #55 and #56 which comprise compounds with *MFPSA* <0.2335 and ≥ 0.2335. In addition, Leaf ID #57 consist of compounds with *MFPSA* <0.2645 (compounds **A002**, **A005**, **A008**, **A019**, **A032**, **A044, A049**). Lastly, Leaf ID #63 and #64 contain compounds with *MW* <366.354 and

≥ 366.354 which is a part of *MFPSA* ≥ 0.2645. Both of these Leaf IDs are not suitable for the favourable activity of HDAC11 inhibition.

5.5 SARpy analysis

To identify the key structural alerts for potent HDAC11 inhibition, a SARpy-mediated structural analysis has been performed on the dataset molecules. The SARpy analysis applied in this work yielded a collection of 22 structural fragments of these HDAC11 inhibitors that served as active rulesets that have shown a positive impact on their inhibition. From **Table 6**, it can be observed that the training set population achieves 78% for *Se*, 83% *Sp*, and 81% A*cc*. Whereas, the external validation with the test set yields 67% *Se*, 89% *Sp*, and 80% A*cc* in the SARpy analysis. Some other statistical measures were also performed for both training and test sets such as *Pr* (*0.*776, 671), G-means (0.803, 0.802), *F1* (0.780, 0.729), etc.

Table 6. Outcomes from SARpy analysis of the training and test set compounds

Dataset	*TP*	*FP*	*TN*	*FN*	*Sen*	*Spe*	*Acc*	*Pr*	*G - means*	*F1*	AUC_b	*MCC*	*γ*	*ρ+*	*ρ-*
Train	184	53	246	51	0.783	0.823	0.805	0.776	0.803	0.780	0.802	0.605	0.605	4.417	0.263
Test	47	23	96	12	0.797	0.807	0.803	0.671	0.802	0.729	0.801	0.581	0.603	4.12	0.252

Many of the segments have shown their potential features for providing powerful HDAC11 inhibition in terms of structural alerts. Information regarding structural alert (SA), SMARTS along with its likelihood ratio (LR) is mentioned in **Table 7**. Structural alert 1 (**SA1**) is *6-trifluromethyl-benzimidazole* moiety having infinite LR value in compounds like **A007**, and **A008** indicating the potent features of the HDAC11 inhibitor. **SA2** revealed the importance of *5-oxo-N-(1-oxoheptan-2-yl)pyrrolidine-2-carboxamide* moiety (LR = inf) in compounds **A036 A041** and **A045** whereas **SA3** represented the significance of *N-phenylbenzo-oxazole* (LR = inf) structure for imparting effective HDAC11 inhibition, this scaffold can be seen in compound **A013** and slightly with **A004**. Moreover, **SA4** uncovers the importance of *5-fluro-benzimidazole*, **SA5** of (*benzyloxy*)*benzene*, **SA6** of *trifluoromethyl aniline*, **SA7** of *6-methyl tetrahydro-benzimidazole* and all are having infinite LR value, possess better inhibition. Several additional structural alerts such as **SA8** (*5-methyl-benzimidazole amine*, LR = 33.84), **SA9** (*2-amino-N-phenylheptanamide*, LR = 20.05, eg: **A053**), **SA10** (*5-methyl-1H-benzimidazol-2-amine*, LR = 14.41) and **SA11** (*5-chloro-benzimidazole*, LR = 13.78, eg: **A013**)

have shown an effective impact on HDAC11 inhibiting efficacy according to their LR values. Lastly, **SA1**, **SA4**, **SA8**, and **SA10** are strongly indicated towards the compounds **A007**, **A008**, and **A012** which conclude that all the generated alerts and the compounds are interrelated with each other.

Table 7: Active structural ruleset

SL. no	***SMARTS***	***Structural Alert***	***Likelihood ratio***
1	c1c2c(nc([nH]2)N)ccc1C(F)(F)F	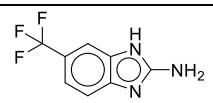	inf
2	N1C(CCC1=O)C(=O)NC(CCCCC)C(=O)	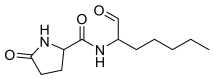	inf
3	N1C(CCC1=O)C(=O)NC(CCCCC)C(=O)	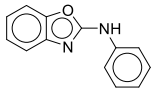	inf
4	c1c2c(cc(c1F))n(c(n2)N)	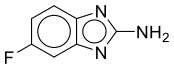	inf
5	c1ccc(cc1)OCc1ccccc1	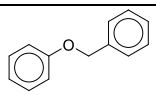	inf
6	c1ccc(cc1C(F)(F)F)NCCCC	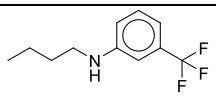	inf
7	c1[nH]c2c(n1)CCC(C2)(C)	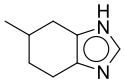	inf
8	c1(c(cc2c(c1)nc([nH]2)N))C	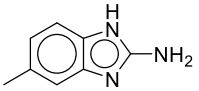	33.84
9	c1cccc(c1)NC(=O)C(CCCCC)N	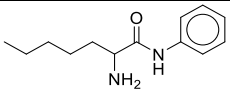	20.05
10	c1c2c(cc(c1C))n(c(n2)N)	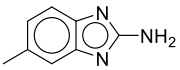	14.41
11	c1c2c(cc(c1Cl))n(c(n2))	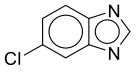	13.78

5.6 Molecular Docking Analysis

Molecular docking analysis helps validate the significance of identified crucial structural fingerprints obtained through multiple classification-based molecular modelling studies. It is also possible to classify and identify the role that these fragments play in achieving selective and promising HDAC11 inhibition.

At first, some potent compounds containing good molecular fingerprints were chosen to understand the binding mode patterns of HDAC11 inhibitors with the receptor. Among all, some of the highly potent compounds (**A004**, **A007**, **A013**, **A053**) having efficient HDAC11 inhibitory activity were selected for docking. In addition, **Figure 20** demonstrates the interactions of essential structural fingerprints identified using various classification-based QSAR techniques and validates them through molecular docking.

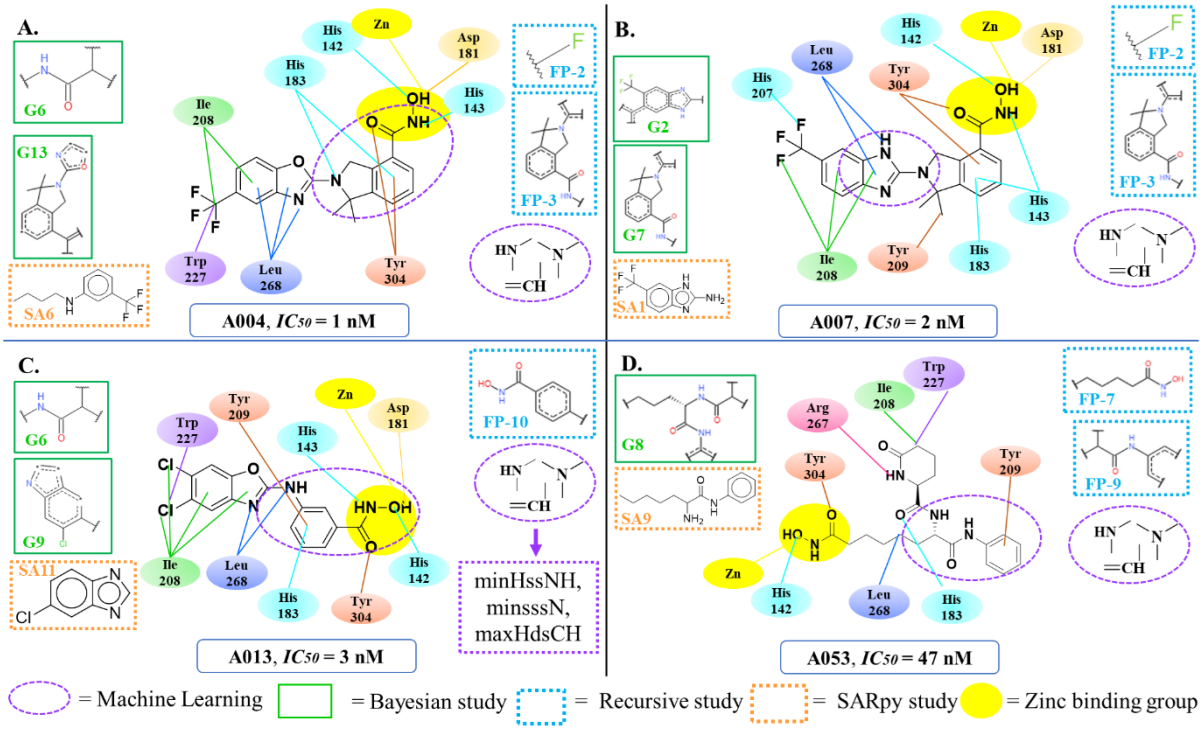

Figure 20: Compounds containing different fingerprints through Bayesian study, RP study, SARpy, and machine-learning-based QSAR techniques.

Here, compound **A004** contains crucial fingerprints like G6, G7, G13**,** and **A007** contains G2 and G7 whereas **A013** contains G6 and G9**,** respectively. The information regarding the activity and similarities of the fingerprints was already discussed in the Bayesian classification portion (**Figure 15**). Since the X-ray crystal structure of HDAC11 has not yet been discovered, so, we have decided to pick the AlphaDB Fold model of HDAC11 (https://alphafold.ebi.ac.uk/entry/B5MCU6) which has been collected from the AlphaFold

Database (https://alphafold.ebi.ac.uk/). Binding site determination was done with the active site of hydroxamate bound HDAC homolog complex (as mentioned in the materials and method section) for the molecular docking simulation. However, after analyzing the results, the selected compounds exhibit well-estimated free energy of binding in terms of "Dock score" after interaction with the active site residues of HDAC11 (**Table 8**). From **Figure 21** it can be observed that all the compounds show identical Zn^{2+} metal coordination with the hydroxamate group.

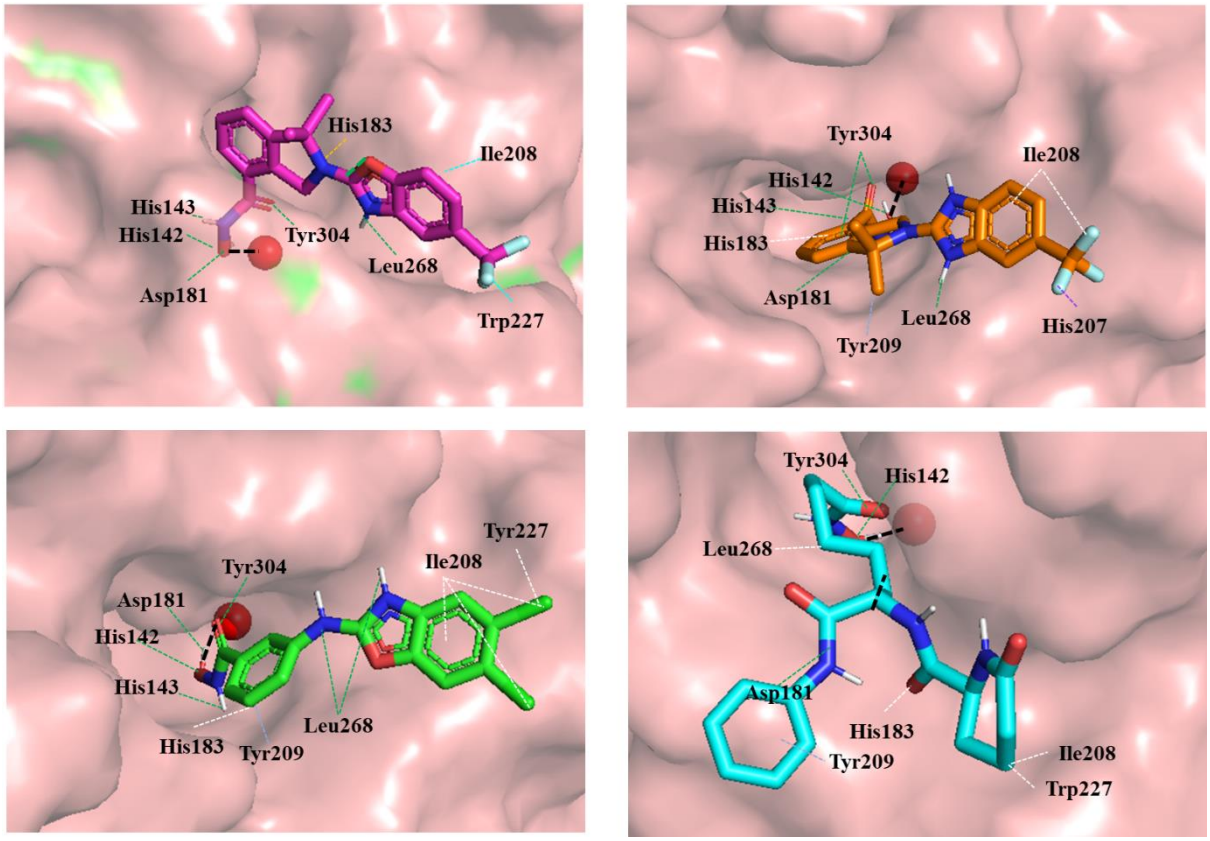

Figure: 21 Analysis of zinc-binding interactions in the compounds **A004**, **A007**, **A013**, and **A053** using molecular docking studies. All the compounds are coordinated with zinc metal via the carboxamide group (CONHOH). The dotted lines indicate different interactions: black lines (metal coordination with zinc metal), green lines (H-bonding), white lines (π-alkyl), blue lines (π-σ), orange lines (π-cation), and purple lines (halogen interaction).

Now, by considering the **A004** compound, the nitrogen atom in the oxazole ring, and the phenyl ring in the G13 fingerprint have conventional H-bond interaction with **Leu268** and **Tyr304**. The trifluoromethyl benzene of the G17 fingerprint has π-alkyl interaction with **Ile208** and **Trp227**. In the G6 fingerprint, the double-bonded oxygen and the amide form H-bond interaction with **Tyr304** and **His143** respectively. The hydroxyl group of the hydroxamate functional group forms an H-bonding with **Asp181** and **His142**. On the other hand, for the

A007 compound, the hydroxamate functional group of the G7 fingerprint forms multiple H-bonding interactions with **Tyr304**, **Asp181**, **His142**, and **His143**. The methyl group forms π-σ interaction with **Tyr209** and the phenyl ring forms π- π stacked interaction with **His183**. The G2 fingerprint forms C-H bonding with **Ile208** residue and has conventional H-bond interaction with **Leu268**. The trifluoromethyl group of the G2 fingerprint has a halogen interaction with **His207**.

In the case of **A013**, the chlorophenyl ring of the G9 fingerprint shows engagement with **Ile208** and **Trp227** through π-alkyl. Then, multiple hydrogen bonds can be noticed in the hydroxamate moiety of the acetamide ring with Tyr304, Asp181, His142, and His143 residue, and also π- π stacked interaction with His183 and Tyr209.

From these observations, it can be hypothesized that these molecular fingerprints may have a key role in modulating the important amino acid interactions towards the active site. Also, the interaction of the specific regions of these fingerprints with important amino acid residues like **Leu268**, **Tyr209**, **Ile208**, **Trp227**, **His143**, **Asp181**, **His142**, and **His183** can be important for accommodating the ligands inside the binding cavity.

Table 8. Docking results, H-Bond interacting residues with good fingerprints of selected compounds

Compound ID	Dock Score (kcal/mol)	H-Bond Interaction	Fingerprints involved in H-Bond interaction
A004	-8.43	Tyr304, Asp181, His142, His143 and Leu268	G6, G7, G13 and G17
A007	-9.17	Tyr304, Asp181, Ile208, His142, His143 and Leu268	G2 and G7
A013	-8.28	Tyr304, Asp181, His142, His143 and Leu268	G6 and G9
A053	-6.15	His183, Arg267, Tyr304, His142	G6, G8 and G10

Chapter 6: Conclusion and Future Perspective

6. Conclusion

The purpose of this work was to find significant fingerprints necessary for HDAC11 inhibition. Since the human crystal structure of HDAC11 has not yet been discovered, so, ligand-based drug design, particularly fragment-based in-silico drug design, is a viable alternative for accelerating the anti-HDAC11 drug development approach. Here, we have developed binary-QSAR models (i.e., bayesian classification, recursive partitioning, SARpy analysis, and machine learning analysis) and molecular docking on a dataset containing N_{Train} = 534 and N_{Test} =178, that have successfully well-performed in all the validation metrics. These models pointed towards several significant structural attributes of these compounds which can define the *active* and *inactive* classes of HDAC11 inhibitors. The observations from the overall modeling strategy are very helpful in understanding the mechanisms underlying the fingerprints associated with supported inhibition processes. For instance, the Bayesian classification model accurately distinguishes good and detrimental structural features of HDAC11 inhibitors. Positive contributors include *benzimidazole* moiety, *carboxamide* group, and *isoindoline* moiety. Conversely, some scaffolds such as substituted *1,3-dimethyl-2,4-dimethylenehexahydropyrimidine, methyl substituted-divinyl amine,* and certain *2-propyloxazole* scaffolds should be omitted in the design of HDAC11 inhibitors. Structural fragments obtained from the RP study such as *diisopropyl amine* moiety, *fluromethane* scaffold, and *isoindoline* moiety fused with *carboxamide* positively influence HDAC11 inhibition, while *isobutyramide* and *methyl indene* have a negative impact. The SARpy analysis revealed that *trifluromethyl-benzimidazole* moiety (SA1), *5-oxo-N-(1-oxoheptan-2-yl)pyrrolidine-2-carboxamide* moiety (SA2) having infinite likelihood ratios positively influence the HDAC11 inhibitory activity. Upon interpreting descriptors using SHAP plots discovered some influential features like minHBint5, GATS1m and some electrotopological descriptors which provide insight into their roles in inhibiting HDAC11 activity.

Moreover, the importance of the discovered structural fragments in attaining effective and selective HDAC11 inhibition was further validated by the molecular docking study, with compounds **A004**, **A007**, **A013**, and **A053**, exhibiting highly potent inhibitory activity. We hope this study will help researchers design and discover highly effective and promising HDAC11 inhibitors, mainly for anticancer and immunosuppressive drugs. We anticipate that these will lead to new insights when designing selective HDAC11 inhibitors in the near future. It is crucial to remember that further in vitro and in vivo research is required to properly interpret our results.

Furthermore, forthcoming investigations could focus on refining the binary-QSAR models by incorporating advanced ML techniques such as deep learning, neural networks, ensemble methods, etc, which could enhance predictive accuracy. Additionally, expanding the molecular fingerprint database and integrating multi-omics data could provide a more comprehensive understanding of HDAC11 inhibition mechanisms. This work has the potential to identify novel inhibitors with high specificity, paving the way for targeted therapies with fewer side effects.

Annexure-I

All HDAC11 compounds in SMILES format.

Training set of compounds of HDAC11 inhibitors in SMILES format

Compound ID	SMILES	IC_{50} (nM)	Binary
A001	C1(=O)[C@@H](C(C)C)NC(=O)C[C@H]2OC(=O)[C@H](C(C)C)NC(=O)/C(=C/C)/NC(=O)[C@@H](CSSCC/C=C/2)N1	0.3	1
A002	c1cc2n(cc(c2cc1)CNCC1CCN(CC1)c1ncc(cn1)C(=O)NO)C	0.37	1
A003	N1[C@@H](CCCC1=O)C(=O)N[C@@H](CCCCCS)C(=O)Nc1cc(ccc1)C	1	1
A004	O=C(NO)c1c2c(C(C)(C)N(c3oc4ccc(cc4n3)C(F)(F)F)C2)ccc1	1	1
A005	O=C(NO)/C=C/c1ccc(CNCCc2c3c([nH]c2C)cccc3)cc1	1.6	1
A006	c1(oc2c(n1)nccc2)N1C(C)(C)c2cccc(c2C1)C(=O)NO	2	1
A007	O=C(NO)c1c2c(C(C)(C)N(c3[nH]c4cc(ccc4n3)C(F)(F)F)C2)ccc1	2	1
A008	c1([nH]c2c(n1)ccc(c2)C(F)(F)F)N1Cc2c(cccc2C1)C(=O)NO	2	1
A009	c1cc2c(cc1S(=O)(=O)N1CCN(CC1)c1ncc(cn1)C(=O)NO)cccc2	2.1	1
A010	O=C(NO)c1c2c(C(C)(C)N(C2)c2ccc(nc2)C(F)(F)F)ccc1	3	1
A011	s1c2nc(c1)C1=N[C@@](CS1)(C(=O)N[C@@H](C(=O)O[C@H](/C=C/CCS)CC(=O)NC2)C(C)C)C	3	1
A012	O=C(NO)c1c2c(C(C)(C)N(C2)c2cnc(cn2)C(F)(F)F)ccc1	3	1
A013	c1(c(cc2c(c1)oc(n2)Nc1cc(ccc1)C(=O)NO)Cl)Cl	3	1
A014	N1[C@@H](CCCC1=O)C(=O)N[C@@H](CCCCCS)C(=O)Nc1ccc(cc1)C	3	1
A017	c1cccc(c1)NC(=O)[C@H](CCCCCS)NC(=O)[C@H]1N(C(=O)CCC1)C	5	1
A019	c1cc(ccc1/C=C/C(=O)NO)CN(CCO)CCc1c[nH]c2c1cccc2	5.6	1
A021	O=C(NO)c1c2c(C(C)(C)N(C2)c2ccc(cn2)C(F)(F)F)ccc1	6	1
A022	c1(oc2c(n1)cccc2)N1Cc2c(cccc2C1)C(=O)NO	7	1
A023	N1(Cc2c(cccc2C1)C(=O)NO)c1ccc(cn1)C(F)(F)F	7	1
A025	N1[C@@H](CC1=O)C(=O)N[C@@H](CCCCCS)C(=O)Nc1ccccc1	10	1
A027	ONC(=O)/C=C/C(=C/[C@H](C(=O)c1ccc(N(C)C)cc1)C)/C	11	1
A032	C(=O)(NCCOc1ccc(cc1)C(=O)NO)c1c(c2c(cccc2)o1)CN(C)C	14	1
A033	c1cc(ccc1C(=O)/C(=C/[C@@H](C)/C=C/C(=O)NO)/C)N(C)C	14	1
A036	c1cc(cc(c1)NC(=O)[C@H](CCCCCC(=O)NO)NC(=O)[C@@H]1NC(=O)CC1)C	15	1
A037	c1cccc(c1)NC(=O)[C@H](CCCCCS)NC(=O)[C@@H]1C(=O)NCCC1	15	1
A038	c1c(ccc(c1)C(=O)NO)/C=C/C(=O)N[C@@H](Cc1c[nH]c2c1cccc2)C(=O)Nc1ccc(cc1)Cl	16	1
A039	[C@H](N1CCN(CC1)c1ncc(cn1)C(=O)NO)(/C=C/c1ccc(cc1)F)CO	21	1
A041	N1C(=O)[C@@H]([C@@H](C1)c1ccccc1)C(=O)N[C@@H](CCCCCS)C(=O)Nc1ccccc1	24	1
A042	N1(Cc2c(cccc2C1)C(=O)NO)c1ccc2c(n1)cccc2	26	1
A043	O=C(NO)c1c2c(C(C)(C)N(C2)c2cnc(nc2)C(F)(F)F)ccc1	27	1
A044	c1([nH]c2c(n1)cccc2)N1CCc2c(CC1)c(ccc2)C(=O)NO	30	1
A045	N1[C@@H](CCC1=O)C(=O)N[C@@H](CCCCCS)C(=O)Nc1ccccc1	30	1
A046	C(n1ncc(c1)c1c2c(ncn1)[nH]cc2)CCCCCC(=O)NO	31	1
A047	c1(sc2c(n1)cccc2)N1Cc2c(cccc2C1)C(=O)NO	35	1
A048	c1cccc(c1)NC(=O)[C@H](CCCCCC(=O)NO)NC(=O)[C@H]1NC(=O)C1	37	1
A049	c12c(cccc1)[nH]cc2CN1CCN(CC1)c1ncc(cn1)C(=O)NNCCCCCC	41	1

A050	O=S(=O)(Nc1ccc(C(=O)NO)cc1)c1ccc(cc1)C(C)(C)C	44	1
A053	c1cccc(c1)NC(=O)[C@H](CCCCCC(=O)NO)NC(=O)[C@H]1NC(=O)CCC1	47	1
A054	C(=O)(c1c(cccc1)OC)N[C@H](COc1cc(ccc1)/C=C/C(=O)NO)Cc1c[nH]c2c1cccc2	53	1
A055	C(=O)(/C=C/c1c(=O)n(ccc1)CCCc1cc2c(cc1)cccc2)NO	55	1
A056	c1(cc2cc(c1)/C=C\CO[C@@H](C(=O)Nc1c(OC2)cccc1)CCCCCC(=O)NO)OC	58	1
A057	N1[C@@H](CCC1=O)C(=O)N[C@@H](CCCCCS)C(=O)Nc1cc(ccc1)C	62	1
A058	N1([C@H](CCC1=O)C(=O)N[C@@H](CCCCCS)C(=O)Nc1ccccc1)C	67	1
A060	S(=O)(=O)(c1c(c(c(c(c1F)F)F)F)F)N(Cc1ccc(cc1)C(=O)NO)Cc1ccc(cc1)C	73	1
A061	c1cccc(c1)NC(=O)[C@H](CCCCCC(=O)NO)NC(=O)[C@@H]1NC(=O)CC1	75	1
A062	c1ccc(cc1C(F)(F)F)NC(=O)CCCCCCC(=O)NO	75	1
A063	c1c(ccc(c1)C(=O)NO)/C=C/C(=O)N[C@@H](Cc1c[nH]c2c1cccc2)C(=O)Nc1cccc(c1)Cl	76	1
A064	n1c(sc(c1C(=O)N[C@H](c1ccc(cc1)C(=O)NO)C)C1CC1)c1ncc(s1)c1ccccc1	78	1
A065	c1c(ccc(c1)NC(=O)CCCCCCC(=O)NO)C	79	1
A066	c1(ccc2c3c1cccc3c(=O)n(c2=O)CCCCCC(=O)NO)NCCC	80	1
A067	N1[C@@H](CCCC1=O)C(=O)N[C@@H](CCCCCS)C(=O)NC1CCCC1	89	1
A068	c1(cc2cc(c1)/C=C\CO[C@@H](C(=O)Nc1c(OC2)cccc1)CCCCCC(=O)NO)OC	97	1
A070	N1[C@H](CCC1=O)C(=O)N[C@H](CCCCCS)C(=O)Nc1ccccc1	102	1
A071	c1(cc2cc(c1)CCCO[C@H](C(=O)Nc1c(OC2)cccc1)CCCCCC(=O)NO)OC	103	1
A072	c12ccc(nc1cccc2)N(CCCCCCC(=O)NO)c1ccccn1	112	1
A073	S(=O)(=O)(c1c(c(c(c(c1)F)F)F)F)N(Cc1ccc(cc1)C(=O)NO)Cc1ccccc1	115	1
A075	c1c(ccc(c1)NC(=O)[C@H](CCCCCC(=O)NO)NC(=O)[C@@H]1NC(=O)CC1)C	127	1
A076	c1cc2c(cc1)nc1n(c2=O)nc(c2c1cccc2)NCCCCCCCC(=O)NO	130	1
A077	c1cc2c(cc1)nc1n(c2=O)nc(c2c1cccc2)NCCCCCCC(=O)NO	130	1
A078	C(=O)(Nc1ccccc1)CCCCCCCS	133	1
A079	c1cccc(c1)NC(=O)[C@H](CCCCCC(=O)NO)NC(=O)[C@H]1C(=O)NCC1	150	1
A080	c1(ccc2c3c1cccc3c(=O)n(c2=O)CCCCCC(=O)NO)NCc1ccccc1	150	1
A081	n1(cccc(c1=O)/C=C/C(=O)NO)CCc1cc2c(cc1)cccc2	161	1
A082	c1(cc2cc(c1)CCCO[C@@H](C(=O)Nc1c(OC2)cccc1)CCCCCC(=O)NO)OC	174	1
A083	c1c(ccc(c1)C(=O)NO)/C=C/C(=O)N[C@@H](Cc1c[nH]c2c1cccc2)C(=O)Nc1ccc(cc1)Br	176	1
A084	C(CCCCC)NNC(=O)c1ccc(cc1)c1ccc(cc1)CNC(=O)C	180	1
A085	c1(ccc2c3c1cccc3c(=O)n(c2=O)CCCCCC(=O)NO)Nc1ccccc1	190	1
A086	c1(ccc2c3c1cccc3c(=O)n(c2=O)CCCCCC(=O)NO)Nc1cccc(c1)F	210	1
A087	O=S(=O)(Nc1ccc(C(C)(C)C)cc1)c1ccc(C(=O)NO)cc1	223	1
A088	c1(cc2cc(c1)CCCO[C@H](C(=O)Nc1c(OC2)cccc1)CCCCCC(=O)NO)OC	226	1
A090	O=S(=O)(N(Cc1ccc(cc1)C(=O)NO)C)c1c(c(c(c(c1F)F)F)F)F	246	1
A092	c1cccc(c1)NC(=O)CCCCCCS	262	1
A095	C(=O)(CCCCCn1c(=O)c2c3c(c1=O)ccc(c3ccc2)N1CCOCC1)NO	290	1
A096	N1[C@@H](CCCC1=O)C(=O)N[C@@H](CCCCCS)C(=O)N1Cc2c(CC1)cccc2	293	1
A098	c1c(c([nH]c1c1ccc(cc1)O)C(=O)NCc1ccc(cc1)C(=O)NO)c1ccsc1	319	1
A099	c1c(c([nH]c1c1ccc(cc1)OC)C(=O)NCc1ccc(cc1)C(=O)NO)c1ccoc1	340	1
A101	C(=O)(c1ccc(cc1)CNc1cccc2cccnc12)NO	376	1
A102	C(c1c[nH]c2c1cccc2)(c1c[nH]c2c1cccc2)c1ccc(cc1)/C=C/C(=O)NO	410	1
A103	C(=O)(c1ccc(cc1)C1CCCCC1)Nc1ccc(cc1)C(=O)NO	411	1

A104	C(=O)(CCCCCC(c1c[nH]c2c1cccc2)c1c[nH]c2c1cccc2)NO	430	1
A105	C(c1ccc(cc1)NC(=O)c1ccc(C(=O)NO)cc1)(C)(C)C	447	1
A106	S(=O)(=O)(c1c(c(c(c(c1)F)F)F)F)N(Cc1ccc(cc1)C(=O)NO)Cc1ccncc1	472	1
A107	c1c(cc2c(c1)n(c1c2C[S@](=O)CC1)Cc1ccc(cc1)C(=O)NO)F	500	1
A108	C(=O)(c1c(cc(c(c1)C(C)C)O)O)N1CCc2onc(c2C1)C(=O)NCCCCCCCC(=O)NO	521	1
A110	N1(Cc2ccc(cc2)C(=O)NO)c2c(CC[C@H]3[C@H]1CCCC3)cccc2	540	1
A111	c1cccc2c1OCCCCCCCCO[C@H](C(=O)N2)CCCCCC(=O)NO	546	1
A112	c1cccc2c1OCCCCCCCO[C@@H](C(=O)N2)CCCCCC(=O)NO	564	1
A113	c12c(cccc1)[nH]cc2CN1CCN(CC1)c1ncc(cn1)C(=O)NNCCC	570	1
A114	c1ccncc1c1ccnc(n1)NCc1ccc(cc1)C(=O)Nc1c(cccc1)N	590	1
A117	c1c(cc2c(c1)c(cn2Cc1ccc(cc1)C(=O)NO)C(=O)c1cc(c(c(c1)OC)OC)OC)OC	651	1
A118	C(=O)(Nc1ccccc1)CCCCCS	659	1
A120	O=S(=O)(c1cc(ccc1)C(F)(F)F)N(c1ccc(cc1)C(=O)NO)CC	695	1
A121	O=S(=O)(N(CC(=O)N(c1ccc(cc1)C(=O)NO)Cc1ccc(cc1)C(C)(C)C)C)c1ccc(cc1)F	697	1
A122	C(=O)(c1c(c(c(c(c1F)F)F)F)F)Nc1ccc(cc1)C(=O)NO	700	1
A125	C1c2c(N(CC1)Cc1ccc(cc1)C(=O)NO)ccc(c2)Cl	746	1
A126	c1(c(cc2c(c1)nc([nH]2)Nc1cc(C(=O)NO)ccc1)S(=O)(=O)C)C#N	750	1
A127	c1c2c(nc([nH]2)Nc2cc(C(=O)NO)ccc2)cc(c1F)F	750	1
A129	c1c2c(nc([nH]2)Nc2cc(C(=O)NO)ccc2)cc(c1OC)Cl	750	1
A130	c1c2c(nc([nH]2)Nc2cc(C(=O)NO)ccc2)ccc1[N+](=O)[O-]	750	1
A132	c1c2c(nc(n2C)Nc2cc(C(=O)NO)ccc2)cc(c1C(F)(F)F)c1cccnc1	750	1
A133	c1cc2c(c(c1)C(=O)NO)C[C@]1(C2)C(=O)N(CC1)Cc1ccc(cc1)F	750	1
A134	c1ccc2c(c1C(=O)NO)C[C@]1(C2)C(=O)N(CC1)c1cc(ccc1)C(F)(F)F	750	1
A135	c12c(cccc1C(=O)NO)C[C@]1(C2)CCN(C1=O)Cc1cccc(c1)C	750	1
A136	c12c(cccc1C(=O)NO)C[C@@]1(C2)CCN(C1=O)Cc1c(cccc1Cl)Cl	750	1
A137	c12c(cccc1C(=O)NO)C[C@]1(C2)CCN(C1=O)Cc1ccccc1C(F)(F)F	750	1
A138	c12c(cccc1C(=O)NO)C[C@@]1(C2)CCN(C1=O)Cc1c(cccc1)OC(F)(F)F	750	1
A139	c12c(cccc1C(=O)NO)C[C@@]1(C2)CCN(C1=O)Cc1ccc(c(c1)C)C	750	1
A143	c1(cccc2c1C[C@]1(CC2)C(=O)N(CC1)c1ccc(cc1)C(F)(F)F)C(=O)NO	750	1
A144	c12c(c(ccc1)C(=O)NO)CC[C@@]1(C2)C(=O)N(CC1)c1cccc(c1)C(F)(F)F	750	1
A145	c1c(cc2c([nH]c(n2)Nc2cc(C(=O)NO)ccc2)c1)[N+](=O)[O-]	750	1
A146	N1(Cc2c(C1)c(ccc2)C(=O)NO)c1[nH]c2c(n1)CCC(C2)(C)C	750	1
A148	c1ccc(c2c1CN(C2)c1ccc2c(c1)OCCN2)C(=O)NO	750	1
A150	N1(C(c2c(C1)c(ccc2)C(=O)NO)(C)C)C(=O)Nc1cnc(cc1)C(F)(F)F	750	1
A151	c12c(cc(nc1)NC(=O)N1C(c3c(C1)c(ccc3)C(=O)NO)(C)C)CCCC2	750	1
A152	c1cc(ncc1C(F)(F)F)N1C(c2c(C1)c(ncc2)C(=O)NO)(C)C	750	1
A153	N1(Cc2c(C1)c(ccc2)C(=O)NO)c1[nH]c2c(n1)cc(cc2c1ccccc1)C(F)(F)F	750	1
A154	c12c(c(ccc1)C(=O)NO)[nH]c(c2)c1ccc(cc1)C(F)(F)F	750	1
A155	c1([nH]c2c(c1)c(ccc2)C(=O)NO)c1ccc(cc1)C(F)(F)F	750	1
A156	c12c(c(ccc1)C(=O)NO)N[C@@H](C2)c1ccc(cc1)C(F)(F)F	750	1
A157	c1cc(ccc1C(F)(F)F)[C@H]1C(c2c(N1)c(ccc2)C(=O)NO)(C)C	750	1
A158	c1ccc2c(c1C(=O)NO)CCN(C2)c1[nH]c2c(n1)cccc2	750	1
A159	c1ncccc1/C=C/C(=O)NCc1ccc(cc1)C(=O)Nc1ccc(cc1N)F	760	1

A160	c1(ccc(cc1)C(=O)NO)Cn1nc(nn1)c1ncccn1	762	1
A161	C(=O)(CCCCCCS)NC1CCCC1	776	1
A162	S(=O)(=O)(c1c(c(c(c(c1F)F)F)F)F)N(Cc1ccc(cc1)C(=O)NO)Cc1ccc(cc1)F	787	1
A163	c1c(ccc(c1)/C=C/C(=O)NO)/C=N/OCc1ccc(cc1)[N+](=O)[O-]	790	1
A164	O=S(=O)(c1cc(ccc1)C(C)(C)C)N(c1ccc(cc1)C(=O)NO)CC	802	1
A165	C1Cc2c(N(Cc3ccc(cc3)C(=O)NO)[C@H]3[C@H](C1)CCCC3)cc(cc2)C(F)(F)F	820	1
A168	C(=O)(CCCCc1nn(cc1)Cc1ccc(cc1)n1ccc2ccccc12)NO	897	1
A169	c1cc(ccc1/C=C/C(=O)NO)OC[C@@H](NC(=O)c1ccc(cc1)Cl)Cc1c2ccccc2[nH]c1	900	1
A170	N(Cc1ccc(cc1)C(=O)Nc1ccccc1N)C(=O)OCc1cccnc1	900	1
A171	c1cc2cc(c1)COC/C=C/COCc1c(ccc(Nc3nccc2n3)c1)OCCCCCCCC(=O)NO	930	1
A172	S(=O)(=O)(c1c(c(c(c(c1F)F)F)F)F)N(Cc1ccc(cc1)C(=O)NO)Cc1ncccc1	941	1
A173	c1cc(ccc1C(=O)NO)CN(S(=O)(=O)c1c(c(c(c(c1F)F)F)F)F)C(C)C	941	1
A175	C(CCCCC(=O)NO)ONC(=O)c1cc(c(cc1)C)C	997	1
A176	C(=O)(c1ccc(cc1)CNc1c2cccnc2ccc1)NO	1,004	0
A177	c1(ccc(cc1)C(=O)NO)Cn1c(nnn1)c1cccs1	1,015	0
A178	c1(ccc2c3c1cccc3c(=O)n(c2=O)CCCCCC(=O)NO)[N+](=O)[O-]	1,020	0
A181	C1c2c(N(Cc3ccc(cc3)C(=O)NO)[C@H]3[C@H]1CCCCC3)cccc2	1,200	0
A182	C(=C\c1nnn(c1)[C@H]1C[C@H](N(C1)Cc1ccccc1)CO)/C(=O)NO	1,200	0
A184	c1(ccc2c3c1cccc3c(=O)n(c2=O)CCCCCC(=O)NO)N(Cc1ccccc1)C	1,220	0
A185	c1c(ccc(c1)/C=C/C(=O)NO)C(=O)N[C@@H](Cc1c[nH]c2c1cccc2)C(=O)Nc1ccc(cc1)Cl	1,365	0
A186	N(C(=O)[C@H](CCCCCC(=O)NO)NC(=O)[C@H]1NC(=O)CCC1)C1CCCC1	1,440	0
A187	C1[C@H]2[C@H](N(Cc3ccc(cc3)C(=O)NO)c3c1cccc3)CCCC2	1,500	0
A188	c1c(ccc(c1)/C=C/C(=O)NO)C(=O)N[C@@H](Cc1c[nH]c2c1cccc2)C(=O)Nc1ccc(cc1)Br	1,577	0
A190	c1(c(c(cc(c1)/C=C\c1ccc(c(c1)/C=C/C(=O)Nc1ccccc1N)OC)OC)OC)OC	1,620	0
A191	c12cc(ccc1n(cc2)Cc1ccc(cc1)OC)C(=O)NO	1,700	0
A192	C(=O)(CCCCc1nn(cc1)Cc1ccc(cc1)c1ccccc1)NO	1,725	0
A193	C(CC)NNC(=O)c1ccc(cc1)c1ccc(cc1)CNC(=O)C	1,800	0
A194	C(=O)(CCCCCCS)NCCc1cc(ccc1)C	1,870	0
A195	c12c(c(cc(n1)C#N)N(c1cc(c(cc1)OC)/C=C/C(=O)NO)C)cccc2	1,900	0
A196	c1(ccccc1)CNc1ncc(cn1)C(=O)NNCCC	2,000	0
A197	C(=O)(CCCCCCS)NCc1ccc(cc1)C(F)(F)F	2,070	0
A198	C(CCCCC(=O)NO)ONC(=O)c1cc(ccc1)C	2,135	0
A199	c1cc(c(cc1)NC(=O)/C=C/c1nnn(c1)[C@H]1C[C@H](N(C1)Cc1ccccc1)CO)N	2,140	0
A200	C(=O)(CCCCc1nn(cc1)Cc1cc(ccc1)c1ccccc1)NO	2,342	0
A201	O=S1(=O)c2ccccc2N([C@@H]2[C@H](C1)CCCC2)Cc1ccc(cc1)C(=O)NO	2,400	0
A203	C1Cc2c(N(Cc3ccc(cc3)C(=O)NO)[C@H]3[C@H](C1)CCCC3)cccc2	2,400	0
A204	C1(NC(=O)CCCCCCC(=O)NO)CCCC1	2,630	0
A205	C[C@@H](/C=C/C(=O)NO)/C=C(\C)/C(=O)c1ccc(cc1)N(C)C	2,684	0
A206	c1(ccc(cc1)C(=O)Nc1ccccc1N)NC(=O)C	2,830	0
A207	ONC(=O)c1ccc(cc1)Cn1sc2ncccc2c1=O	2,840	0
A209	c1(c(cc(cc1F)C(=O)NO)F)Cn1nc(nn1)c1ncccn1	3,071	0
A210	c1c(ccc(c1)/C=C/C(=O)NO)C(=O)N[C@@H](Cc1c[nH]c2c1cccc2)C(=O)Nc1cc2c(cc1)cccc2	3,164	0
A211	c12c(c(nc(n1)C)N(c1cc(c(cc1)OC)/C=C/C(=O)NO)C)cccc2	3,200	0

A214	c1cc(ccc1C(=O)NO)C(=O)N[C@@H](c1c2c([nH]c1)cccc2)C(=O)Nc1ccc(cc1)C	3,500	0
A215	C1[C@H]2C[C@@H]3C[C@@H](C[C@]1(C3)N(c1ncc(cn1)C(=O)NO)C)C2	3,600	0
A218	C(=O)(Cc1ccccc1)N(CCO)C(=O)Cc1ccc(cc1)C(=O)NO	3,705	0
A219	c1ccc2c(c1)n(c1c2CN(CC1)C)Cc1ccc(cc1)C(=O)NO	3,790	0
A221	C(=C\C(=O)NO)/c1cc(ccc1)S(=O)(=O)N[C@H](C(=O)Nc1c2ccccc2ccc1)c1ccccc1	3,850	0
A222	c1c(ccc(c1)/C=C/C(=O)NO)C(=O)N[C@@H](Cc1c[nH]c2c1cccc2)C(=O)Nc1cccc(c1)Br	3,962	0
A223	c1ccc2c(c1)N(c1c(S2)cccc1)Cc1ncc(cc1)C(=O)NO	4,304	0
A224	c1(nccc(c1)/C=C/c1ccc(cc1)C(=O)NO)c1c(cc(cc1)C)F	4,930	0
A225	N(C(=O)CCCC(=O)NCCc1ccccc1)O	5,000	0
A226	c1(c(c(cc(c1)C(=C)c1ccc2c(c1)c(cn2C)/C=C/C(=O)NO)OC)OC)OC	5,000	0
A227	c1ccc(CCNC(=O)CCCNC(=O)OCC)cc1	5,000	0
A228	c1(ccc(cc1)/C=C/C(=O)NO)c1ccc(cc1)O	5,010	0
A229	o1c(cc(n1)C(=O)NO)CCNC(=O)c1cc(c(cc1)Cl)Cl	5,120	0
A230	ONC(=O)CCCCCn1c(=O)c2cccc3cccc(c1=O)c23	5,200	0
A231	C1c2cc(ccc2N(CC1)Cc1ccc(cc1)C(=O)NO)C(=O)N	5,310	0
A232	c1c(ccc(c1)/C=C/C(=O)NO)/C=N/OCc1c(c(c(c(c1F)F)F)F)F	5,480	0
A233	c1c(cc2c(c1)c(=O)n(c(=O)n2Cc1ccc(cc1)C(=O)NO)CCc1ccccc1)O	5,501	0
A234	C(=O)(/C=C/c1ccc(cc1)C(F)(F)F)NO	5,530	0
A235	c1(cc(cc(c1Cn1c(nnn1)c1sccc1)F)C(=O)NO)F	5,662	0
A236	c1c(c([nH]c1c1ccc(cc1)O)C(=O)NCc1ccc(cc1)C(=O)Nc1c(cccc1)N)c1ccoc1	5,662	0
A237	n1(c(=O)n(c(=O)c2c1scc2)CCc1ccccc1)Cc1ccc(cc1)C(=O)NO	5,686	0
A238	C(=O)(CCCCCC(c1c[nH]c2c1cccc2)c1c[nH]c2c1cccc2)Nc1ccccc1N	5,800	0
A240	c1(cc(on1)CN1CCOCC1)c1ccc(cc1)/C=C/C(=O)NO	6,260	0
A241	n1c(nc2c(c1N1CCOCC1)ccn2CCCCCCC(=O)NO)c1cnc(nc1)N	6,300	0
A242	c1c(cc2c(c1)c(=O)n(c(=O)n2Cc1ccc(cc1)C(=O)NO)CCc1ccccc1)C(F)(F)F	7,392	0
A243	c1(c(c(cc(c1)C(=C)c1ccc(cc1/C=C/C(=O)NO)OC)OC)OC)OC	8,000	0
A244	c1(ccc2c3c1cccc3c(=O)n(c2=O)CCCCCC(=O)Nc1c(cccc1)N)N1CCOCC1	8,120	0
A245	C1[C@H]2C[C@]3(C[C@@H]1C[C@H](C3)C2)c1c(ccc(c1)c1ccc(cc1)C=CC(=O)O)O[C@@H](C(=O)NO)C	8,230	0
A246	C(CCCCC)NNC(=O)c1cccc(c1)NCc1ccccc1	8,600	0
A249	S1Cc2c(CC1)n(c1c2cc(cc1)F)Cc1ccc(cc1)C(=O)NO	9,700	0
A251	c1(ncnc2c1nc[nH]2)N[C@H](c1nc(c2c(n1)cccc2)CCCCCC(=O)NO)CC	9,819	0
A252	C1[C@@H]2C[C@@H]3C[C@H]1C[C@](C2)(C3)CN(Cc1c(cc(cc1)C(=O)NO)F)C	10,000	0
A253	c1ccc(cc1)NC(=O)CCCCCC(=O)NO	10,000	0
A254	c1(c(c(cc(c1)C(=C)c1ccc(c(c1)/C=C/C(=O)NO)OC)OC)OC)OC	10,000	0
A255	c1ccc2c(c1)c(=O)n(c(=O)n2Cc1ccc(cc1)C(=O)NO)CCc1cccs1	10,020	0
A256	C(=O)(/C=C/c1ccc(cn1)NC(=O)[C@H](Cc1ccccc1)c1ccccc1)NO	10,200	0
A257	c1c(cc2c(c1)c(=O)n(c(=O)n2Cc1ccc(cc1)C(=O)NO)CCc1ccccc1)C1CC1	10,500	0
A258	c1ccc2c(c1)c(=O)n(c(=O)n2Cc1ccc(cc1)C(=O)NO)CCc1cc(ccc1)F	10,660	0
A259	c1c(ccc(c1)/C=C/C(=O)NO)/C=N/OCc1ccc(cc1)C(=O)OC	10,800	0
A260	c1(c(c(cc(c1)C(=C)c1ccc(c(c1)C#CCCC(=O)NO)OC)OC)OC)OC	11,000	0
A261	c1ccc2c(c1)c(=O)n(c(=O)n2Cc1ccc(cc1)C(=O)NO)CCc1ccc(cc1)O	11,290	0
A262	c1c(c(cc(c1)C(=O)NO)F)Cn1c(nc2c1cccc2)C	12,900	0
A263	c1ccc2c(c1)c(=O)n(c(=O)n2Cc1ccc(cc1)C(=O)NO)CCc1ccc(cc1)OC	13,850	0

A264	c1ccc2c(c1)c(=O)n(c(=O)n2Cc1ccc(cc1)C(=O)NO)CCc1ccccc1	13,900	0
A265	c1([C@H]2CN(C[C@@H]2C(=O)Nc2ccc(cc2)Cl)C)ccc(/C=C/C(=O)Nc2c(cccc2)N)cc1	14,000	0
A266	c1cccc(c1)NC(=O)[C@@H](CCCCCS)NC(=O)[C@H]1NC(=O)CCC1	14,200	0
A267	c1ccc2c(c1)c(=O)n(c(=O)n2Cc1ccc(cc1)C(=O)NO)CCc1ccc(cc1)F	14,730	0
A268	c1c(ccc(c1)C(=O)NO)NCc1csc2c1cc(cc2)Br	15,000	0
A269	c1c(cc2c(c1)c(=O)n(c(=O)n2Cc1ccc(cc1)C(=O)NO)CCc1ccccc1)F	15,400	0
A270	c1ccc2c(c1)c(c([nH]2)C)/C=C/c1c(cccc1)c1ccc(cc1)/C=C/C(=O)NO	16,200	0
A272	c1(ccc2c(c1)c(=O)n(c(=O)n2Cc1ccc(cc1)C(=O)NO)CCc1ccccc1)F	16,740	0
A275	c1([C@@H]2CN(C[C@H]2C(=O)Nc2ccc(cc2)Cl)C)ccc(/C=C/C(=O)Nc2c(cccc2)N)cc1	20,000	0
A278	N1CC2(OC1=O)CCN(c1ccc(cn1)C(=O)Nc1c(ccc(c1)c1sccc1)N)CC2	25,000	0
A279	c1cccc(c1)NS(=O)(=O)c1cc(ccc1)/C=C/C(=O)NO	25,000	0
A280	c1cnc2c(c1)c(=O)n(c(=O)n2Cc1ccc(cc1)C(=O)NO)CCc1ccccc1	25,050	0
A281	C1N(Cc2n(C1)cc(c2)C(=O)NO)C(=O)c1cccn1C	29,000	0
A282	[C@H](CCCCCS)(C(=O)NC1CCCC1)NC(=O)OC(C)(C)C	30,700	0
A283	c1ccc(cc1)/C=C/c1scc(n1)CCCC(=O)NO	32,800	0
A284	c1ccc2c(c1)c(=O)n(c(=O)n2Cc1ccc(cc1)C(=O)NO)CCc1c(cccc1)OC	34,370	0
A285	C(/C(=C/c1ccc(cc1)/C=C/C(=O)NO)/c1ccc(cc1)F)NC1CC1	37,000	0
A286	c1ccc2c(c1)c(=O)n(c(=O)n2Cc1ccc(cc1)C(=O)NO)Cc1ccccc1	37,500	0
A287	C(=O)(NO)/C=C/C=C/c1ccc(c2ccc(c(c2)[C@]23C[C@@H]4C[C@H](C2)C[C@@H](C4)C3)OC)cc1	38,000	0
A288	c1cc(ccc1C(=O)NNCCCC)Br	44,500	0
A289	c1c(cc2c(c1)c(=O)n(c(=O)n2Cc1ccc(cc1)C(=O)NO)CCc1ccccc1)C	52,050	0
A290	c1(c(ccc(c1)c1ccc(cc1)/C=C/C(=O)NO)O)[C@]12C[C@@H]3C[C@H](C1)C[C@@H](C3)C2	57,000	0
A291	c1(cc(ccc1CC#N)c1c(cc(cc1)/C=C/C(=O)NO)Cl)[C@]12C[C@@H]3C[C@H](C1)C[C@@H](C3)C2	63,000	0
A293	c1c(cc2c(c1)cc(c(=O)o2)C(=O)/C=C/C=C/c1ccc(c(c1)OC)OC)OC	74,000	0
A297	N1(C(=O)c2c(C1)c(ccc2)C(=O)NO)c1oc2c(n1)cc(cc2)C(F)(F)F	<500	1
A298	N1(Cc2c(C1)c(ccc2)C(=O)NO)c1[nH]c2c(n1)cc(c(c2)c1ccccc1)C(F)(F)F	<500	1
A299	c12c(c(ccc1)C(=O)NO)[nH]c(c2)c1ncc(nc1)C(F)(F)F	<500	1
A301	c12c(c(ccc1)C(=O)NO)N[C@H](C2)c1ccc(cc1)C(F)(F)F	<500	1
A302	c1cc(ncc1C(F)(F)F)[C@@H]1C(c2c(N1)c(ccc2)C(=O)NO)(C)C	<500	1
A303	n1cc(ncc1C(F)(F)F)[C@H]1C(c2c(N1)c(ccc2)C(=O)NO)(C)C	<500	1
A305	N1(Cc2c(C1)c(ccc2)C(=O)NO)c1[nH]c2c(n1)CC[C@H](C2)C(F)(F)F	<500	1
A306	N1(Cc2c(C1)c(ccc2)C(=O)NO)c1[nH]c2c(n1)CC[C@@H](C2)C(F)(F)F	<500	1
A308	c1c(cc2c(c1)sc(n2)N1Cc2c(C1)c(ccc2)C(=O)NO)C(F)(F)F	<500	1
A309	C1[C@@H](Cc2c(C1)oc(n2)N1Cc2c(C1)c(ccc2)C(=O)NO)C(F)(F)F	<500	1
A310	c1(ccc2c(c1)oc(n2)N1C(c2c(C1)c(ccc2)C(=O)NO)(C)C)C(F)(F)F	<500	1
A311	C1[C@@H](Cc2c(C1)oc(n2)N1C(c2c(C1)c(ccc2)C(=O)NO)(C)C)C(F)(F)F	<500	1
A312	[C@H]1(CCc2c(C1)oc(n2)N1C(c2c(C1)c(ccc2)C(=O)NO)(C)C)C(F)(F)F	<500	1
A313	c1c(cc2c(c1)sc(n2)N1C(c2c(C1)c(ccc2)C(=O)NO)(C)C)C(F)(F)F	<500	1
A314	c1ncc2c(c1)oc(n2)N1C(c2c(C1)c(ccc2)C(=O)NO)(C)C	<500	1
A315	c1ccc2c(c1)sc(n2)N1C(c2c(C1)c(ccc2)C(=O)NO)(C)C	<500	1
A316	c1ccc2c(c1)nc(cc2)N1Cc2c(C1(C)C)cccc2C(=O)NO	<500	1
A317	c1c(cc2c(c1)nc(cc2)N1Cc2c(C1(C)C)cccc2C(=O)NO)C(F)(F)F	<500	1
A320	c1(N2C(c3c(C2)c(ccc3)C(=O)NO)(C)C)oc2c(n1)nc(cc2)C(F)(F)F	<500	1

A321	c1(N2C(c3c(C2)c(ccc3)C(=O)NO)(C)C)oc2c(n1)ncc(c2)C(F)(F)F	<500	1
A322	c1(N2C(c3c(C2)c(ccc3)C(=O)NO)(C)C)nc(c(cc1)C(F)(F)F)C#N	<500	1
A325	N1(C(c2c(C1)c(ccc2)C(=O)NO)(C)C)C(=O)Nc1cc(ncc1)C(F)(F)F	<500	1
A326	N1(C(c2c(C1)c(ccc2)C(=O)NO)(C)C)C(=O)Nc1nccc(c1)C(F)(F)F	<500	1
A327	[N+](=O)(c1c(cc2c([nH]c(n2)Nc2cc(C(=O)NO)ccc2)c1)Cl)[O-]	<500	1
A328	c1c2c(nc([nH]2)Nc2cc(C(=O)NO)ccc2)cc(c1F)Br	<500	1
A329	C(c1c(cc2c([nH]c(n2)Nc2cc(C(=O)NO)ccc2)c1)C#C)(F)(F)F	<500	1
A330	c1c2c(nc([nH]2)Nc2cc(C(=O)NO)ccc2)ccc1C(F)(F)F	<500	1
A331	c1c2c(nc(n2C)Nc2cc(C(=O)NO)ccc2)cc(c1c1cnccc1)C(F)(F)F	<500	1
A332	c1c2c(nc(n2C)Nc2cc(C(=O)NO)ccc2)cc(c1c1ccccc1)C(F)(F)F	<500	1
A333	c1c2c(nc([nH]2)Nc2cc(C(=O)NO)ccc2)cc(c1C(F)(F)F)c1ccccc1	<500	1
A334	c1c2c(nc([nH]2)Nc2cc(C(=O)NO)ccc2)cc(c1c1cccnc1)C(F)(F)F	<500	1
A335	c1c2c(nc([nH]2)Nc2cc(C(=O)NO)ccc2)cc(c1C(F)(F)F)c1ccncc1	<500	1
A336	c1c2c(nc([nH]2)Nc2cc(C(=O)NO)ccc2)cc(c1c1cccc(c1)OCC)C(F)(F)F	<500	1
A337	c1c2c(nc([nH]2)Nc2cc(C(=O)NO)ccc2)cc(c1c1ccc(cc1)SC)C(F)(F)F	<500	1
A338	c1c2c(nc([nH]2)Nc2cc(C(=O)NO)ccc2)cc(c1c1ccc(cc1)C(=O)N(C)C)C(F)(F)F	<500	1
A341	ONC(=O)c1cc(ccc1)Nc1[nH]c2c(n1)cc(c(c2)C(F)(F)F)c1cc2OC=COc2cc1	<500	1
A342	c1c2c(nc([nH]2)Nc2cc(C(=O)NO)ccc2)cc(c1c1cccc(c1)O)C(F)(F)F	<500	1
A343	c1c2c(nc([nH]2)Nc2cc(C(=O)NO)ccc2)cc(c1c1ccccc1CO)C(F)(F)F	<500	1
A345	c1c2c(nc([nH]2)Nc2cc(C(=O)NO)ccc2)cc(c1c1cnc(nc1)N1CCOCC1)C(F)(F)F	<500	1
A346	c1c2c(nc([nH]2)Nc2cc(C(=O)NO)ccc2)cc(c1c1cc(ccc1)C(=O)N1CCOCC1)C(F)(F)F	<500	1
A348	c1c2c(nc([nH]2)Nc2cc(C(=O)NO)ccc2)cc(c1c1cc(ccc1)COC)C(F)(F)F	<500	1
A349	c1c2c(nc([nH]2)Nc2cc(C(=O)NO)ccc2)cc(c1c1cc2c(cc1)cnn2C)C(F)(F)F	<500	1
A350	c1c2c(nc([nH]2)Nc2cc(C(=O)NO)ccc2)cc(c1c1cc(ccc1)C(=O)N(C)C)C(F)(F)F	<500	1
A351	c1c2c(nc([nH]2)Nc2cc(C(=O)NO)ccc2)cc(c1c1ccc(cc1)N1CCOCC1)C(F)(F)F	<500	1
A352	c1c2c(nc([nH]2)Nc2cc(C(=O)NO)ccc2)cc(c1c1cocc1)C(F)(F)F	<500	1
A353	c1ccc2c(c1C(=O)NO)C[C@]1(C2)C(=O)N(CC1)Cc1ccc(cc1)Cl	<500	1
A354	c1ccc2c(c1C(=O)NO)C[C@@]1(C2)C(=O)N(CC1)Cc1ccc(c(c1)C(F)(F)F)Cl	<500	1
A355	Clc1c(cc(CN2C(=O)[C@@]3(CC2)Cc2cccc(c2C3)C(=O)NO)cc1)C(F)(F)F	<500	1
A356	Fc1cc(CN2C(=O)[C@@]3(CC2)Cc2cccc(c2C3)C(=O)NO)ccc1C(F)(F)F	<500	1
A357	c1cc2c(c(c1)C(=O)NO)C[C@]1(C2)C(=O)N(CC1)Cc1ccc(cc1)C(F)(F)F	<500	1
A359	c12c(cccc1C(=O)NO)C[C@]1(C2)CCN(C1=O)Cc1cccc(c1)c1ccccc1	<500	1
A360	c12c(cccc1C(=O)NO)C[C@]1(C2)CCN(C1=O)Cc1cccc(c1Cl)Cl	<500	1
A361	c12c(cccc1C(=O)NO)C[C@@]1(C2)CCN(C1=O)Cc1ccc(cc1)OC(F)(F)F	<500	1
A362	c12c(cccc1C(=O)NO)C[C@]1(C2)CCN(C1=O)Cc1cccc(c1)Cl	<500	1
A365	c12c(cccc1C(=O)NO)C[C@]1(C2)CCN(C1=O)Cc1ccccc1c1ccccc1	<500	1
A366	c12c(cccc1C(=O)NO)C[C@@]1(C2)CCN(C1=O)Cc1ccc(c(c1)Cl)Cl	<500	1
A367	c12c(cccc1C(=O)NO)C[C@]1(C2)CCN(C1=O)Cc1ccc(cc1)OCc1ccccc1	<500	1
A368	c12c(cccc1C(=O)NO)C[C@@]1(C2)CCN(C1=O)Cc1cccc(c1)OC(F)(F)F	<500	1
A369	c12c(cccc1C(=O)NO)C[C@]1(C2)CCN(C1=O)Cc1cccc(c1F)C(F)(F)F	<500	1
A370	c1(cccc2c1C[C@]1(CC2)C(=O)N(CC1)Cc1cc(c(cc1)Cl)C(F)(F)F)C(=O)NO	<500	1
A372	c12c(c(ccc1)C(=O)NO)OC1(CC2)CCN(CC1)C(=O)C1(CC1)c1cc(ccc1)C(F)(F)F	<500	1
A375	c12c(c(ccc1)C(=O)NO)CC[C@@]1(C2)C(=O)N(CC1)Cc1ccc(c(c1)F)C(F)(F)F	<500	1

A377	c1c(c(cc2c1oc(n2)Nc1cccc(c1)C(=O)NO)C(F)(F)F)C#C	<500	1
A380	c1c(c(cc2c1oc(n2)Nc1cccc(c1C)C(=O)NO)Cl)Cl	<500	1
A381	c1(c(cc2c(c1)oc(n2)Nc1cc(C(=O)NO)ccc1F)Cl)Cl	<500	1
A382	c1(c(cc2c(c1)oc(n2)Nc1cc(C(=O)NO)cnc1)Cl)Cl	<500	1
A385	c1(c(cc2c(c1)sc(n2)Nc1cc(C(=O)NO)ccc1)Cl)Cl	<500	1
A386	c1(c(cc2c(c1)nc([nH]2)Nc1cc(C(=O)NO)ccc1)S(=O)(=O)C)C(F)(F)F	<500	1
A387	c1(c(cc2c(c1)nc([nH]2)N(c1cc(C(=O)NO)ccc1)C)C#N)C(F)(F)F	<500	1
A389	c1c2c(cc(c1C(F)(F)F)C#N)n(c(n2)Nc1cc(C(=O)NO)ccc1)C	<500	1
A390	c1c2c(cc(c1F)C#N)n(c(n2)Nc1cc(C(=O)NO)ccc1)C	<500	1
A391	c1c2c(cc(c1Cl)Cl)n(c(n2)Nc1cc(C(=O)NO)ccc1)C	<500	1
A392	c1c2c(cc(c1C(F)(F)F)C#N)n(c(n2)Nc1cc(C(=O)NO)ccc1)C(C)C	<500	1
A393	c1c2c(cc(c1C#N)C(F)(F)F)n(c(n2)Nc1cc(C(=O)NO)ccc1)C(C)C	<500	1
A395	c1c2c(cc(c1c1ccccc1)C(F)(F)F)n(c(n2)Nc1cc(C(=O)NO)ccc1)C(C)C	<500	1
A396	c1c2c(cc(c1Cl)Cl)n(c(n2)Nc1cc(C(=O)NO)ccc1)C(C)C	<500	1
A397	c1c2c(cc(c1C(F)(F)F)c1ccccc1)n(c(n2)Nc1cc(C(=O)NO)ccc1)CCOC	<500	1
A399	c1c(c(cc2c1nc(n2CCCCCC)Nc1cccc(c1)C(=O)NO)C(F)(F)F)C#N	<500	1
A400	N(c1cc(C(=O)NO)ccc1)c1n(c2c(n1)cc(c(c2)Cl)Cl)CCCCCN	<500	1
A401	N(c1cc(C(=O)NO)ccc1)c1n(c2c(n1)cc(c(c2)F)Cl)CCCCCN	<500	1
A402	c1(c(cc2c(c1)nc([nH]2)Nc1cc(C(=O)NO)ccc1)C)C	<500	1
A404	c1(c(cc2c(nc([nH]2)Cc2cc(C(=O)NO)ccc2)c1)Cl)Cl	<500	1
A405	c1(c(cc2c([nH]c(c2)Nc2cc(C(=O)NO)ccc2)c1)Cl)Cl	<500	1
A406	c1c2c(oc(n2)Nc2nc(C(=O)NO)ccc2)cc(c1Cl)Cl	<500	1
A407	n1c2c(oc(n2)Nc2cc(C(=O)NO)ccc2)cc(c1)C(F)(F)F	<500	1
A408	c1c2c(nc([nH]2)Nc2cc(C(=O)NO)ccc2)cc(Cl)c1F	<500	1
A409	c1c2c(nc([nH]2)Nc2cc(C(=O)NO)ccc2)cc(c1Cl)C	<500	1
A410	c1c2c(nc([nH]2)Nc2cc(C(=O)NO)ccc2)cc(c1F)C(F)(F)F	<500	1
A411	c1c2c(nc([nH]2)Nc2cc(C(=O)NO)ccc2)cc(c1Cl)C(F)(F)F	<500	1
A412	c1c2c(nc([nH]2)Nc2cc(C(=O)NO)ccc2)cc(C(F)(F)F)c1Br	<500	1
A413	c1c2c(nc([nH]2)Nc2cc(C(=O)NO)ccc2)cc(C)c1F	<500	1
A414	c1c(c(cc2c1oc(n2)Nc1cc(cc(c1)C(=O)NO)C)Br)C(F)(F)F	<500	1
A415	c1c2c(nc([nH]2)Nc2cc(C(=O)NO)ccc2)cc(C)c1Br	<500	1
A417	c1c2c(cc(c1C(F)(F)F)C#N)n(c(n2)Nc1cc(C(=O)NO)ccc1)CCOC	<500	1
A418	N(c1cc(C(=O)NO)ccc1)c1n(c2c(n1)cc(c(c2)C(F)(F)F)C#N)CCCCCN	<500	1
A420	c1c2c(nc([nH]2)Nc2cc(C(=O)NO)ccc2)cc(c1Cl)[N+](=O)[O-]	<500	1
A421	c1c2c(nc([nH]2)Nc2cc(C(=O)NO)ccc2)cc(c1C#N)C(F)(F)F	<500	1
A422	c1c2c(nc([nH]2)Nc2cc(C(=O)NO)ccc2)cc(c1C(F)(F)F)c1ccc2c(c1)OCCO2	<500	1
A424	c1ccc2c(c1C(=O)NO)C[C@]1(C2)C(=O)N(CC1)Cc1ccc(c(c1)F)C(F)(F)F	<500	1
A425	c1(c(cc2c(c1)oc(n2)Nc1cc(ccc1)C(=O)NO)C(F)(F)F)C#N	<500	1
A426	c1(c(cc2c(c1)oc(n2)Nc1cccc(C(=O)NO)c1F)Cl)Cl	<500	1
A427	c1(c(cc2c(c1)oc(n2)Nc1cc(C(=O)NO)ncc1)Cl)Cl	<500	1
A430	c1cc(ccc1C(=O)NO)CN(Cc1cc(c(c(c1F)F)F)F)C(C)C	>1000	0
A432	c1cc2c(cc1C(=O)NO)CCN(C2)S(=O)(=O)c1cc(c(c(c1F)F)F)F	>1000	0
A433	C(=O)(c1c(c(c(c(c1F)F)F)F)F)N(C(C)C)Cc1ccc(cc1)C(=O)NO	>1000	0

A435	C(=O)(c1ccc(cc1)CN(C(=O)Nc1ccccc1)CCCC)NO	>1000	0
A436	N1(Cc2c(C1)c(ccc2)C(=O)NO)c1nc(ccc1)C(F)(F)F	>1000	0
A437	c1c(cc2c(c1)CCN(C2)c1[nH]c2c(n1)cccc2)C(=O)NO	>1000	0
A438	c1(ccc2c(c1)CCN(C2)c1[nH]c2c(n1)cccc2)C(=O)NO	>1000	0
A439	c1cc(c2c(c1)CCN(C2)c1[nH]c2c(n1)cccc2)C(=O)NO	>1000	0
A441	c1([nH]c(c(n1)C)C)N1Cc2c(cccc2C1)C(=O)NO	>1000	0
A443	c12c(c(ccc1)C(=O)OC)CN(C2(C)C)c1ncc(nc1)C(F)(F)F	>1000	0
A445	S(=O)(=O)(c1c(c(c(c(c1F)F)F)F)F)N(Cc1ccc(cc1)C(=O)NO)Cc1ccc(cc1)N(C)C	>1000	0
A446	S(=O)(=O)(c1c(c(c(c(c1F)F)F)F)F)N(Cc1ccc(cc1)C(=O)NO)Cc1ccncc1	>1000	0
A448	S(=O)(=O)(c1c(c(c(c(c1)F)F)F)F)N(Cc1ccc(cc1)C(=O)NO)Cc1cnccc1	>1000	0
A451	O=S(=O)(N(Cc1ccc(cc1)C(=O)NO)C1CC1)c1c(c(cc(c1F)F)F)F	>1000	0
A452	O=S(=O)(N(Cc1ccc(cc1)C(=O)NO)C1CC1)c1ccc(cc1)F	>1000	0
A453	O=S(=O)(N(Cc1ccc(cc1)C(=O)NO)C1CC1)c1cc(c(c(c1)F)F)F	>1000	0
A455	O=S(=O)(N(Cc1cccc(c1)C(=O)NO)C1CC1)c1c(c(c(c(c1F)F)F)F)F	>1000	0
A457	O=S(=O)(N(Cc1ccc(cc1)C(=O)NO)C1CC1)c1c(c(c(c(c1F)F)Cl)F)F	>1000	0
A458	O=S(=O)(N(Cc1ccc(cc1)C(=O)NO)C1CC1)c1cc(c(c(c1F)F)F)F	>1000	0
A461	c1cc(ccc1C(=O)NO)CN(S(=O)(=O)c1cc(c(c(c1F)F)F)F)C1CCCC1	>1000	0
A462	c1nc(ccc1C(=O)NO)CN(S(=O)(=O)c1cc(c(c(c1F)F)F)F)C(C)C	>1000	0
A463	c1cc(ccc1C(=O)NO)CN(S(=O)(=O)c1cc(c(c(c1F)F)F)F)CC(C)C	>1000	0
A464	C(=O)(c1ccc(cc1)C(C)(C)C)N(Cc1ccc(cc1)C(=O)NO)C1CC1	>1000	0
A465	C(=O)(c1c(c(c(c(c1F)F)F)F)F)N(Cc1ccc(cc1)C(=O)NO)C1CC1	>1000	0
A466	C(=O)(c1c(c(c(c(c1F)F)F)F)F)NCc1ccc(cc1)/C=C/C(=O)NO	>1000	0
A467	C(=O)(c1c(c(c(c(c1F)F)F)F)F)N(Cc1ccc(cc1)/C=C/C(=O)NO)C1CC1	>1000	0
A468	C(=O)(c1ccc(cc1)C(C)(C)C)N(c1ccc(cc1)C(=O)NO)CC	>1000	0
A469	C(=O)(c1c(c(c(c(c1F)F)F)F)F)N(C)Cc1ccc(cc1)C(=O)NO	>1000	0
A470	c1c(ccc(c1)/C=C/C(=O)NO)CN(C[C@]12C[C@H]3C[C@H](C[C@@H](C1)C3)C2)C	>1000	0
A471	c1(c(ccc(c1)/C=C/C(=O)NO)CN(C[C@]12C[C@H]3C[C@H](C[C@@H](C1)C3)C2)C)F	>1000	0
A472	N1(Cc2c(C1)c(ccc2)C(=O)NO)c1[nH]c(cn1)CCC	>1000	0
A473	N1(Cc2c(C1)c(ccc2)C(=O)NO)c1[nH]c2c(n1)cncc2	>1000	0
A474	N1(Cc2c(C1)c(ccc2)C(=O)NO)c1[nH]c2c(n1)nccc2	>1000	0
A475	N1(Cc2c(C1)c(ccc2)C(=O)NO)c1nc2c(o1)cncc2	>1000	0
A476	N1(Cc2c(C1)c(ccc2)C(=O)NO)c1nc2c(o1)nccc2	>1000	0
A477	n1c(nc2c(c1)cccc2)N1Cc2c(C1)c(ccc2)C(=O)NO	>1000	0
A478	c1c(nc2c(c1)nccc2)N1Cc2c(C1)c(ccc2)C(=O)NO	>1000	0
A479	N1(Cc2c(C1)c(ccc2)C(=O)NO)c1[nH]c(cn1)C	>1000	0
A480	c1cnc2c(c1)ncc(c2)N1Cc2c(C1)c(ccc2)C(=O)NO	>1000	0
A481	c1c(cc2c(c1)OCCN2)N1Cc2c(C1)c(ccc2)C(=O)NO	>1000	0
A482	c1cnc2c(c1)sc(n2)N1Cc2c(C1)c(ccc2)C(=O)NO	>1000	0
A483	C1NCc2c(C1)nc([nH]2)N1Cc2c(C1)c(ccc2)C(=O)NO	>1000	0
A484	C1N(Cc2c(C1)nc([nH]2)N1Cc2c(C1)c(ccc2)C(=O)NO)C(=O)C	>1000	0
A485	c1cnc2c(c1)sc(n2)N1C(c2c(C1)c(ccc2)C(=O)NO)(C)C	>1000	0
A487	C(=O)(N1C(c2c(C1)c(ccc2)C(=O)NO)(C)C)c1ccc(cc1)C(F)(F)F	>1000	0
A488	C(=O)(N1C(c2c(C1)c(ccc2)C(=O)NO)(C)C)c1cc(ccc1)C(F)(F)F	>1000	0

A489	N1(C(c2c(C1)c(ccc2)C(=O)NO)(C)C)C(=O)Nc1ncc(cc1)C(F)(F)F	>1000	0
A490	N1(C(c2c(C1)c(ccc2)C(=O)NO)(C)C)C(=O)Nc1cncc(c1)C(F)(F)F	>1000	0
A492	N1(C(c2c(C1)c(ccc2)C(=O)NO)(C)C)C(=O)Nc1oc2c(n1)cccc2	>1000	0
A493	N1(C(c2c(C1)c(ccc2)C(=O)NO)(C)C)Cc1ccc(cc1)OC	>1000	0
A494	N1(Cc2c(C1)c(ccc2)C(=O)NO)c1[nH]c2c(n1)cccc2c1ccccc1	>1000	0
A495	N1(C(=O)c2c(C1)c(ccc2)C(=O)NO)c1oc2c(n1)cccc2	>1000	0
A496	[C@H]1(Nc2c(C1)c(ccc2)C(=O)NO)c1ccc(cc1)C(F)(F)F	>1000	0
A497	c12c(c(ccc1)C(=O)NO)N[C@@H](C2)c1ccc(cc1)C(F)(F)F	>1000	0
A499	n1cc(ncc1C(F)(F)F)[C@@H]1C(c2c(N1)c(ccc2)C(=O)NO)(C)C	>1000	0
A501	N1(Cc2c(C1)c(ccc2)C(=O)NO)c1n(c2c(n1)cccc2)CCOC	>1000	0
A502	N1(Cc2c(C1)c(ccc2)C(=O)NO)C(=O)[C@H](c1ccc(cc1)OC)CC	>1000	0
A503	N1(Cc2c(C1)c(ccc2)C(=O)NO)C(=O)c1ccccc1	>1000	0
A504	N1(Cc2c(C1)c(ccc2)C(=O)NO)Cc1ccc(cc1)OC	>1000	0
A506	N1(Cc2c(C1)c(ccc2)C(=O)NO)C1=N[C@@](C(=N1)c1ccccc1)(O)C(F)(F)F	>1000	0
A507	c1(cc(ccc1)C(=O)Nc1ccc(cc1)C(=O)NO)C(C)(C)C	>1000	0
A508	c1(cc(ccc1)C(=O)N(c1ccc(cc1)C(=O)NO)CC)C(C)(C)C	>1000	0
A509	c1(cc(ccc1)C(=O)N(c1ccc(cc1)C(=O)NO)CC)C(F)(F)F	>1000	0
A510	O=S(=O)(c1cc(cc(c1)C(F)(F)F)C(F)(F)F)N(c1ccc(cc1)C(=O)NO)CC	>1000	0
A511	c1(cc(cc(c1)C(C)(C)C)C(=O)N(c1ccc(cc1)C(=O)NO)CC)C(C)(C)C	>1000	0
A513	c1c(c(ccc1)C(=O)N(c1ccc(cc1)C(=O)NO)CC)C(F)(F)F	>1000	0
A514	c1(cc(ccc1)CN(c1ccc(cc1)C(=O)NO)C(=O)C)C(F)(F)F	>1000	0
A515	c1(cc(cc(c1)C(F)(F)F)CN(c1ccc(cc1)C(=O)NO)C(=O)C)C(F)(F)F	>1000	0
A516	c1(cc(ccc1)C(=O)N(c1ccc(cc1)C(=O)NO)CC1CC1)C(F)(F)F	>1000	0
A517	c1(cc(ccc1)C(=O)N(c1ccc(cc1)C(=O)NO)C(C)C)C(F)(F)F	>1000	0
A519	c1(cc(cc(c1)C(C)(C)C)C(=O)N(c1ccc(cc1)C(=O)NO)CC1CC1)C(C)(C)C	>1000	0
A521	c1(cc(ccc1)C(=O)N(c1ccc(cc1)C(=O)NO)C(C)C)OC(F)(F)F	>1000	0
A523	c1(cc(ccc1F)C(=O)N(c1ccc(cc1)C(=O)NO)C(C)C)C(F)(F)F	>1000	0
A525	c1(cc(ccc1)NC(=O)c1ccc(cc1)C(=O)NO)C(C)(C)C	>1000	0
A527	c1cc(ccc1NC(=O)c1ccc(cc1)C(C)(C)C)C(=O)NO	>1000	0
A528	C(=O)(c1ccc(cc1)NC(=O)c1ccc(cc1)C)NO	>1000	0
A530	FC(F)(F)c1ccc(C(=O)Nc2ccc(cc2)C(=O)NO)cc1	>1000	0
A532	C(=O)(c1ccc(cc1)NC(=O)Cc1ccc(cc1)C(C)(C)C)NO	>1000	0
A533	C(=O)(c1ccc(cc1)C(C)(C)C)NCc1ccc(cc1)C(=O)NO	>1000	0
A534	O=S(=O)(NCc1ccc(C(=O)NO)cc1)c1ccc(cc1)C(C)(C)C	>1000	0
A537	c12c(c(ccc1)C(=O)NO)C[C@@]1(C2)CCN(CC1)C1CC1	>1000	0
A539	c12c(CC3(C2=O)CCN(CC3)Cc2ccccc2)c(ccc1)C(=O)NO	>1000	0
A540	c12c(CC3([C@H]2O)CCN(CC3)Cc2ccccc2)c(ccc1)C(=O)NO	>1000	0
A541	c12c(c(ccc1)C(=O)NO)C[C@@]1(CC2)C(=O)N(CC1)Cc1ccc(cc1)Cl	>1000	0
A544	c1(cccc2c1OC1(CC2)CCN(CC1)C(=O)N(C)C)C(=O)NO	>1000	0
A545	c12c(c(ccc1)C(=O)NO)OC1(CC2)CCN(CC1)C(=O)c1ccc(cc1)F	>1000	0
A546	c12c(c(ccc1)C(=O)NO)OC1(CC2)CCN(CC1)S(=O)(=O)C1CCCCC1	>1000	0
A547	c12c(c(ccc1)C(=O)NO)OC1(CC2)CCN(CC1)C(=O)C1(CCOCC1)C	>1000	0
A548	c12c(c(ccc1)C(=O)NO)OC1(CC2)CCN(CC1)C(=O)Cc1ccccc1	>1000	0

A552	c12c(c(ccc1)C(=O)NO)OC1(CC2)CCN(CC1)c1cc(c(cc1)C)F	>1000	0
A553	c12c(c(ccc1)C(=O)NO)CC[C@]1(C2)C(=O)N(CC1)Cc1ccc(cc1)Cl	>1000	0
A554	c12c(c(ccc1)C(=O)NO)CC[C@@]1(C2)C(=O)N(CC1)c1ccccc1C(F)(F)F	>1000	0
A556	c12c(c(ccc1)C(=O)NO)CCC1(O2)CCN(CC1)c1ccccc1	>1000	0
A558	O=S(=O)(N(CC(=O)N(c1ccc(cc1)C(=O)NO)C)Cc1c(c(c(c(c1F)F)F)F)F)c1ccc(cc1)F	>1000	0
A560	c1cc(ccc1NCc1ccc(cc1)C(C)(C)C)C(=O)NO	>1000	0
A562	O=S(=O)(N(CC(=O)N(c1ccc(cc1)C(=O)NO)Cc1ccc(cc1)C(C)(C)C)Cc1c(c(c(c(c1F)F)F)F)F)C	>1000	0
A563	n1cnc2c(c1C)cc(cc2OCCCCCCCC(=O)NO)c1cc(c(nc1)OC)F	>1000	0
A564	c1(c(cc2c(c1)oc(n2)Nc1nc(C(=O)NO)ccn1)Cl)Cl	>1000	0
A565	c1ccc2c(c1)nc([nH]2)Nc1cc(C(=O)NO)ccc1	>1000	0
A566	c1ccc2c(c1)n(c(n2)Nc1cc(ccc1)C(=O)NO)CCOC	>1000	0
A567	c1c(c2c(cc1Nc1[nH]c3c(cccc3)n1)cccc2)C(=O)NO	>1000	0
A568	c12n(c(nc1cccc2)Nc1cc2c(c(c1)C(=O)NO)cccc2)CCOC	>1000	0
A569	c1cc(c2c(c1)n(c(n2)Nc1cc(C(=O)NO)ccc1)CCOC)OC	>1000	0
A571	c1c2c(cc(c1C#N)C(F)(F)F)n(c(n2)Nc1cc(C(=O)NO)ccc1)CCOC	>1000	0
A573	n1cnc2c(nc([nH]2)Nc2cc(C(=O)NO)ccc2)c1	>1000	0
A577	O(c1c(cc2c([nH]c(n2)Nc2cc(C(=O)NO)ccc2)c1)O)C	>1000	0
A578	c12c(cc3c([nH]c(n3)Nc3cc(C(=O)NO)ccc3)c1)OCC(=O)N2	>1000	0
A579	c1c2c(nc([nH]2)Nc2cc(C(=O)NO)ccc2)ccc1Cl	>1000	0
A582	c1c2c(nc(n2C)N(c2cc(C(=O)NO)ccc2)C)cc(c1C(F)(F)F)c1cccnc1	>1000	0
A583	c1c2c(nc(n2C)N(c2cc(C(=O)NO)ccc2)C)cc(c1c1cnccc1)C(F)(F)F	>1000	0
A584	c1ccccc1CNC(=O)ONC(=O)c1cccc(c1)N(c1[nH]c2cc(c(cc2n1)C(F)(F)F)C#N)C	>1000	0
A585	c1cc2c(c(c1)C(=O)NO)C[C@]1(C2)C(=O)N(CC1)C	>1000	0
A586	c12c(cccc1C(=O)NO)C[C@@]1(C2)CCN(C1=O)Cc1ccc(cc1)S(=O)(=O)C	>1000	0
A587	c1ccc2c(c1C(=O)NO)C[C@]1(C2)C(=O)N(CC1)C1CC1	>1000	0
A588	C1(CCC1)CN1C(=O)[C@@]2(CC1)Cc1cccc(c1C2)C(=O)NO	>1000	0
A590	c1cc2c(c(c1)C(=O)NO)C[C@@]1(C2)C(=O)N(CC1)c1c(cccc1)C(F)(F)F	>1000	0
A592	c12c(cccc1C(=O)NO)C[C@]1(C2)CCN(C1=O)CCCc1ccccc1	>1000	0
A596	c12c(cccc1C(=O)NO)C[C@]1(C2)CCN(C1=O)Cc1cnccc1	>1000	0
A597	c12c(cccc1C(=O)NO)C[C@@]1(C2)CCN(C1=O)Cc1c(cccc1)Cl	>1000	0
A598	c12c(cccc1C(=O)NO)C[C@]1(C2)CCN(C1=O)Cc1cccc(c1)F	>1000	0
A600	c12c(cccc1C(=O)NO)C[C@]1(C2)CCN(C1=O)Cc1csc(n1)c1ccccc1	>1000	0
A603	c12c(cccc1C(=O)NO)C[C@@]1(C2)CCN(C1=O)Cc1cc(cc(c1)OC)OC	>1000	0
A608	c12c(cccc1C(=O)NO)C[C@]1(C2)CCN(C1=O)Cc1noc(n1)C1CCOCC1	>1000	0
A609	c12c(cccc1C(=O)NO)C[C@]1(C2)CCN(C1=O)Cc1c(onc1C)C	>1000	0
A612	c12c(cccc1C(=O)NO)C[C@@]1(C2)CCN(C1=O)Cc1nnn(c1)c1ccccc1	>1000	0
A615	c1ccc2c(c1C(=O)NO)C[C@]1(C2)CN(CC1)C(=O)c1ccc(cc1)C(F)(F)F	>1000	0
A616	c1ccc2c(c1C(=O)NO)C[C@@]1(C2)CN(CC1)C(=O)C	>1000	0
A617	c1ccc2c(c1C(=O)NO)CC1(C2)CCN(CC1)C(=O)C	>1000	0
A618	c1c2c(nc([nH]2)Nc2cc(C(=O)NO)ccc2)cc(c1OC)OC	>1000	0
A619	c1c2c(nc([nH]2)Nc2cc(C(=O)NO)ccc2)cc2c1OCC(=O)N2	>1000	0
A621	c1ccc2c(c1C(=O)OCC1CCC1)C[C@]1(C2)C(=O)N(CC1)CC1CCC1	>1000	0
A622	c1ccc2c(nc([nH]2)N(c2cc(C(=O)NO)ccc2)CCOC)c1	>1000	0

A623	c1(c(cc2c(nc([nH]2)Oc2cc(C(=O)NO)ccc2)c1)C#N)C(F)(F)F	>1000	0
A624	c1ccc2c(c1)c(=O)n(c(=O)n2Cc1cc(ccc1)C(=O)NO)CCc1ccccc1	>10000	0
A625	c1ccc2c(c1)c(=O)n(c(=O)n2Cc1csc(c1)C(=O)NO)CCc1ccccc1	>10000	0
A627	SCC/C=C/[C@@H]1CC(=O)NCc2scc(C(=O)N/C(=C\C)/C(=O)N[C@H](C(=O)O1)C(C)C)n2	>10000	0
A628	S(CC/C=C/[C@@H]1CC(=O)NCc2scc(C(=O)N/C(=C\C)/C(=O)N[C@H](C(=O)O1)C(C)C)n2)C(=O)C	>10000	0
A629	[nH]1nc(cc1C(=O)NCCCCCCS)c1ccncc1	>10000	0
A630	[nH]1nc(cc1C(=O)NCCCCCCS)c1cccnc1	>10000	0
A631	[nH]1nc(cc1C(=O)NCCCCCCS)c1cnccn1	>10000	0
A632	c1ccc2c(c1)c(nc(n2)C)N(c1cc(c(cc1)OC)OCCCC(=O)NO)C	>10000	0
A633	C1[C@H]2C[C@]3(C[C@@H]1C[C@H](C3)C2)c1c(ccc(c1)c1ccc(cc1)C=CC(=O)O)O	>10000	0
A634	n1c(nc2c(c1N1CCOCC1)ncn2CCCCCCC(=O)NO)c1ccc(nc1)N	>10000	0
A635	C(=O)(/C=C/c1cc2nc(n(c2cc1)CCN(CC)CC)CCCC)NO	>10000	0
A636	OCCN(C(=O)Cc1ccc(C(=O)NO)cc1)c1ccccc1	>10000	0
A638	n1c2c(c3n(c1N)nc(n3)c1occc1)cnn2CCc1ccc(cc1)C(=O)Nc1ccccc1N	>10000	0
A639	c1(ccc(cc1N)F)NC(=O)c1ccc(cc1)CSc1nc(c2n(n1)ccc2)Nc1cc([nH]n1)C	>10000	0
A640	N(c1c(N)cccc1)C(=O)CCCCCCC(=O)Nc1ccccc1	>10000	0
A641	n1(Cc2ccc(cc2)C(=O)NO)sc2c(c1=O)cccc2	>10000	0
A642	N1(Cc2c(CC1)n1c(=NCC1)n(c2=O)Cc1c(cccc1)OC)Cc1ccc(cc1)C(=O)Nc1ccccc1N	>10000	0
A643	C1(CCOCC1)(CNC(=O)c1cccc(c2nc(on2)C(F)(F)F)c1)c1nc(cs1)c1ccccc1	>10000	0
A645	c1ccc(c(c1)CN1C[C@H](CC1)O)NC(=O)CCCCCCC(=O)NO	>10000	0
A646	C(=O)(c1ccc(cc1)CCn1c(=O)c2c3c(c1=O)ccc(c3ccc2)N1CCOCC1)NO	>10000	0
A647	c1c(c(c(cc1O)C)c1[nH]c2c(n1)cc(cc2)C(=O)NO)C	>10000	0
A648	c1c(c(ccc1)c1[nH]c2c(n1)cc(cc2)C(=O)NO)C(F)(F)F	>10000	0
A649	C(=O)(NO)c1cnc(N(Cc2onc(n2)C2CCN(CC2)Cc2ccc(cc2)C)C)nc1	>10000	0
A650	n1c([nH]c(=O)c2c1sc1c2CCN(C1)C)c1cc(c(c(c1)C)OCCCCCC(=O)NO)C	>10000	0
A651	N(Cc1ccc(cc1)C(=O)Nc1ccccc1N)C1=N[C@@H]([C@@H](O1)c1ccccc1)c1ccccc1	>100000	0
A652	c1(ccc2c(c1)C[C@@H](CC2)Nc1nccc(n1)c1cccnc1)C(=O)NO	>100000	0
A653	c1c(ccc(c1)/C=C/C=C/C(=O)NO)c1ccc(cc1)OC	>100000	0
A654	c1ccc2c(c1)C(=O)c1c(C2=O)ccc(c1)/C=C/C(=O)NO	>100000	0
A655	C1(NC(=O)CCCCCC[C@@H](C(=O)NC)N=O)c2c(cccc2)c2c1cccc2	>100000	0
A656	c1cccc(c1)NC(=O)CCCCCC[C@@H](C(=O)NC)N=O	>100000	0
A657	c1cc(cc2c1cccc2)NC(=O)CCCCCC[C@@H](C(=O)NC)N=O	>100000	0
A658	n1cc(cc2c1cccc2)NC(=O)CCCCCC[C@@H](C(=O)NC)N=O	>100000	0
A659	C1(=O)N([C@@H](C(=O)N1c1ccc(cc1)Cl)CCC(=O)Nc1ccc(cc1)C(=O)NO)Cc1ccccc1	>100000	0
A660	C1(=O)N([C@@H](C(=O)N1c1ccc(cc1)Cl)CCC(=O)Nc1ccc(cc1)C(=O)NO)Cc1ccc(cc1)Br	>100000	0
A661	C1(=O)N([C@@H](C(=O)N1c1ccc(cc1)Cl)CCC(=O)Nc1ccc(cc1)C(=O)NO)Cc1ccc(cc1)C	>100000	0
A662	c1cc(cc(c1)NC(=O)CCCCCC[C@@H](C(=O)NC)N=O)Br	>100000	0
A663	c1(cc(ccc1)C(=O)N(c1ccc(cc1)C(=O)NO)Cc1ccccc1)C(F)(F)F	>2000	0
A664	c1c(cc2c(c1)ccn2Cc1ccc(cc1)OC)C(=O)NO	>20000	0
A665	[O-][N+](=O)c1c(N)cc(N2CCN(CC2)C)cc1	>200000	0
A667	n1n(cc(n1)c1cccc(c1)NC(=O)N1CCOCC1)Cc1ncc(cc1)c1nnc(o1)C(F)F	>30000	0

A669	c1(ccc(cc1)c1nnc(o1)C(F)F)Cn1cc(nn1)c1cc2c(cc1)nc([nH]2)N	>30000	0
A670	c1(ncc(cc1)c1nnc(o1)C(F)F)Cn1cc(nn1)c1ccc2c(c1)nc([nH]2)Cl	>30000	0
A673	c1(ccc(cn1)c1ncn(c1)Cc1ccc(cn1)c1oc(nn1)C(F)F)N	>30000	0
A677	n1n(cc(n1)c1cc(ccc1)NC(=O)N1CCOCC1)Cc1ccc(c(c1)F)c1nnc(o1)C(F)F	>30000	0
A678	c1(n(c2c(n1)cc(cc2)c1nnn(c1)Cc1ccc(cn1)c1oc(nn1)C(F)F)C)N	>30000	0
A679	c1([nH]c2c(n1)ccc(c2)c1nnn(c1)Cc1ccc(cn1)c1oc(nn1)C(F)F)NCC	>30000	0
A683	C1(=NCCN1)Nc1ccc(cc1)c1ncn(c1)Cc1ccc(cc1)c1oc(nn1)C(F)F	>30000	0
A684	n1n(cc(n1)c1cc2c(n(c(n2)N)C)cc1)Cc1ccc(cc1)c1nnc(o1)C(F)F	>30000	0
A688	n1n(cc(n1)c1ccc2sc(nc2c1)N)Cc1ncc(cc1)c1nnc(o1)C(F)F	>30000	0
A690	c1(ccc(cn1)c1nnn(c1)Cc1ccc(cn1)c1oc(nn1)C(F)F)N	>30000	0
A691	CN1C[C@H](c2c(cc(/C=C/C(=O)Nc3c(cccc3)N)cc2)F)[C@H](C1)C(=O)Nc1ccc(cc1)Cl	>30000	0
A693	c1(C(=O)N[C@H](C(=O)NO)C(N)(C)C)ccc(cc1)OCC#CC	>30000	0
A695	c1c(ccc(c1)C(=O)NNCCC)CNC(=O)c1cc2c([nH]1)cccc2	>5000	0
A696	C(=O)(NCc1ccc(cc1)C(=O)NNCCC)/C=C/c1ccccc1	>5000	0
A697	C\1(=C\2/C(=O)Nc3c2cccc3)/C(=N/OCCCC(=O)NO)/c2c(N1)cccc2	>5000	0
A699	C\1(=C\2/C(=O)N(c3c2cccc3)CC#C)/C(=N/OCCCC(=O)NO)/c2c(N1)cccc2	>5000	0
A700	[C@@H](Oc1cc(N(c2c3ccccc3nc(n2)C)C)ccc1OC)(C(=O)NO)C(C)C	>5000	0
A701	O=S1(=O)c2c3c(n(Cc4ccc(cc4)C(=O)NO)c2CC1)cccc3	>5000	0
A702	c1c(c(ccc1c1ccccc1)N)NC(=O)c1ccccc1	>50000	0
A703	c1c(c(ccc1)N)NC(=O)c1ccccc1	>50000	0
A704	c1c(c(ccc1c1sccc1)N)NC(=O)c1ccccc1	>50000	0
A705	C(=O)(c1ccc(cc1)CN(C(=O)Nc1ccc(cc1)CN)CCCCO)NO	>50000	0
A706	c1cc(cc2c1CN(CC2)C(=O)c1cccn1C)C(=O)NO	>50000	0
A708	c1c(ccc(c1)C(=O)NO)CN(CCCCO)C(=O)Nc1ccccc1	>50000	0
A709	c1c(c(ccc1)N)NC(=O)c1cccnc1	>50000	0
A710	c1c(c(ccc1c1ccccc1)O)NC(=O)c1ccccc1	>50000	0
A711	c1c(c(ccc1c1ccccc1)N)NC(=O)c1cccnc1	>50000	0

Here 1 is depicted as active, and 0 is depicted as inactive classes

Test set compounds of HDAC11 inhibitors in SMILES format

Compound ID	SMILES	IC_{50} (nM)	Binary
A015	N1C(=O)[C@H]([C@@H](C1)c1ccccc1)C(=O)N[C@@H](CCCCCS)C(=O)Nc1ccccc1	4	1
A016	O=C(NO)c1c2c(C(C)(C)N(C2)c2ncc(cn2)C(F)(F)F)ccc1	5	1
A018	N1[C@H](CCC1=O)C(=O)N[C@@H](CCCCCS)C(=O)Nc1cc(ccc1)C	5	1
A020	c1cccc(c1)NC(=O)[C@H](CCCCCS)NC(=O)[C@H]1NC(=O)CCC1	6	1
A024	c1cccc(c1)NC(=O)[C@H](CCCCCS)NC(=O)[C@H]1C(=O)NCCC1	9	1
A026	c1cccc(c1)NC(=O)[C@H](CCCCCS)NC(=O)[C@@H]1NC(=O)CCC1	10	1
A028	N1([C@H](CCC1=O)C(=O)N[C@@H](CCCCCS)C(=O)Nc1cc(ccc1)C)C	12	1
A029	N1C(=O)[C@@H]([C@H](C1)c1ccccc1)C(=O)N[C@@H](CCCCCS)C(=O)Nc1ccccc1	12	1
A030	c1cccc(c1)NC(=O)[C@H](CCCCCC(=O)NO)NC(=O)[C@H]1NC(=O)CC1	13	1

A031	N1C(=O)[C@H]([C@H](C1)c1ccccc1)C(=O)N[C@@H](CCCCCS)C(=O)Nc1ccccc1	13	1
A034	c1cccc(c1)NC(=O)[C@H](CCCCCS)NC(=O)[C@@H]1NC(=O)CC1	14	1
A035	N1[C@@H](CCC1=O)C(=O)N[C@H](CCCCCS)C(=O)Nc1ccccc1	14	1
A040	c1(cc2cc(c1)/C=C\CO[C@H](C(=O)Nc1c(OC2)cccc1)CCCCCC(=O)NO)OC	23	1
A051	N1[C@H](CCC1=O)C(=O)N[C@@H](CCCCCS)C(=O)Nc1cc(ccc1)C(F)(F)F	44	1
A052	O=S(=O)(N(Cc1ccc(cc1)C(=O)NO)C1CC1)c1c(c(c(c(c1F)F)F)F)F	47	1
A059	[nH]1c(c(cc1c1ccc(cc1)O)c1cocc1)C(=O)NCc1ccc(cc1)C(=O)NO	72	1
A069	C(=O)(CCCCSc1nc(cc(=O)[nH]1)c1ccc(cc1)c1ccccc1)NO	100	1
A074	S(=O)(=O)(c1c(c(c(c(c1F)F)F)F)F)N(Cc1ccc(cc1)C(=O)NO)Cc1ccccc1	122	1
A089	S(=O)(=O)(c1c(c(c(c(c1)F)F)F)F)N(Cc1ccc(cc1)C(=O)NO)Cc1cc(ccc1)F	235	1
A091	c1cccc(c1)NC(=O)[C@H](CCCCCC(=O)NO)NC(=O)[C@H]1C(=O)NCCC1	255	1
A093	S(=O)(=O)(c1c(c(c(c(c1)F)F)F)F)N(Cc1ccc(cc1)C(=O)NO)Cc1c(cccc1)F	263	1
A094	C(=O)(Nc1ccc(C(=O)NO)cc1)OCc1cc2c(cc(CN(CC)CC)cc2)cc1	287	1
A097	C1(=N[C@H]2[C@H](N1)CCCC2)N1Cc2c(cccc2C1)C(=O)NO	300	1
A100	O=S(=O)(N(Cc1ccc(cc1)C(=O)NO)C1CC1)c1c(c(c(c(c1F)Cl)F)Cl)F	364	1
A109	c1(cc(ccc1)C(=O)N(c1ccc(cc1)C(=O)NO)Cc1cccc(c1)C(F)(F)F)C(F)(F)F	526	1
A115	[n+]1(onc(c1S(=O)(=O)c1ccccc1)OCCCCCC(=O)NO)[O-]	608	1
A116	c1(ccc(cc1N)F)NC(=O)c1ccc(cc1)CNC(=O)/C=C/1\NC(=O)c2c1cccc2	632	1
A119	O=S(=O)(NCC(=O)N(c1ccc(cc1)C(=O)NO)Cc1ccc(cc1)C(C)(C)C)c1ccc(cc1)F	665	1
A123	C(=O)(c1ccc(cc1)C1CC1)Nc1ccc(cc1)C(=O)NO	704	1
A124	c1c(c([nH]c1c1ccc(cc1)OC)C(=O)NCc1ccc(cc1)C(=O)NO)c1ccsc1	718	1
A128	c1c2c(nc([nH]2)Nc2cc(C(=O)NO)ccc2)cc2c1OCCO2	750	1
A131	c1c2c(nc(n2C)N(c2cc(C(=O)NO)ccc2)C)cc(c1c1ccccc1)C(F)(F)F	750	1
A140	c12c(cccc1C(=O)NO)C[C@]1(C2)CCN(C1=O)Cc1c(ccc(c1)Cl)Cl	750	1
A141	c1ccc2c(c1C(=O)NO)C[C@]1(C2)CN(CC1)Cc1ccc(cc1)C(F)(F)F	750	1
A142	c1(cccc2c1C[C@]1(CC2)C(=O)N(CC1)Cc1ccc(cc1)C(F)(F)F)C(=O)NO	750	1
A147	N1(Cc2c(C1)c(ccc2)C(=O)NO)c1oc2c(n1)cncc2	750	1
A149	c1(ccc2c(c1)nc(cc2)N1Cc2c(C1(C)C)cccc2C(=O)NO)C(F)(F)F	750	1
A166	c1cc(ccc1N(C(=O)OC(C)(C)C)Cc1ccc(cc1)C(C)(C)C)C(=O)NO	837	1
A167	C(CCCCC(=O)NO)ONC(=O)c1cc(cc(c1)C)C	852	1
A174	C(=O)(CCCCCCS)N1Cc2c(CC1)cccc2	949	1
A179	c1(cc(ccc1Cl)C(=O)NCc1ccc(cc1)C(=O)NO)Cl	1,050	0
A180	C(NC(=O)CCCCCCC(=O)NO)Cc1ccccc1	1,130	0
A183	c1cccc2c1OCCCCCO[C@@H](C(=O)N2)CCCCCC(=O)NO	1,210	0
A189	c1cc(cc(c1)NC(=O)CCCCCCC(=O)NO)C	1,600	0
A202	O=S1(=O)C[C@@H]2[C@H](N(c3c1cccc3)Cc1ccc(cc1)C(=O)NO)CCCC2	2,400	0
A208	c1c(ccc(c1)/C=C/C(=O)NO)/C=N/OCCN1CCOCC1	3,060	0

A212	c1c(ccc(c1)/C=C/C(=O)NO)C(=O)N[C@@H](Cc1c[nH]c2c1cccc2)C(=O)Nc1ccc(cc1)I	3,229	0
A213	[nH]1cc(c2c1cccc2)C[C@H](NC(=O)c1ccc(C(=O)NO)cc1)C(=O)Nc1ccc(cc1)C	3,500	0
A216	C[C@H](/C=C/C(=O)NO)/C=C(\C)/C(=O)c1ccc(cc1)N(C)C	3,642.50	0
A217	c1ccc(cc1)CC(=O)N(CCO)Cc1ccc(cc1)C(=O)NO	3,700	0
A220	c1ccc2c(c1)c(=O)n(c(=O)n2Cc1ccc(cc1)C(=O)NO)CCc1ccc(cc1)NC	3,800	0
A239	C1[C@H]2C[C@]3(C[C@@H]1C[C@H](C3)C2)c1c(ccc(c1)c1ccc(cc1)C=CC(=O)O)OCC(=O)NO	6,090	0
A247	n1(c(=O)c2c3c(c1=O)cccc3ccc2)CCCCCC(=O)Nc1c(N)cccc1	9,350	0
A248	O=S(=O)(c1ccc(cc1)c1cn(nc1)C)n1ccc(c1)/C=C/C(=O)Nc1ccccc1N	9,700	0
A250	n1c(nc2c(c1N1CCOCC1)ncn2CCCCCCC(=O)NO)c1cc(ccc1)CO	9,700	0
A271	c1ccc2c(c1)c(=O)n(c(=O)n2Cc1ccc(cc1)C(=O)NO)CCc1c(cccc1)O	16,700	0
A273	O=S1(=O)[C@H]2c3c(N(Cc4ccc(cc4)C(=O)NO)[C@@H]2CC1)cccc3	17,000	0
A274	c1ccc2c(c1)c(=O)n(c(=O)n2Cc1sc(cc1)C(=O)NO)CCc1ccccc1	19,800	0
A276	c1ccc2c(c1)c(=O)n(c(=O)n2Cc1ccc(cc1)C(=O)NO)CCc1ccc(cc1)N1CCOCC1	22,750	0
A277	c1(ncnc2c1nc[nH]2)N[C@H](c1nc(c2c(n1)cccc2)CCCCC(=O)NO)CC	23,030	0
A292	c1(ccc(cc1)/C=C/C(=O)NO)c1ccc(cc1)OC	73,000	0
A294	c1(ccc2c(c1)CN(CC2)Cc1ccc(o1)c1cccc(c1)[N+](=O)[O-])C(=O)NO	75,300	0
A295	c1(c(ccc(c1)c1ccc(cc1)/C=C/C(=O)NO)OC)[C@]12C[C@@H]3C[C@H](C1)C[C@@H](C3)C2	77,000	0
A296	c1ccc2c(c1)C(=O)c1c(C2=O)ccc(c1)C(=O)NO	80,020	0
A300	c1([nH]c2c(c1)c(ccc2)C(=O)NO)c1ncc(nc1)C(F)(F)F	<500	1
A304	N1(Cc2c(C1)c(ccc2)C(=O)NO)c1[nH]c2c(n1)CC[C@H](C2)C(F)(F)F	<500	1
A307	N1(Cc2c(C1)c(ccc2)C(=O)NO)c1oc2c(n1)nccc2	<500	1
A318	c1c(nc2c(c1)nc(cc2)N1Cc2c(C1(C)C)cccc2C(=O)NO)C(F)(F)F	<500	1
A319	c1(N2C(c3c(C2)c(ccc3)C(=O)NO)(C)C)oc2c(n1)cccc2	<500	1
A323	c1(N2C(c3c(C2)c(ccc3)C(=O)NO)(C)C)ncc(c(c1)C#N)C(F)(F)F	<500	1
A324	N1(C(c2c(C1)c(ccc2)C(=O)NO)(C)C)C(=O)Nc1ccc(cc1)C(F)(F)F	<500	1
A339	c1c2c(nc([nH]2)Nc2cc(C(=O)NO)ccc2)cc(c1c1ccc(cc1)COC)C(F)(F)F	<500	1
A340	c1c2c(nc([nH]2)Nc2cc(C(=O)NO)ccc2)cc(c1C(F)(F)F)c1ccc2c(c1)cccn2	<500	1
A344	c1c2c(nc([nH]2)Nc2cc(C(=O)NO)ccc2)cc(c1c1ccc(nc1)N(C)C)C(F)(F)F	<500	1
A347	c1c2c(nc([nH]2)Nc2cc(C(=O)NO)ccc2)cc(c1c1cc(ccc1CO)F)C(F)(F)F	<500	1
A358	c12c(cccc1C(=O)NO)C[C@]1(C2)CCN(C1=O)Cc1ccc(cc1)c1ccccc1	<500	1
A363	c12c(cccc1C(=O)NO)C[C@]1(C2)CCN(C1=O)Cc1cccc(c1)C(F)(F)F	<500	1
A364	c12c(cccc1C(=O)NO)C[C@@]1(C2)CCN(C1=O)Cc1cccc(c1)Br	<500	1
A371	c12c(c(ccc1)C(=O)NO)C[C@]1(CC2)C(=O)N(CC1)Cc1ccc(c(c1)F)C(F)(F)F	<500	1
A373	c12c(c(ccc1)C(=O)NO)CC[C@@]1(C2)C(=O)N(CC1)Cc1ccc(c(c1)C(F)(F)F)Cl	<500	1
A374	c12c(c(ccc1)C(=O)NO)CC[C@@]1(C2)C(=O)N(CC1)Cc1ccc(cc1)C(F)(F)F	<500	1
A376	c12c(c(ccc1)C(=O)NO)CC[C@@]1(C2)C(=O)N(CC1)c1ccc(cc1)C(F)(F)F	<500	1
A378	c1(c(cc2c(c1)oc(n2)Nc1cc(ccc1)C(=O)NO)C(F)(F)F)c1ccccc1	<500	1

A379	c1(c(cc2c(c1)oc(n2)Nc1cc(C(=O)NO)c(cc1)F)Cl)Cl	<500	1
A383	c1c(c(cc2c1oc(n2)Nc1cnnc(c1)C(=O)NO)Cl)Cl	<500	1
A384	c1c(c(cc2c1oc(n2)Nc1ncnc(c1)C(=O)NO)Cl)Cl	<500	1
A388	c1(c(cc2c(c1)n(c(n2)Nc1cc(C(=O)NO)ccc1)C)C#N)C(F)(F)F	<500	1
A394	c1c2c(cc(c1C(F)(F)F)c1ccccc1)n(c(n2)Nc1cc(C(=O)NO)ccc1)C(C)C	<500	1
A398	c1c2c(cc(c1c1ccccc1)C(F)(F)F)n(c(n2)Nc1cc(C(=O)NO)ccc1)CCOC	<500	1
A403	c1(c(cc2c(nc([nH]2)Cc2cc(C(=O)NO)ccc2)c1)C#N)C(F)(F)F	<500	1
A416	c1c2c(nc([nH]2)Nc2cc(C(=O)NO)ccc2)cc(c1Cl)Cl	<500	1
A419	c1c2c(nc([nH]2)Nc2cc(C(=O)NO)ccc2)cc(c1Br)OC(F)(F)F	<500	1
A423	c1ccc2c(c1C(=O)NO)C[C@@]1(C2)C(=O)N(CC1)Cc1ccc(c(c1)F)C(F)(F)F	<500	1
A428	c1(c(cc2c(c1)oc(n2)Nc1cc(C(=O)NO)ccn1)Cl)Cl	<500	1
A429	c1cc(ccc1C(=O)NO)CN(S(=O)(=O)c1cc(c(c(c1F)F)F)F)CCOC	>1000	0
A431	c1c(c(ccc1C(=O)NO)CN(S(=O)(=O)c1cc(c(c(c1F)F)F)F)C(C)C)OC	>1000	0
A434	c1ccccc1NC(=O)CCCCCCC(=O)NO	>1000	0
A440	c1([nH]c2c(n1)cccc2)N1Cc2c(cccc2C1)C(=O)NO	>1000	0
A442	N1(Cc2c(C1)c(ccc2)C(=O)NO)c1[nH]c2c(n1)CCCC2	>1000	0
A444	S(=O)(=O)(c1c(c(c(c(c1F)F)F)F)F)NCc1ccc(cc1)C(=O)NO	>1000	0
A447	S(=O)(=O)(c1c(c(c(c(c1)F)F)F)F)N(Cc1ccc(cc1)C(=O)NO)Cc1ccc(cc1)F	>1000	0
A449	n1cnc2c(c1C)cc(cc2OCCN(c1ncc(cn1)C(=O)NO)C)c1ccc(nc1)OC	>1000	0
A450	C(=O)(c1c(c(c(c(c1F)F)F)F)F)NCc1ccc(cc1)C(=O)NO	>1000	0
A454	O=S(=O)(N(Cc1ccc(cc1)C(=O)NO)C1CC1)c1c(cc(cc1F)F)F	>1000	0
A456	O=S(=O)(N(Cc1ccc(cc1)C(=O)NO)C1CC1)c1c(cc(c(c1F)Cl)F)F	>1000	0
A459	c1cc(ccc1C(=O)NO)CN(S(=O)(=O)c1cc(c(c(c1F)F)F)F)C(C)C	>1000	0
A460	c1cc(ccc1CC(=O)NO)CN(S(=O)(=O)c1cc(c(c(c1F)F)F)F)C(C)C	>1000	0
A486	c1(N2C(c3c(C2)c(ccc3)C(=O)NO)(C)C)scc(n1)C(F)(F)F	>1000	0
A491	N1(C(c2c(C1)c(ccc2)C(=O)NO)(C)C)C(=O)Nc1nc(ccc1)C(F)(F)F	>1000	0
A498	c1cc(ncc1C(F)(F)F)[C@H]1C(c2c(N1)c(ccc2)C(=O)NO)(C)C	>1000	0
A500	c1cc(ccc1C(F)(F)F)[C@@H]1C(c2c(N1)c(ccc2)C(=O)NO)(C)C	>1000	0
A505	N1(Cc2c(C1)c(ccc2)C(=O)NO)c1ccccc1	>1000	0
A512	c1(cc(ccc1)C(=O)Nc1ccc(cc1)C(=O)NO)C(F)(F)F	>1000	0
A518	c1(cc(ccc1)C(=O)N(c1ccc(cc1)C(=O)NO)CC1CC1)C(C)(C)C	>1000	0
A520	c1(cc(cc(c1)C(C)(C)C)C(=O)Nc1ccc(cc1)C(=O)NO)C(C)(C)C	>1000	0
A522	c1(c(c(ccc1)C(=O)N(c1ccc(cc1)C(=O)NO)C(C)C)F)C(F)(F)F	>1000	0
A524	c1(cc(cc(c1)C(C)(C)C)C(=O)N(c1ccc(cc1)C(=O)NO)C(C)C)C(C)(C)C	>1000	0
A526	c1(cc(ccc1)N(C(=O)c1ccc(cc1)C(=O)NO)CC)C(C)(C)C	>1000	0
A529	C(=O)(c1ccc(cc1)NC(=O)c1ccc(cc1)N1CCOCC1)NO	>1000	0
A531	C(=O)(c1ccc(cc1)F)Nc1ccc(cc1)C(=O)NO	>1000	0

A535	c12c(c(ccc1)C(=O)NO)CC1(C2)CCN(CC1)C(=O)c1ccc(cc1)Cl	>1000	0
A536	c12c(c(ccc1)C(=O)NO)CC1(C2)CCN(CC1)Cc1ccc(cc1)Cl	>1000	0
A538	c12c(CC3(C2)CCN(CC3)Cc2ccccc2)c(ccc1)C(=O)NO	>1000	0
A542	c1(cccc2c1C[C@]1(CC2)C(=O)N(CC1)c1cccc(c1)C(F)(F)F)C(=O)NO	>1000	0
A543	c1(cccc2c1C[C@@]1(CC2)C(=O)N(CC1)c1ccccc1C(F)(F)F)C(=O)NO	>1000	0
A549	c1(cccc2c1OC1(CC2)CCN(CC1)Cc1ccc(cc1)F)C(=O)NO	>1000	0
A550	c12c(c(ccc1)C(=O)NO)O[C@@]1(CC2)CCN(CC1)C1CCCCC1	>1000	0
A551	c1(cccc2c1OC1(CC2)CCN(CC1)c1ccc(cn1)C(F)(F)F)C(=O)NO	>1000	0
A555	c12c(c(ccc1)C(=O)NO)CCC1(O2)CCN(CC1)C(=O)C	>1000	0
A557	c12c(c(ccc1)C(=O)NO)CCC1(O2)CCN(CC1)c1ccc(cc1)F	>1000	0
A559	O=S(=O)(N(CC(=O)N(c1ccc(cc1)C(=O)NO)C)C)c1ccc(cc1)F	>1000	0
A561	c1cc(ccc1N(Cc1ccc(cc1)C(C)(C)C)C(=O)C)C(=O)NO	>1000	0
A570	c1ccc2c(n(c(n2)Nc2cc(C(=O)NO)ccc2)CCOC)c1OC	>1000	0
A572	c1cnc2c(nc([nH]2)Nc2cc(C(=O)NO)ccc2)n1	>1000	0
A574	n1c2c(oc(n2)Nc2cc(C(=O)NO)ccc2)ccc1	>1000	0
A575	c1c2c(nc([nH]2)Nc2cc(C(=O)NO)ccc2)cc2c1OCO2	>1000	0
A576	c1c2c(nc([nH]2)Nc2cc(C(=O)NO)ccc2)cc2c1OCCCO2	>1000	0
A580	c1c2c(nc([nH]2)Nc2cc(C(=O)NO)ccc2)ccc1S(=O)(=O)C	>1000	0
A581	c1c2c(nc([nH]2)Nc2cc(C(=O)NO)ccc2)ccc1S(=O)(=O)N	>1000	0
A589	c1ccc2c(c1C(=O)NO)C[C@]1(C2)C(=O)N(CC1)c1ccc(cc1)C(F)(F)F	>1000	0
A591	c1ccc2c(c1C(=O)NO)C[C@]1(C2)C(=O)N(CC1)Cc1ccccc1	>1000	0
A593	c12c(cccc1C(=O)NO)C[C@@]1(C2)CCN(C1=O)Cc1ccc(cc1)OC	>1000	0
A594	c12c(cccc1C(=O)NO)C[C@@]1(C2)CCN(C1=O)Cc1cccc(c1)OC	>1000	0
A595	c12c(cccc1C(=O)NO)C[C@@]1(C2)CCN(C1=O)Cc1c(cccc1)C	>1000	0
A599	c12c(cccc1C(=O)NO)C[C@]1(C2)CCN(C1=O)Cc1cc(cc(c1)F)F	>1000	0
A601	c12c(cccc1C(=O)NO)C[C@]1(C2)CCN(C1=O)Cc1c(cc(cc1)F)F	>1000	0
A602	c12c(cccc1C(=O)NO)C[C@@]1(C2)CCN(C1=O)Cc1c(cccc1)OC	>1000	0
A604	c12c(cccc1C(=O)NO)C[C@]1(C2)CCN(C1=O)CC1CCCCC1	>1000	0
A605	c12c(cccc1C(=O)NO)C[C@@]1(C2)CCN(C1=O)Cc1onc(c1)c1ccccc1	>1000	0
A606	c12c(cccc1C(=O)NO)C[C@]1(C2)CCN(C1=O)Cc1cnc(cc1)n1cccn1	>1000	0
A607	c12c(cccc1C(=O)NO)C[C@]1(C2)CCN(C1=O)Cc1cnc(cc1)C(F)(F)F	>1000	0
A610	c12c(cccc1C(=O)NO)C[C@]1(C2)CCN(C1=O)Cc1cccc(n1)C(F)(F)F	>1000	0
A611	c12c(cccc1C(=O)NO)C[C@]1(C2)CCN(C1=O)CCN1CCOCC1	>1000	0
A613	c12c(cccc1C(=O)NO)C[C@]1(C2)CCN(C1=O)CC1CC1	>1000	0
A614	c1ccc2c(c1C(=O)NO)C[C@]1(C2)CN(CC1)C1CC1	>1000	0
A620	c1cc2c(c(c1)C(=O)NO)C[C@]1(C2)C(=O)N(CC1)Cc1ccc(cc1)C	>1000	0
A626	SCC/C=C/[C@@H]1CC(=O)N[C@@H](c2scc(C(=O)N/C(=C\C)/C(=O)N[C@H](C(=O)O1)C(C)C)n2)C(C)C	>10000	0

A637	c1(nccc(c1)/C=C/c1ccc(cc1)C(=O)NO)c1c(cccc1)O	>10000	0
A644	O=C(N)c1c2c(C(C)(C)N(C2)c2cnc(cn2)C(F)(F)F)ccc1	>10000	0
A666	c12cc(oc1cccc2)c1nc2c(cccc2)c(c1)C(=O)NC(c1ccccc1)c1ccccc1	>200000	0
A668	o1c(nc2c1ccc(c2)c1nn(nn1)Cc1ccc(cn1)c1oc(nn1)C(F)F)N	>30000	0
A671	C1(=NCCN1)Nc1ccc(cc1)c1nnn(c1)Cc1ccc(cc1)c1oc(nn1)C(F)F	>30000	0
A672	c1(c2nnc(o2)C(F)F)ccc(cc1)Cn1nc(nn1)c1ccc2c(c1)nc(n2C)N	>30000	0
A674	c1(ccc(cn1)c1cnn(c1)Cc1ccc(cn1)c1oc(nn1)C(F)F)N	>30000	0
A675	n1n(cc(n1)c1cc2c(nc(s2)N)cc1)Cc1ccc(cc1)c1nnc(o1)C(F)F	>30000	0
A676	n1n(cc(n1)c1ccc(nc1)N)Cc1ccc(c(c1)F)c1nnc(o1)C(F)F	>30000	0
A680	n1n(cc(n1)c1cc2c(NC(=O)C32CCNCC3)cc1)Cc1ncc(cc1)c1nnc(o1)C(F)F	>30000	0
A681	c1(ccc(cn1)c1nnc(o1)C(F)F)Cn1cc(nc1)c1ccc(cc1)NC1=NCCN1	>30000	0
A682	c1(ccc(cn1)c1nnn(c1)Cc1c(c(c(cc1)c1oc(nn1)C(F)F)F)F)N	>30000	0
A685	C(c1ccc(cc1)C(=O)NO)n1c(=O)c2c3c(c1=O)cccc3c(cc2)OC	>30000	0
A686	n1n(cc(n1)c1cc2c(nc(s2)N)cc1)Cc1ncc(cc1)c1nnc(o1)C(F)F	>30000	0
A687	n1n(nc(n1)c1ccc(c(c1)NC(=O)N1CCOCC1)O)Cc1ccc(cn1)c1nnc(o1)C(F)F	>30000	0
A689	c1(nnc(o1)C(F)F)c1cnc(cc1)Cn1nc(nn1)c1cc2c(cc1)CNC2=O	>30000	0
A692	c1ccc(c(c1)C(=O)N)Nc1cccc(c1)OCCc1ccccc1	>30000	0
A694	C(C)(C)(CNC(=O)c1cccc(c1)c1noc(C(F)(F)F)n1)c1nc(oc1)c1ccccc1	>5000	0
A698	C\1(=C\2/C(=O)Nc3c2cccc3)/C(=N/OCCCC(=O)O)/c2c(N1)cccc2	>5000	0
A707	C(=O)(c1ccc(cc1)CN(C(=O)Nc1ccc(cc1)CN)CCCC)NO	>50000	0
A712	c1c(c(ccc1c1cccs1)N)NC(=O)c1cccnc1	>50000	0

Here 1 is depicted as active, and 0 is depicted as inactive classes

Chapter 7: References

Reference

Ahamed TS, Rajan VK, Sabira K, Muraleedharan K. QSAR classification-based virtual screening followed by molecular docking studies for identification of potential inhibitors of 5-lipoxygenase. Computational Biology and Chemistry. 2018 Dec 1;77:154-66.

Ambure P, Aher RB, Gajewicz A, Puzyn T, Roy K. "NanoBRIDGES" software: open access tools to perform QSAR and nano-QSAR modeling. Chemometrics and Intelligent Laboratory Systems. 2015 Oct 15;147:1-3.

Amin SA, Adhikari N, Jha T. Exploration of histone deacetylase 8 inhibitors through classification QSAR study: Part II. Journal of Molecular Structure. 2020 Mar 15;1204:127529.

Amin SA, Khatun S, Gayen S, Das S, Jha T. Are inhibitors of histone deacetylase 8 (HDAC8) effective in hematological cancers especially acute myeloid leukemia (AML) and acute lymphoblastic leukemia (ALL)?. European Journal of Medicinal Chemistry. 2023 Jun 25:115594.

Amin SA, Kumar J, Khatun S, Das S, Qureshi IA, Jha T, Gayen S. Binary quantitative activity-activity relationship (QAAR) studies to explore selective HDAC8 inhibitors: In light of mathematical models, DFT-based calculation and molecular dynamic simulation studies. Journal of Molecular Structure. 2022 Jul 15;1260:132833.

Amin SA, Nandi S, Kashaw SK, Jha T, Gayen S. A critical analysis of urea transporter B inhibitors: molecular fingerprints, pharmacophore features for the development of next-generation diuretics. Molecular Diversity. 2022 Oct 1:1-1.

Arts J, King P, Marin A, Floren W, Belin A, Janssen L, Pilatte I, Roux B, Decrane L, Gilissen R, Hickson I. JNJ-26481585, a novel second-generation oral histone deacetylase inhibitor, shows broad-spectrum preclinical antitumoral activity. Clinical Cancer Research. 2009 Nov 15;15(22):6841-51.

Auzzas L, Larsson A, Matera R, Baraldi A, Deschênes-Simard B, Giannini G, Cabri W, Battistuzzi G, Gallo G, Ciacci A, Vesci L. Non-natural macrocyclic inhibitors of histone deacetylases: design, synthesis, and activity. Journal of medicinal chemistry. 2010 Dec 9;53(23):8387-99.

Baderna D, Gadaleta D, Lostaglio E, Selvestrel G, Raitano G, Golbamaki A, Lombardo A, Benfenati E. New in silico models to predict in vitro micronucleus induction as marker of genotoxicity. Journal of hazardous materials. 2020 Mar 5;385:121638.

Baek SY, Lee J, Kim T, Lee H, Choi HS, Park H, Koh M, Kim E, Jung ME, Iliopoulos D, Lee JY. Development of a novel histone deacetylase inhibitor unveils the role of HDAC11 in alleviating depression by inhibition of microglial activation. Biomedicine & Pharmacotherapy. 2023 Oct 1;166:115312.

Bagchi RA, Ferguson BS, Stratton MS, Hu T, Cavasin MA, Sun L, Lin YH, Liu D, Londono P, Song K, Pino MF. HDAC11 suppresses the thermogenic program of adipose tissue via BRD2. JCI insight. 2018 Aug 8;3(15).

Balasubramanian S, Verner E, Buggy JJ. Isoform-specific histone deacetylase inhibitors: the next step?. Cancer letters. 2009 Aug 8;280(2):211-21.

Banerjee A, Roy K. Prediction-inspired intelligent training for the development of classification read-across structure–activity relationship (c-RASAR) models for organic skin sensitizers: assessment of classification error rate from novel similarity coefficients. Chemical Research in Toxicology. 2023 Aug 16;36(9):1518-31.

Banerjee S, Amin SA, Jha T. A fragment-based structural analysis of MMP-2 inhibitors in search of meaningful structural fragments. Computers in Biology and Medicine. 2022 May 1;144:105360.

Banerjee S, Baidya SK, Ghosh B, Jha T, Adhikari N. Exploration of structural alerts and fingerprints for novel anticancer therapeutics: a robust classification-QSAR dependent structural analysis of drug-like MMP-9 inhibitors. SAR and QSAR in Environmental Research. 2023 Apr 3;34(4):299-319.

Baselious F, Hilscher S, Robaa D, Barinka C, Schutkowski M, Sippl W. Comparative Structure-Based Virtual Screening Utilizing Optimized AlphaFold Model Identifies Selective HDAC11 Inhibitor. International Journal of Molecular Sciences. 2024 Jan 22;25(2):1358.

Baselious F, Robaa D, Sippl W. Utilization of AlphaFold models for drug discovery: Feasibility and challenges. Histone deacetylase 11 as a case study. Computers in Biology and Medicine. 2023 Dec 1;167:107700.

Bhattacharya A, Amin SA, Kumar P, Jha T, Gayen S. Exploring structural requirements of HDAC10 inhibitors through comparative machine learning approaches. Journal of Molecular Graphics and Modelling. 2023 Sep 1;123:108510.

Bi L, Ren Y, Feng M, Meng P, Wang Q, Chen W, Jiao Q, Wang Y, Du L, Zhou F, Jiang Y. HDAC11 regulates glycolysis through the LKB1/AMPK signaling pathway to maintain hepatocellular carcinoma stemness. Cancer research. 2021 Apr 15;81(8):2015-28.

Boltz TA, Khuri S, Wuchty S. Promoter conservation in HDACs points to functional implications. BMC genomics. 2019 Dec;20:1-2.

Bora-Singhal N, Mohankumar D, Saha B, Colin CM, Lee JY, Martin MW, Zheng X, Coppola D, Chellappan S. Novel HDAC11 inhibitors suppress lung adenocarcinoma stem cell self-renewal and overcome drug resistance by suppressing Sox2. Scientific reports. 2020 Mar 13;10(1):4722.

Box GE, Tiao GC. Bayesian inference in statistical analysis. John Wiley & Sons; 2011 Jan 25.

Broide RS, Redwine JM, Aftahi N, Young W, Bloom FE, Winrow CJ. Distribution of histone deacetylases 1–11 in the rat brain. Journal of Molecular Neuroscience. 2007 Jan;31:47-58.

Bryant DT, Landles C, Papadopoulou AS, Benjamin AC, Duckworth JK, Rosahl T, Benn CL, Bates GP. Disruption to schizophrenia-associated gene Fez1 in the hippocampus of HDAC11 knockout mice. Scientific Reports. 2017 Sep 19;7(1):11900.

Buglio D, Khaskhely NM, Voo KS, Martinez-Valdez H, Liu YJ, Younes A. HDAC11 plays an essential role in regulating OX40 ligand expression in Hodgkin lymphoma. Blood, The Journal of the American Society of Hematology. 2011 Mar 10;117(10):2910-7.

Cao J, Sun L, Aramsangtienchai P, Spiegelman NA, Zhang X, Huang W, Seto E, Lin H. HDAC11 regulates type I interferon signaling through defatty-acylation of SHMT2. Proceedings of the National Academy of Sciences. 2019 Mar 19;116(12):5487-92.

Carreiras MD, Marco-Contelles J. Hydrazides as Inhibitors of Histone Deacetylases. Journal of Medicinal Chemistry. 2024 Aug 2.

Chatterjee M, Roy K. Predictive binary mixture toxicity modeling of fluoroquinolones (FQs) and the projection of toxicity of hypothetical binary FQ mixtures: a combination of 2D-QSAR and machine-learning approaches. Environmental Science: Processes & Impacts. 2024;26(1):105-18.

Chen H, Xie C, Chen Q, Zhuang S. HDAC11, an emerging therapeutic target for metabolic disorders. Frontiers in Endocrinology. 2022 Oct 20;13:989305.

Chen IC, Sethy B, Liou JP. Recent update of HDAC inhibitors in lymphoma. Frontiers in cell and developmental biology. 2020 Sep 3;8:576391.

Chen J, Cheng F, Sahakian E, Powers J, Wang Z, Tao J, Seto E, Pinilla-Ibarz J, Sotomayor EM. HDAC11 regulates expression of C/EBPβ and immunosuppressive molecules in myeloid-derived suppressor cells. Journal of Leucocyte Biology. 2021 May;109(5):891-900.

Chen L, Li Y, Zhao Q, Peng H, Hou T. ADME evaluation in drug discovery. 10. Predictions of P-glycoprotein inhibitors using recursive partitioning and naive Bayesian classification techniques. Molecular pharmaceutics. 2011 Jun 6;8(3):889-900.

Cheng F, Lienlaf M, Perez-Villarroel P, Wang HW, Lee C, Woan K, Woods D, Knox T, Bergman J, Pinilla-Ibarz J, Kozikowski A. Divergent roles of histone deacetylase 6 (HDAC6) and histone deacetylase 11 (HDAC11) on the transcriptional regulation of IL10 in antigen presenting cells. Molecular immunology. 2014 Jul 1;60(1):44-53.

Cheshmazar N, Hamzeh-Mivehroud M, Charoudeh HN, Hemmati S, Melesina J, Dastmalchi S. Current trends in development of HDAC-based chemotherapeutics. Life Sciences. 2022 Nov 1;308:120946.

Dallavalle S, Musso L, Cincinelli R, Darwiche N, Gervasoni S, Vistoli G, Guglielmi MB, La Porta I, Pizzulo M, Modica E, Prosperi F. Antitumor activity of novel POLA1-HDAC11 dual inhibitors. European Journal of Medicinal Chemistry. 2022 Jan 15;228:113971.

Das RN, Roy K. Predictive in silico modeling of ionic liquids toward inhibition of the acetyl cholinesterase enzyme of electrophorus electricus: a predictive toxicology approach. Industrial & Engineering Chemistry Research. 2014 Jan 15;53(2):1020-32.

Deubzer HE, Schier MC, Oehme I, Lodrini M, Haendler B, Sommer A, Witt O. HDAC11 is a novel drug target in carcinomas. International journal of cancer. 2013 May 1;132(9):2200-8.

Discovery Studio 3.0 (DS 3.0), Accelrys Inc., CA, USA, 2015. Available at www.accelrys. com.

Fan XD, Wan LL, Duan M, Lu S. HDAC11 deletion reduces fructose-induced cardiac dyslipidemia, apoptosis and inflammation by attenuating oxidative stress injury. Biochemical and biophysical research communications. 2018 Sep 5;503(2):444-51.

Fang J, Li Y, Liu R, Pang X, Li C, Yang R, He Y, Lian W, Liu AL, Du GH. Discovery of multitarget-directed ligands against Alzheimer's disease through systematic prediction of chemical–protein interactions. Journal of chemical information and modeling. 2015 Jan 26;55(1):149-64.

Fawcett T. Roc analysis in pattern recognition. Pattern Recognition Letters. 2005;8:861-74.
Feng W, Lu Z, Luo RZ, Zhang X, Seto E, Liao WS, Yu Y. Multiple histone deacetylases repress tumor suppressor gene ARHI in breast cancer. International journal of cancer. 2007 Apr 15;120(8):1664-8.

Ferrari T, Cattaneo D, Gini G, Golbamaki Bakhtyari N, Manganaro A, Benfenati E. Automatic knowledge extraction from chemical structures: the case of mutagenicity prediction. SAR and QSAR in Environmental Research. 2013 May 1;24(5):365-83.

Furumai R, Komatsu Y, Nishino N, Khochbin S, Yoshida M, Horinouchi S. Potent histone deacetylase inhibitors built from trichostatin A and cyclic tetrapeptide antibiotics including trapoxin. Proceedings of the National Academy of Sciences. 2001 Jan 2;98(1):87-92.

Gao L, Cueto MA, Asselbergs F, Atadja P. Cloning and functional characterization of HDAC11, a novel member of the human histone deacetylase family. Journal of Biological Chemistry. 2002 Jul 12;277(28):25748-55.

Glozak MA, Seto E. Acetylation/deacetylation modulates the stability of DNA replication licensing factor Cdt1. Journal of Biological Chemistry. 2009 Apr 24;284(17):11446-53.

Golbamaki A, Benfenati E, Golbamaki N, Manganaro A, Merdivan E, Roncaglioni A, Gini G. New clues on carcinogenicity-related substructures derived from mining two large datasets of chemical compounds. Journal of Environmental Science and Health, Part C. 2016 Apr 2;34(2):97-113.

Gong D, Zeng Z, Yi F, Wu J. Inhibition of histone deacetylase 11 promotes human liver cancer cell apoptosis. American Journal of Translational Research. 2019;11(2):983.

Gridelli C, Rossi A, Carbone DP, Guarize J, Karachaliou N, Mok T, Petrella F, Spaggiari L, Rosell R. Non-small-cell lung cancer. Nature reviews Disease primers. 2015 May 21;1(1):1-6.

Hauer MH, Gasser SM. Chromatin and nucleosome dynamics in DNA damage and repair. Genes & development. 2017 Nov 15;31(22):2204-21.

He L, Chen Y, Lin S, Shen R, Pan H, Zhou Y, Wang Y, Chen S, Ding J. Regulation of Hsa-miR-4639-5p expression and its potential role in the pathogenesis of Parkinson's disease. Aging Cell. 2023 Jun;22(6):e13840.

Heim CE, Bosch ME, Yamada KJ, Aldrich AL, Chaudhari SS, Klinkebiel D, Gries CM, Alqarzaee AA, Li Y, Thomas VC, Seto E. Lactate production by Staphylococcus aureus biofilm inhibits HDAC11 to reprogramme the host immune response during persistent infection. Nature microbiology. 2020 Oct;5(10):1271-84.

Ho TT, Peng C, Seto E, Lin H. Trapoxin A analogue as a selective nanomolar inhibitor of HDAC11. ACS chemical biology. 2023 Mar 28;18(4):803-9.

Host L, Dietrich JB, Carouge D, Aunis D, Zwiller J. Cocaine self-administration alters the expression of chromatin-remodelling proteins; modulation by histone deacetylase inhibition. Journal of psychopharmacology. 2011 Feb;25(2):222-9.

Huang J, Wang L, Dahiya S, Beier UH, Han R, Samanta A, Bergman J, Sotomayor EM, Seto E, Kozikowski AP, Hancock WW. Histone/protein deacetylase 11 targeting promotes Foxp3+ Treg function. Scientific reports. 2017 Aug 17;7(1):8626.

Hurtado E, Núñez-Álvarez Y, Muñoz M, Gutiérrez-Caballero C, Casas J, Pendás AM, Peinado MA, Suelves M. HDAC11 is a novel regulator of fatty acid oxidative metabolism in skeletal muscle. The FEBS journal. 2021 Feb;288(3):902-19.

Ito T, Wang YH, Duramad O, Hanabuchi S, Perng OA, Gilliet M, Qin FX, Liu YJ. OX40 ligand shuts down IL-10-producing regulatory T cells. Proceedings of the National Academy of Sciences. 2006 Aug 29;103(35):13138-43.

Jagielska A, Lowe AL, Makhija E, Wroblewska L, Guck J, Franklin RJ, Shivashankar GV, Van Vliet KJ. Mechanical strain promotes oligodendrocyte differentiation by global changes of gene expression. Frontiers in cellular neuroscience. 2017 Apr 20;11:93.

Jenke R, Reßing N, Hansen FK, Aigner A, Büch T. Anticancer therapy with HDAC inhibitors: Mechanism-based combination strategies and future perspectives. Cancers 2021, 13, 634.

Jordan MI, Mitchell TM. Machine learning: Trends, perspectives, and prospects. Science. 2015 Jul 17;349(6245):255-60.

Joshi P, Greco TM, Guise AJ, Luo Y, Yu F, Nesvizhskii AI, Cristea IM. The functional interactome landscape of the human histone deacetylase family. Molecular systems biology. 2013 Jun 11;9(1):672.

Kar S, Roy K. First report on predictive chemometric modeling, 3D-toxicophore mapping and in silico screening of in vitro basal cytotoxicity of diverse organic chemicals. Toxicology in Vitro. 2013 Mar 1;27(2):597-608.

Keedy KS, Archin NM, Gates AT, Espeseth A, Hazuda DJ, Margolis DM. A limited group of class I histone deacetylases acts to repress human immunodeficiency virus type 1 expression. Journal of virology. 2009 May 15;83(10):4749-56.

Khatun S, Amin SA, Gayen S, Jha T. In Silico Discovery of Class IIb HDAC Inhibitors: The State of Art. Current Trends in Computational Modeling for Drug Discovery. 2023 Jul 1:25-55.

Khatun S, Bhagat RP, Amin SA, Jha T, Gayen S. Density functional theory (DFT) studies in HDAC-based chemotherapeutics: Current findings, case studies and future perspectives. Computers in Biology and Medicine. 2024 Apr 16:108468.

Khatun S, Bhagat RP, Dutta R, Datta A, Jaiswal A, Halder S, Jha T, Amin SA, Gayen S. Unraveling HDAC11: Epigenetic orchestra in different diseases and structural insights for inhibitor design. Biochemical Pharmacology. 2024 May 22:116312.

Kim JI, Jung KJ, Jang HS, Park KM. Gender-specific role of HDAC11 in kidney ischemia-and reperfusion-induced PAI-1 expression and injury. American Journal of Physiology-Renal Physiology. 2013 Jul 1;305(1):F61-70.

Kirchner M, Kluck K, Brandt R, Volckmar AL, Penzel R, Kazdal D, Endris V, Neumann O, Seker-Cin H, Goldschmid H, Glade J. The immune microenvironment in EGFR-and ERBB2-mutated lung adenocarcinoma. ESMO open. 2021 Oct 1;6(5):100253.

Kleinbaum DG, Dietz K, Gail M, Klein M, Klein M. Logistic regression. New York: Springer-Verlag; 2002 Aug.

Kluyver T, Ragan-Kelley B, Pérez F, Granger B, Bussonnier M, Frederic J, Kelley K, Hamrick J, Grout J, Corlay S, Ivanov P. Jupyter Notebooks–a publishing format for reproducible computational workflows. InPositioning and power in academic publishing: Players, agents and agendas 2016 (pp. 87-90). IOS press.

Kouzarides T. Chromatin modifications and their function. Cell. 2007 Feb 23;128(4):693-705.

Kumar V, Kaur S, Kapil L, Singh C, Singh A. HDAC11: A novel inflammatory biomarker in Huntington's disease. EXCLI journal. 2022;21:647.

Kumar V, Kundu S, Singh A, Singh S. Understanding the role of histone deacetylase and their inhibitors in neurodegenerative disorders: current targets and future perspective. Current neuropharmacology. 2022 Jan 1;20(1):158.

Kutil Z, Mikešová J, Zessin M, Meleshin M, Nováková Z, Alquicer G, Kozikowski A, Sippl W, Bařinka C, Schutkowski M. Continuous activity assay for HDAC11 enabling reevaluation of HDAC inhibitors. ACS omega. 2019 Nov 15;4(22):19895-904.

Kutil Z, Novakova Z, Meleshin M, Mikesova J, Schutkowski M, Barinka C. Histone deacetylase 11 is a fatty-acid deacylase. ACS Chemical Biology. 2018 Jan 16;13(3):685-93.

Lau KW, Wu QH. Online training of support vector classifier. Pattern Recognition. 2003 Aug 1;36(8):1913-20.

Leslie PL, Chao YL, Tsai YH, Ghosh SK, Porrello A, Van Swearingen AE, Harrison EB, Cooley BC, Parker JS, Carey LA, Pecot CV. Histone deacetylase 11 inhibition promotes breast cancer metastasis from lymph nodes. Nature communications. 2019 Sep 13;10(1):4192.

Li J, Li X, Wang X, Hou J, Zang J, Gao S, Xu W, Zhang Y. PXD 101 analogs with L-phenylglycine-containing branched cap as histone deacetylase inhibitors. Chemical Biology & Drug Design. 2016 Oct;88(4):574-84.

Li MY, Zhu M, Linghu EQ, Feng F, Zhu B, Wu C, Guo MZ. Interleukin-13 suppresses interleukin-10 via inhibiting A20 in peripheral B cells of patients with food allergy. Oncotarget. 2016 Nov 11;7(48):79914.

Li R, Wu X, Zhao P, Xue K, Li J. A pan-cancer analysis identifies HDAC11 as an immunological and prognostic biomarker. The FASEB Journal. 2022 Jul;36(7):e22326.

Li X, Zhang J, Xie Y, Jiang Y, Yingjie Z, Xu W. Progress of HDAC inhibitor panobinostat in the treatment of cancer. Current drug targets. 2014 Jun 1;15(6):622-34.

Lipinski CA. Lead-and drug-like compounds: the rule-of-five revolution. Drug discovery today: Technologies. 2004 Dec 1;1(4):337-41.

Liu H, Hu Q, D'ercole AJ, Ye P. Histone deacetylase 11 regulates oligodendrocyte-specific gene expression and cell development in OL-1 oligodendroglia cells. Glia. 2009 Jan 1;57(1):1-2.

Liu H, Hu Q, Kaufman A, D'Ercole AJ, Ye P. Developmental expression of histone deacetylase 11 in the murine brain. Journal of neuroscience research. 2008 Feb 15;86(3):537-43.

Liu SS, Wu F, Jin YM, Chang WQ, Xu TM. HDAC11: a rising star in epigenetics. Biomedicine & pharmacotherapy. 2020 Nov 1;131:110607.

Liu Y, Tong X, Hu W, Chen D. HDAC11: A novel target for improved cancer therapy. Biomedicine & Pharmacotherapy. 2023 Oct 1;166:115418.

Lombardo A, Pizzo F, Benfenati E, Manganaro A, Ferrari T, Gini G. A new in silico classification model for ready biodegradability, based on molecular fragments. Chemosphere. 2014 Aug 1;108:10-6.

Lozada EM, Andrysik Z, Yin M, Redilla N, Rice K, Stambrook PJ. Acetylation and deacetylation of Cdc25A constitutes a novel mechanism for modulating Cdc25A functions with implications for cancer. Oncotarget. 2016 Apr 4;7(15):20425.

Lundberg SM, Erion GG, Lee SI. Consistent individualized feature attribution for tree ensembles. arXiv preprint arXiv:1802.03888. 2018 Feb 12.

Luo XQ, Shao JB, Xie RD, Zeng L, Li XX, Qiu SQ, Geng XR, Yang LT, Li LJ, Liu DB, Liu ZG. Micro RNA-19a interferes with IL-10 expression in peripheral dendritic cells of patients with nasal polyposis. Oncotarget. 2017 Jul 7;8(30):48915.

Mangalathu S, Hwang SH, Jeon JS. Failure mode and effects analysis of RC members based on machine-learning-based SHapley Additive exPlanations (SHAP) approach. Engineering Structures. 2020 Sep 15;219:110927.

Mao L, Liu L, Zhang T, Qin H, Wu X, Xu Y. Histone deacetylase 11 contributes to renal fibrosis by repressing KLF15 transcription. Frontiers in Cell and Developmental Biology. 2020 Apr 17;8:235.

Mármol I, Sánchez-de-Diego C, Pradilla Dieste A, Cerrada E, Rodriguez Yoldi MJ. Colorectal carcinoma: a general overview and future perspectives in colorectal cancer. International journal of molecular sciences. 2017 Jan 19;18(1):197.

Martin MW, Lee JY, Lancia Jr DR, Ng PY, Han B, Thomason JR, Lynes MS, Marshall CG, Conti C, Collis A, Morales MA. Discovery of novel N-hydroxy-2-arylisoindoline-4-carboxamides as potent and selective inhibitors of HDAC11. Bioorganic & medicinal chemistry letters. 2018 Jul 1;28(12):2143-7.

Marzo M, Kulkarni S, Manganaro A, Roncaglioni A, Wu S, Barton-Maclaren TS, Lester C, Benfenati E. Integrating in silico models to enhance predictivity for developmental toxicity. Toxicology. 2016 Aug 31;370:127-37.

Miano JM. Vascular smooth muscle cell differentiation–2010. Journal of biomedical research. 2010 May 1;24(3):169-80.

Moinul M, Amin SA, Khatun S, Das S, Jha T, Gayen S. A detail survey and analysis of selectivity criteria for indole-based histone deacetylase 8 (HDAC8) inhibitors. Journal of Molecular Structure. 2023 Jan 5;1271:133967.

Mombelli E, Raitano G, Benfenati E. In silico prediction of chemically induced mutagenicity: how to use QSAR models and interpret their results. In silico methods for predicting drug toxicity. 2016:87-105.

Morales PE, Bucarey JL, Espinosa A. Muscle lipid metabolism: role of lipid droplets and perilipins. Journal of diabetes research. 2017;2017(1):1789395.

Mrug M, Sanders PW. Beware the low Hdac11: Males at risk for ischemic kidney injury. American Journal of Physiology-Renal Physiology. 2013 Oct 1;305(7):F973-4.

Núñez-Álvarez Y, Hurtado E, Munoz M, García-Tuñon I, Rech GE, Pluvinet R, Sumoy L, Pendás AM, Peinado MA, Suelves M. Loss of HDAC11 accelerates skeletal muscle regeneration in mice. The FEBS Journal. 2021 Feb;288(4):1201-23.

Núñez-Álvarez Y, Suelves M. HDAC11: a multifaceted histone deacetylase with proficient fatty deacylase activity and its roles in physiological processes. The FEBS Journal. 2022 May;289(10):2771-92.

Olsen CA, Ghadiri MR. Discovery of potent and selective histone deacetylase inhibitors via focused combinatorial libraries of cyclic α3β-tetrapeptides. Journal of medicinal chemistry. 2009 Dec 10;52(23):7836-46.

Pal M., Random forest classifier for remote sensing classification. International journal of remote sensing. 2005 Jan 1;26(1):217-22.

Pan H, Cao J, Xu W. Selective histone deacetylase inhibitors. Anti-Cancer Agents in Medicinal Chemistry (Formerly Current Medicinal Chemistry-Anti-Cancer Agents). 2012 Mar 1;12(3):247-70.

Rana Z, Diermeier S, Hanif M, Rosengren RJ. Understanding failure and improving treatment using HDAC inhibitors for prostate cancer. Biomedicines. 2020 Jan 30;8(2):22.

Rogers D, Hahn M. Extended-connectivity fingerprints. Journal of chemical information and modeling. 2010 May 24;50(5):742-54.

Roy K, Kar S, Das RN. Understanding the basics of QSAR for applications in pharmaceutical sciences and risk assessment. Academic press; 2015 Mar 3.

Ruijter AJ, GENNIP AH, Caron HN, Kemp S, KUILENBURG AB. Histone deacetylases (HDACs): characterization of the classical HDAC family. Biochemical Journal. 2003 Mar 15;370(3):737-49.

Sahakian E, Chen J, Powers JJ, Chen X, Maharaj K, Deng SL, Achille AN, Lienlaf M, Wang HW, Cheng F, Sodré AL. Essential role for histone deacetylase 11 (HDAC11) in neutrophil biology. Journal of leukocyte biology. 2017 Aug;102(2):475-86.

Sahakian E, Powers JJ, Chen J, Deng SL, Cheng F, Distler A, Woods DM, Rock-Klotz J, Sodre AL, Youn JI, Woan KV. Histone deacetylase 11: A novel epigenetic regulator of myeloid derived suppressor cell expansion and function. Molecular immunology. 2015 Feb 1;63(2):579-85.

Santos-Martins D, Forli S, Ramos MJ, Olson AJ. AutoDock4Zn: an improved AutoDock force field for small-molecule docking to zinc metalloproteins. Journal of chemical information and modeling. 2014 Aug 25;54(8):2371-9.

Sardar S, Jyotisha, Amin SA, Khatun S, Qureshi IA, Patil UK, Jha T, Gayen S. Identification of structural fingerprints among natural inhibitors of HDAC1 to accelerate nature-inspired drug discovery in cancer epigenetics. Journal of Biomolecular Structure and Dynamics. 2024 Jul 23;42(11):5642-56.

Schlüter A, Aksan B, Fioravanti R, Valente S, Mai A, Mauceri D. Histone deacetylases contribute to excitotoxicity-triggered degeneration of retinal ganglion cells in vivo. Molecular neurobiology. 2019 Dec;56:8018-34.

Shanmugam G, Rakshit S, Sarkar K. HDAC inhibitors: Targets for tumor therapy, immune modulation and lung diseases. Translational Oncology. 2022 Feb 1;16:101312.

Shao JB, Luo XQ, Wu YJ, Li MG, Hong JY, Mo LH, Liu ZG, Li HB, Liu DB, Yang PC. Histone deacetylase 11 inhibits interleukin 10 in B cells of subjects with allergic rhinitis. InInternational Forum of Allergy & Rhinology 2018 Nov (Vol. 8, No. 11, pp. 1274-1283).

Shogren-Knaak M, Ishii H, Sun JM, Pazin MJ, Davie JR, Peterson CL. Histone H4-K16 acetylation controls chromatin structure and protein interactions. Science. 2006 Feb 10;311(5762):844-7.

Shouksmith AE, Shah F, Grimard ML, Gawel JM, Raouf YS, Geletu M, Berger-Becvar A, de Araujo ED, Luchman HA, Heaton WL, Bakhshinyan D. Identification and characterization of AES-135, a hydroxamic acid-based HDAC inhibitor that prolongs survival in an orthotopic mouse model of pancreatic cancer. Journal of medicinal chemistry. 2019 Feb 18;62(5):2651-65.

Son SI, Cao J, Zhu CL, Miller SP, Lin H. Activity-guided design of HDAC11-specific inhibitors. ACS chemical biology. 2019 Jul 2;14(7):1393-7.

Son SI, Su D, Ho TT, Lin H. Garcinol is an HDAC11 inhibitor. ACS chemical biology. 2020 Oct 9;15(11):2866-71.

Sriramareddy SN, Faião-Flores F, Emmons MF, Saha B, Chellappan S, Wyatt C, Smalley I, Licht JD, Durante MA, Harbour JW, Smalley KS. HDAC11 activity contributes to MEK inhibitor escape in uveal melanoma. Cancer gene therapy. 2022 Dec;29(12):1840-6.

Štrumbelj E, Kononenko I. Explaining prediction models and individual predictions with feature contributions. Knowledge and information systems. 2014 Dec;41:647-65.

Sui L, Zhang S, Huang R, Li Z. HDAC11 promotes meiotic apparatus assembly during mouse oocyte maturation via decreasing H4K16 and α-tubulin acetylation. Cell Cycle. 2020 Feb 1;19(3):354-62.

Sun L, De Evsikova CM, Bian K, Achille A, Telles E, Pei H, Seto E. Programming and regulation of metabolic homeostasis by HDAC11. EBioMedicine. 2018 Jul 1;33:157-68.

Sun L, Telles E, Karl M, Cheng F, Luetteke N, Sotomayor EM, Miller RH, Seto E. Loss of HDAC11 ameliorates clinical symptoms in a multiple sclerosis mouse model. Life science alliance. 2018 Oct 1;1(5).

Takase K, Oda S, Kuroda M, Funato H. Monoaminergic and neuropeptidergic neurons have distinct expression profiles of histone deacetylases. PLoS One. 2013 Mar 4;8(3):e58473.

Tao R, De Zoeten EF, Özkaynak E, Chen C, Wang L, Porrett PM, Li B, Turka LA, Olson EN, Greene MI, Wells AD. Deacetylase inhibition promotes the generation and function of regulatory T cells. Nature medicine. 2007 Nov;13(11):1299-307.

Thangapandian S, John S, Lee Y, Arulalapperumal V, Lee KW. Molecular modeling study on tunnel behavior in different histone deacetylase isoforms. PLoS One. 2012 Nov 29;7(11):e49327.

Tian Y, Lv W, Li X, Wang C, Wang D, Wang PG, Jin J, Shen J. Stabilizing HDAC11 with SAHA to assay slow-binding benzamide inhibitors. Bioorganic & Medicinal Chemistry Letters. 2017 Jul 1;27(13):2943-5.

Tiwari S, Dharmarajan S, Shivanna M, Otteson DC, Belecky-Adams TL. Histone deacetylase expression patterns in developing murine optic nerve. BMC developmental biology. 2014 Dec;14:1-8.

Todd PK, Oh SY, Krans A, Pandey UB, Di Prospero NA, Min KT, Taylor JP, Paulson HL. histone deacetylases suppress CGG repeat–induced neurodegeneration via transcriptional silencing in models of fragile X tremor ataxia syndrome. PLoS genetics. 2010 Dec 9;6(12):e1001240.

Toropova AP, Toropov AA, Veselinović JB, Miljković FN, Veselinović AM. QSAR models for HEPT derivates as NNRTI inhibitors based on Monte Carlo method. European journal of medicinal chemistry. 2014 Apr 22;77:298-305.

Toropova AP, Toropov AA. CORAL: binary classifications (active/inactive) for drug-induced liver injury. Toxicology Letters. 2017 Feb 15;268:51-7.

Tropsha A. Best practices for QSAR model development, validation, and exploitation. Molecular informatics. 2010 Jul 12;29(6-7):476-88.

Villagra A, Cheng F, Wang HW, Suarez I, Glozak M, Maurin M, Nguyen D, Wright KL, Atadja PW, Bhalla K, Pinilla-Ibarz J. The histone deacetylase HDAC11 regulates the expression of interleukin 10 and immune tolerance. Nature immunology. 2009 Jan;10(1):92-100.

Wang J, Zibetti C, Shang P, Sripathi SR, Zhang P, Cano M, Hoang T, Xia S, Ji H, Merbs SL, Zack DJ. ATAC-Seq analysis reveals a widespread decrease of chromatin accessibility in age-related macular degeneration. Nature communications. 2018 Apr 10;9(1):1364.

Wang W, Wei C. Advances in the early diagnosis of hepatocellular carcinoma. Genes & diseases. 2020 Sep 1;7(3):308-19.

Watanabe Y, Khodosevich K, Monyer H. Dendrite development regulated by the schizophrenia-associated gene FEZ1 involves the ubiquitin proteasome system. Cell reports. 2014 Apr 24;7(2):552-64.

Witt O, Deubzer HE, Milde T, Oehme I. HDAC family: What are the cancer relevant targets?. Cancer letters. 2009 May 8;277(1):8-21.

Woods DM, Woan KV, Cheng F, Sodré AL, Wang D, Wu Y, Wang Z, Chen J, Powers J, Pinilla-Ibarz J, Yu Y. T cells lacking HDAC11 have increased effector functions and mediate enhanced alloreactivity in a murine model. Blood, The Journal of the American Society of Hematology. 2017 Jul 13;130(2):146-55.

Xanthopoulos P, Pardalos PM, Trafalis TB, Xanthopoulos P, Pardalos PM, Trafalis TB. Linear discriminant analysis. Robust data mining. 2013:27-33.

Yadav V, Banerjee S, Baidya SK, Adhikari N, Jha T. Applying comparative molecular modelling techniques on diverse hydroxamate-based HDAC2 inhibitors: an attempt to identify promising structural features for potent HDAC2 inhibition. SAR and QSAR in Environmental Research. 2022 Jan 2;33(1):1-22.

Yang H, Chen L, Sun Q, Yao F, Muhammad S, Sun C. The role of HDAC11 in obesity-related metabolic disorders: A critical review. Journal of Cellular Physiology. 2021 Aug;236(8):5582-91.

Yang H, Li C, Che M, Liang J, Tian X, Yang G, Sun C. HDAC11 deficiency resists obesity by converting adipose-derived stem cells into brown adipocyte-like cells. International Journal of Biological Macromolecules. 2024 Feb 1;258:128852.

Yang H, Li J, Wu Z, Li W, Liu G, Tang Y. Evaluation of different methods for identification of structural alerts using chemical ames mutagenicity data set as a benchmark. Chemical Research in Toxicology. 2017 Jun 19;30(6):1355-64.

Yang X, Shen Z, Tian M, Lin Y, Li L, Chai T, Zhang P, Kang M, Lin J. LncRNA C9orf139 can regulate the progression of esophageal squamous carcinoma by mediating the miR-661/HDAC11 axis. Translational Oncology. 2022 Oct 1;24:101487.

Yanginlar C, Logie C. HDAC11 is a regulator of diverse immune functions. Biochimica et Biophysica Acta (BBA)-Gene Regulatory Mechanism

Yao Y, Tu Z, Liao C, Wang Z, Li S, Yao H, Li Z, Jiang S. Discovery of novel class I histone deacetylase inhibitors with promising in vitro and in vivo antitumor activities. Journal of Medicinal Chemistry. 2015 Oct 8;58(19):7672-80.

Yap CW. PaDEL-descriptor: An open source software to calculate molecular descriptors and fingerprints. Journal of computational chemistry. 2011 May;32(7):1466-74.

Yoon S, Eom GH. HDAC and HDAC inhibitor: from cancer to cardiovascular diseases. Chonnam medical journal. 2016 Jan;52(1):1-1.

Yuan Y, Zhao K, Yao Y, Liu C, Chen Y, Li J, Wang Y, Pei R, Chen J, Hu X, Zhou Y. HDAC11 restricts HBV replication through epigenetic repression of cccDNA transcription. Antiviral research. 2019 Dec 1;172:104619.

Zhang R, Pan Y, Feng W, Zhao Y, Yang Y, Wang L, Zhang Y, Cheng J, Jiang Q, Zheng Z, Jiang M. HDAC11 regulates the proliferation of bovine muscle stem cells through the notch signaling pathway and inhibits muscle regeneration. Journal of Agricultural and Food Chemistry. 2022 Jul 15;70(29):9166-78.

Zhao H, Zhang XM, Xiao S, Wu ZR, Shi YJ, Xie MJ. HDAC11 is related to breast cancer prognosis and inhibits invasion and proliferation of breast cancer cells. International Journal of Clinical and Experimental Pathology. 2023;16(7):172.

Zhou B, Zeng S, Li N, Yu L, Yang G, Yang Y, Zhang X, Fang M, Xia J, Xu Y. Angiogenic factor with G patch and FHA domains 1 is a novel regulator of vascular injury. Arteriosclerosis, Thrombosis, and Vascular Biology. 2017 Apr;37(4):675-84.

Zhou N, Moradei O, Raeppel S, Leit S, Frechette S, Gaudette F, Paquin I, Bernstein N, Bouchain G, Vaisburg A, Jin Z. Discovery of N-(2-aminophenyl)-4-[(4-pyridin-3-ylpyrimidin-2-ylamino) methyl] benzamide (MGCD0103), an orally active histone deacetylase inhibitor. Journal of medicinal chemistry. 2008 Jul 24;51(14):4072-5.

Chapter 8: Publications

Publication Lists

1. Khatun S, **Prasad Bhagat R**, Dutta R, Datta A, Jaiswal A, Halder S, Jha T, Amin SA, Gayen S. Unraveling HDAC11: Epigenetic orchestra in different diseases and structural insights for inhibitor design. Biochem Pharmacol. 2024 Jul;225:116312. doi: 10.1016/j.bcp.2024.11631
2. Khatun S, **Bhagat RP**, Amin SA, Jha T, Gayen S. Density functional theory (DFT) studies in HDAC-based chemotherapeutics: Current findings, case studies and future perspectives. Comput Biol Med. 2024 Jun;175:108468. doi: 10.1016/j.compbiomed.2024.108468

Publication 1

Biochemical Pharmacology 225 (2024) 116312

Contents lists available at ScienceDirect

Biochemical Pharmacology

journal homepage: www.elsevier.com/locate/biochempharm

Review

Unraveling HDAC11: Epigenetic orchestra in different diseases and structural insights for inhibitor design

Samima Khatun [a], Rinki Prasad Bhagat [a], Ritam Dutta [b], Anwesha Datta [a], Abhishek Jaiswal [a], Swapnamay Halder [a], Tarun Jha [c,*], Sk. Abdul Amin [b,*], Shovanlal Gayen [a,*]

[a] Laboratory of Drug Design and Discovery, Department of Pharmaceutical Technology, Jadavpur University, Kolkata 700032, West Bengal, India
[b] Department of Pharmaceutical Technology, JIS University, 81, Nilgunj Road, Agarpara, Kolkata 700109, West Bengal, India
[c] Natural Science Laboratory, Division of Medicinal and Pharmaceutical Chemistry, Department of Pharmaceutical Technology, Jadavpur University, Kolkata 700032, West Bengal, India

ARTICLE INFO

Keywords:
HDAC11
Chemotherapy
Cancer
Epigenetics
Structure-activity relationship

ABSTRACT

Histone deacetylase 11 (HDAC11), a member of the HDAC family, has emerged as a critical regulator in numerous physiological as well as pathological processes. Due to its diverse roles, HDAC11 has been a focal point of research in recent times. Different non-selective inhibitors are already approved, and research is going on to find selective HDAC11 inhibitors. The objective of this review is to comprehensively explore the role of HDAC11 as a pivotal regulator in a multitude of physiological and pathological processes. It aims to delve into the intricate details of HDAC11's structural and functional aspects, elucidating its molecular interactions and implications in different disease contexts. With a primary focus on elucidating the structure–activity relationships (SARs) of HDAC11 inhibitors, this review also aims to provide a holistic understanding of how its molecular architecture influences its inhibition. Additionally, by integrating both established knowledge and recent research, the review seeks to contribute novel insights into the potential therapeutic applications of HDAC11 inhibitors. Overall, the scope of this review spans from fundamental research elucidating the complexities of HDAC11 biology to the potential of targeting HDAC11 in therapeutic interventions.

Abbreviations: Aggf1, Angiogenic factor with G-Patch and FHA domain 1; AMPK, Activated protein kinase; Ang II, Angiotensin II; AP-2α, Activator protein 2 alpha; ARH1, ADP-ribosylhydrolase 1; BAT, Brown adipose tissue; BMR, Basal metabolic rate; BRD2, Bromodomain-containing protein; BRET, Bioluminescence resonance energy transfer; BubR1, Budding uninhibited by benzimidazoles 1-related 1; CCL2, Chemokine C–C motif ligand 2; CD4+, Cluster of differentiation 4 positive; CDC20/APC, Cell division cycle 20/ anaphase-promoting complex; cDNA, circular DNA; CDT1, Chromatin licensing and DNA replication factor 1; CL_{int}, Intrinsic clearance; CU, Connection unit; DISC1, Disruption in schizophrenia 1; DNA, Deoxyribonucleic acid; E2F1, E2F Transcription Factor 1; E2F4, E2F Transcription Factor 4; EAE, Experimental autoimmune encephalomyelitis; ECM, Extracellular matrix; EGR1, Early growth response protein 1; EOMES, Eomesodermin; FDA, Food and Drug Administration; FEZ1, Fasciculation and elongation protein zeta 1; Foxp3+, Forkhead box P3 positive; GLI1, Glioma-associated oncogene family zinc finger-1; H3K27ac, Acetylation on histone H3 at lysine residue 27; H3K9/K14ac, Acetylation on histone H3 at lysine residues 9 and 14; HATs, Histone acetyltransferases; HBV, Hepatitis B virus; HCC, Hepatocellular carcinoma; HDL, High density lipoprotein; HDAC11, Histone deacetylase 11; HEY-1, Hes Related Family BHLH transcription factor with YRPW Motif 1; HL, Hodgkin's lymphoma; Hsa-miR-4639-5p, Homo sapiens microRNA 4639-5p; IL-10, Interleukin-10; I/R, Ischemia-reperfusion; JAK/STAT, Janus kinase/Signal Transducer and Activator of Transcription; KLF4, Krüppel-like factor 4; KLF15, Kruppel-like factor 15; LDL, Low density lipoprotein; *LipE*, Lipophilic efficiency; LKB1, Liver Kinase B1; LPL, Lipoprotein lipase; LPS, Lipopolysaccharide; *Mbp*, Myelin basic protein; MEKi, Mitogen-activated protein kinase inhibitor; MYC, myelocytomatosis; MYOD, Myoblast determination protein 1; NMDA, N-Methyl-D-aspartate; NSCLC, Non-small cell lung cancer; OX40L, OX40 ligand; PAI-1, Plasminogen activator inhibitor type 1; *Plp*, Proteolipid protein; PU.1, Purine-rich box-1; RGC, Retinal ganglion cells; RTECs, Renal tubular epithelial cells; RNS, Reactive nitrogen species; SAR, Structure–activity relationship; SHMT2, Serine hydroxymethyltransferase 2; SIRT1, Sirtuin 1; SMN, Survival of motor neuron; SOX-2, Sex determining region Y-related box 2; TBET, T-box expressed in T cells; TBX2, T-box transcription factor 2; TGI, Tumor growth inhibition; Th1, T-helper 1; TNF, Tumor necrosis factor; Treg, Regulatory T cells; UCP1, Uncoupling protein 1; UCP-25, Uncoupling protein-25; ZBG, Zinc binding group.

* Corresponding authors.
E-mail addresses: tjupharm@yahoo.com (T. Jha), pharmacist.amin@gmail.com, skabdul.amin@jisuniversity.ac.in (Sk.A. Amin), sgayen.pharmacy@jadavpuruniversity.in (S. Gayen).

https://doi.org/10.1016/j.bcp.2024.116312
Received 5 February 2024; Received in revised form 20 May 2024; Accepted 21 May 2024
Available online 22 May 2024

Publication 2

Computers in Biology and Medicine 175 (2024) 108468

Contents lists available at ScienceDirect

Computers in Biology and Medicine

journal homepage: www.elsevier.com/locate/compbiomed

Density functional theory (DFT) studies in HDAC-based chemotherapeutics: Current findings, case studies and future perspectives

Samima Khatun [a,1], Rinki Prasad Bhagat [a,1], Sk Abdul Amin [b], Tarun Jha [c], Shovanlal Gayen [a,*]

[a] Laboratory of Drug Design and Discovery, Department of Pharmaceutical Technology, Jadavpur University, Kolkata, 700032, India
[b] Department of Pharmaceutical Technology, JIS University, 81, Nilgunj Road, Agarpara, Kolkata, West Bengal, India
[c] Natural Science Laboratory, Division of Medicinal and Pharmaceutical Chemistry, Department of Pharmaceutical Technology, Jadavpur University, Kolkata 700032, India

ARTICLE INFO

Keywords:
HDACs
HDACis
DFT
Toxicity
Quantum chemical techniques
Reactivity

ABSTRACT

Density Functional Theory (DFT) is a quantum chemical computational method used to predict and analyze the electronic properties of atoms, molecules, and solids based on the density of electrons rather than wavefunctions. It provides insights into the structure, bonding, and behavior of different molecules, including those involved in the development of chemotherapeutic agents, such as histone deacetylase inhibitors (HDACis). HDACs are a wide group of metalloenzymes that facilitate the removal of acetyl groups from acetyl-lysine residues situated in the N-terminal tail of histones. Abnormal HDAC recruitment has been linked to several human diseases, especially cancer. Therefore, it has been recognized as a prospective target for accelerating the development of anticancer therapies. Researchers have studied HDACs and its inhibitors extensively using a combination of experimental methods and diverse *in-silico* approaches such as machine learning and quantitative structure–activity relationship (QSAR) methods, molecular docking, molecular dynamics, pharmacophore mapping, and more. In this context, DFT studies can make significant contribution by shedding light on the molecular properties, interactions, reaction pathways, transition states, reactivity and mechanisms involved in the development of HDACis. This review attempted to elucidate the scope in which DFT methodologies may be used to enhance our comprehension of the molecular aspects of HDAC inhibitors, aiding in the rational design and optimization of these compounds for therapeutic applications in cancer and other ailments. The insights gained can guide experimental efforts toward developing more potent and selective HDAC inhibitors.

1. Introduction

HDACs belong to a category of metalloenzymes responsible for removing acetyl groups from the ε-N-acetyl lysine amino acid present in histones and non-histone proteins [1]. HDACs control the acetylation status of histones within chromatin and also influence the acetylation of numerous non-histone substrates, such as various proteins linked to human cancerogenesis, which makes HDACs interesting for therapeutic investigation [2]. Consequently, there has been an increasing interest in HDAC inhibitors (HDACis) in recent years. The Food and Drug Administration of the United States (US-FDA) has recognized and authorized multiple HDACis. The US FDA approved Vorinostat (SAHA) for treating cutaneous T-cell lymphoma. Belinostat (PXD101), Panabinostat (LBH589), and Romidepsin are the HDACis with US FDA approval, while Chidamide (HBI8000) has received FDA approval from the Chinese government (Fig. 1) [3]. In recent times, there has been a shift in attention among academic institutions and pharmaceutical companies towards developing selective inhibitors for specific isoforms of HDACs. However, in recent years, both academic institutions and pharmaceutical companies have begun to focus on the development of isoform-selective HDACis [4]. All these HDAC-targeting drugs approved by the FDA are pan-HDAC inhibitors and hence lead to several toxicities even at therapeutic levels. Therefore, there is an ongoing quest to develop cancer treatments that are more precise, safer, and more effective therapeutically.

* Corresponding author.
E-mail address: shovanlal.gayen@gmail.com (S. Gayen).
[1] Authors have equal contribution.

https://doi.org/10.1016/j.compbiomed.2024.108468
Received 2 November 2023; Received in revised form 8 April 2024; Accepted 9 April 2024
Available online 16 April 2024